Understanding Decision-Making Processes at Different Time Scales Using Multi-Modal Neuroimaging Techniques

Yvonne H.C. Yau

Faculty of Medicine

Integrated Program in Neuroscience

McGill University, Montreal

June 2020

A thesis submitted to McGill University in partial fulfillment of the requirements of the degree of Doctor of Philosophy

Abstract (English)

Decision-making is a critical cognitive function for everyday life. In any given day, we are constantly tasked with making decisions, large and small, and we must identify potential options, gather and compare the relevant information, and ultimately make a choice. The brain must infer the most likely state of the world given a variable amount of sensory evidence – a process commonly referred to as "perceptual decision-making". The last two decades bore witness to great strides towards explaining how the brain can enable adaptive action in the face of noisy sensory information. Animal physiology has had success in identifying neural signals that perform the role of a "decision variable" which integrates sensory information in favour of a particular outcome up to an action-triggering threshold. Recently, there has been a push to also consider the aspect of time which may impose an evidence-independent "urgency" factor to the decision-making process. Taken together, animal studies have shown that computational models can be fitted to behaviour and to signals from microelectrode recording in various parts of the brain. This has provoked a search for similar neural processes at work in the human brain, however, this has proven challenging. The present doctoral thesis aimed to bridge this gap in knowledge through three studies that exploit recent advances in neuroimaging methodologies and computational tools to overcome inherent limitations in non-invasive recording techniques. In the first study, we demonstrate that sensory evidence in the human brain can be decoded by model-driven machine-learning neuroimaging techniques. This representation of sensory evidence was found to be relayed between visual, decision, and motor brain regions to inform and enact decisions. Moreover, we observed an inverse-urgency signal rooted in the caudate that slowed decisions. In the second study, we examined perceptual decisions at a faster timescale and disentangled neural signals within a trial. We provide evidence that the neural decision variable reflects the combined influence of both the sensory evidence and an urgency signal. In the third study, we aimed to test how global brain networks may shape perceptual decisions. We found that variability in the functional configuration of the brain captured at rest influenced behavioural performance in task. This relationship was mediated by the activity of subcortical structures, including the thalamus and caudate, that are involved with generating an inverse-urgency signal in task. Understanding the

neuroscience of perceptual decision-making in humans can expose principles of neural processing that underlie a variety of mental functions, providing critical insight into the pathophysiology of disease that compromise cognitive function, and ultimately help elucidate ways to ameliorate cognitive dysfunction.

Résumé (Français)

La prise de décision est une fonction cognitive essentielle pour la vie quotidienne. Chaque jour, nous sommes constamment amenés à prendre des décisions, grandes ou petites, et nous devons identifier les options potentielles, rassembler et comparer les informations pertinentes, et finalement faire un choix. Le cerveau doit déduire l'état le plus probable du monde en fonction d'une quantité variable de preuves sensorielles - un processus communément appelé "prise de décision perceptive". Les deux dernières décennies ont vu de grands progrès dans l'explication de la manière dont le cerveau peut permettre une action adaptative face à des informations sensorielles bruyantes. La physiologie animale a réussi à identifier les signaux neuronaux qui jouent le rôle de "variable de décision" intégrant l'information sensorielle en faveur d'un résultat particulier, jusqu'à un seuil de déclenchement de l'action. Récemment, il a eu un effort de prise en considération l'aspect du temps qui peut imposer un facteur d'"urgence", indépendant des preuves, dans le processus de décision. Dans l'ensemble, les études sur les animaux ont montré que les modèles basés sur des méthodes computationnelles peuvent être ajustés au comportement et aux signaux des microélectrodes enregistrant l'activité dans différentes parties du cerveau. Cela a entrainé la recherche de processus neuronaux similaires, à l'œuvre dans le cerveau humain, ce qui s'est révélé plus difficile. Cette thèse de doctorat vise à combler cette lacune grâce à trois études qui exploitent les récentes avancées dans les méthodologies de neuroimagerie et les outils informatiques pour surmonter les limites inhérentes aux techniques d'enregistrement non invasives. Dans la première étude, nous démontrons que les preuves sensorielles dans le cerveau humain peuvent être décodées par des techniques de neuroimagerie à apprentissage automatique pilotées par des modèles. Cette représentation des preuves sensorielles s'est avérée être relayée entre les régions

visuelles, décisionnelles et motrices du cerveau pour informer et mettre en œuvre des décisions. De plus, nous avons observé un signal d'urgence inverse, enraciné dans le noyau caudé, qui ralentit les décisions. Dans la seconde étude, nous avons examiné les décisions perceptives à une échelle de temps plus rapide et avons démêlé les signaux neuronaux au sein d'un même essai. Nous avons démontré que la variable de décision neurale reflète l'influence combinée des preuves sensorielles et d'un signal d'urgence. Dans la troisième étude, nous avons cherché à tester comment les réseaux cérébraux globaux peuvent façonner les décisions perceptives. Nous avons constaté que la variabilité de la configuration fonctionnelle du cerveau au repos influençait les performances comportementales durant les tâches. Cette relation était médiée par l'activité des structures sous-corticales, y compris le thalamus et le noyau caudé, qui sont impliquées dans la génération d'un signal d'urgence inverse durant la tâche. La compréhension de la neuroscience de la prise de décision perceptive chez l'homme peut exposer les principes du traitement neural. Ces principes sous-tendent une grande variété de fonctions mentales, fournissant un aperçu critique de la physiopathologie des maladies qui compromettent la fonction cognitive. Les comprendre pourra contribuer à élucider les moyens d'améliorer le dysfonctionnement cognitif.

Contents

Acknowledgements

First and foremost, I would like to thank my supervisors (Alain Dagher and Lesley Fellows) for their guidance, encouragement, practical advice, and humour as I navigated this doctoral journey. Without their contributions, my thesis work would not have been possible. Alain has always been a source of innovative ideas that have pushed my work forward, introducing and encouraging me to adopt new techniques to better solve the problem at hand. Lesley brings with her a wealth of knowledge and expertise; she has used them to orient me, making sure I didn't get too distracted or carried away – a trait for which I am guilty of. Together, they are a formidable team that has been instrumental to my academic success. Thanks are also due to my advisory committee (Boris Bernhardt, Madeleine Sharp, and Robert Zatorre) for their consultations and contribution to great scientific discussions during my committee meetings and beyond.

My collaborators and colleagues have served a tremendously important role to the success of my doctoral work and I am grateful for their time and effort. Yashar Zeighami has, in particular, been like a third supervisor to me (who knew you could have so many supervisors?) and has stuck with me through thick and thin. His technical guidance was instrumental to my doctoral research and he remains a figure that I can reliably turn to should I ever need a brain to pick. Mahsa Dadar has been a fountain of knowledge who helped me greatly during my doctoral research. I have never met someone who worked as efficiently as Mahsa; if you have an issue, she can fix it for you within the hour. Madeline Taylor, who I supervised, was quintessential to our data collection efforts and without her work, I would have had no data to analyze. I would also like to thank members of the Dagher and Fellows lab who have provided friendship and peer-support throughout these years. You are too numerous to name but my deepest gratitude goes out to you for your help in making every day fun at work. Having spent the final months of my doctoral studies at a social distance due to an ensuing pandemic has made me appreciate, even more, our office banter.

I would like to acknowledge the Vanier-Banting Secretariat, Desjardins Foundation, Colman-Seivers family, Max Stern Estate, McGill's Faculty of Medicine, and the Integrated Program of Neuroscience for their generous financial support over the years. I thank Josephine

Nalbantoglu and Katherine Vanka for helping me transition to McGill, believing in me, and encouraging me to apply for these scholarships.

To my family and friends who may not know what a pivotal role they have played to the success of my doctoral studies, I give my sincerest thanks. From the early Rotation family (Scott Bell, Nathalie Nilsson, Zahraa Chorghay), the friends made along the way (Marie Franquin, Andréanne Michaud, Isabel Garcia-Garcia, Christine Déry, Selin Neseliler, Filip Morys, Thomas Hinault), and to the original crew (my mother (Shirley Yu) and brother (Justin Yau)), I am thankful for your continued support. An extra thanks goes to Marie for her translation of the abstract and to Nathalie and Zahraa for their proofreading of this thesis.

Like a cliché Oscars acceptance speech, I have probably gone beyond my allocated time and the music is starting to play. So last, but certainly not least, I would like to thank my partner, Basile Durieux. He can somehow cope with my mercurial personality and has held my hand throughout this doctoral journey. His acts of support – be it cooking for me, perhaps in greater frequency when deadlines are due, or cleaning after yet another of the cat's puking spree – do not go unappreciated.

Thank you.

Prologue

Overview of Thesis

In this monograph, I present the results of several years worth of experiments and analyses to help bridge the knowledge gap in what we understand about the neural underpinnings of perceptual decisions in humans. The subsequent chapters are organized as follows: Chapter 1 provides a literature review of topics related to the studies conducted in this thesis. Perceptual decision-making, computational models used to explain the decision process, the putative neural correlates of decision parameters, as well as neuroimaging approaches are discussed. Relevant statistical methods employed in this thesis are also introduced. Chapter 2 examines how decisions parameters are encoded in the human brain using a combination of model-driven machine-learning neuroimaging techniques, psychophysics, and computational modelling. We identify brain regions involved in the accumulation of sensory evidence and the pathway by which this information is relayed across the brain to inform decisions. Chapter 3 examines perceptual decisions at a faster timescale, parsing neural signals within a trial that may contribute to different decision parameters. We further test whether an endogenous urgency signal may affect observed behaviour and captured neural signals. Chapter 4 focuses on how latent brain connectivity may modulate and shape perceptual decisions. We compare and contrast brain connectivity at rest to that during a task, and ask how this may be affected by task demands. Finally, Chapter 5 discusses the overall findings, limitations, and possible future directions of the present thesis.

Contribution of Authors

This thesis integrates original research from three manuscripts of which I am the primary author:

Study 1 (Chapter 2):

Yau, Y.H.C., Dadar, M., Taylor., M., Zeighami., Y., Fellows., L.K.., Cisek, P., & Dagher, A. Neural correlates of evidence and urgency during human perceptual decision-making in dynamically changing conditions.

Contributions: YY and AD designed research; YY and MT collected the data; YY, MD, and YZ analyzed the data and contributed methods; and YY, AD, LF, and PC contributed to result interpretation. YY drafted the initial manuscript; all authors contributed to writing of manuscript.

Study 2 (Chapter 3):

Yau, Y.H.C., Hinault, T., Taylor, M., Fellows, L.K. & Dagher, A. Disentangling the neural decision parameters involved in perceptual decisions in humans.

Contributions: YY, LF, and AD designed research; YY and MT collected the data; YY analyzed the data and contributed methods; and YY, TH, LF, and AD contributed to results interpretation. YY drafted the initial manuscript; all authors contributed to writing of manuscript.

Study 3 (Chapter 4):

Yau, Y.H.C., Morys, F., Fellows, L.K. & Dagher., A. Dynamics of brain connectivity at rest constrains performance in task.

Contributions: YY and AD designed research; YY collected the data; YY and FM analyzed the data and contributed methods; and YY, LF, and AD contributed to results interpretation. YY drafted the initial manuscript; all authors contributed to writing of manuscript.

For completeness, I have also co-authored several other papers and textbook chapters during my doctoral studies. These include published work regarding cognitive disruptions and related topics in Parkinson's disease (Dadar et al., 2018; Tremblay et al., accepted; Yau et al., 2018; Zheng et al., 2019), schizophrenia (Kirschner et al., 2020), obesity (Michaud et al., 2020; Neseliler et al., 2018), and addiction (Banz et al., 2016; Benady-Chorney et al., 2020; Benady-Chorney et al., 2018; Cox et al., 2017; Foster et al., 2015; Mei et al., 2016; Yau & Potenza, 2015; Yau et al., 2015).

List of Abbreviations and Acronyms

BOLD	Blood Oxygen Level-Dependent
CPP	Centroparietal Positivity
DDM	Drift Diffusion Model
DIC	Deviance Information Criterion
DMN	Default Mode Network
EEG	Electroencephalography
ERP	Event-related Potential
FC	Functional Connectivity
fMRI	Functional Magnetic Resonance Imaging
FWE	Familywise Error
GLM	General Linear Model
gPPI	Generalized Psychophysiological-Interaction
HDDM	Hierarchical Drift Diffusion Model
ICA	Independent Component Analysis
ICs	Independent Components
LIP	Lateral Intraparietal Area
MNI	Montreal Neurological Institute
MVPA	Multivariate Pattern Analysis
nDDM	Non-hierarchical Drift Diffusion Model
rs-fMRI	Resting-State Functional Magnetic Resonance Imaging
RSNs	Resting-State Networks
RT	Reaction Time
SVM	Support Vector Machine-leaning
tvFC	Time-Varying Functional Connectivity
UGM	Urgency Gating Model

List of Figures

CHAPTER 1. Introduction

Imagine you are hiking in the forest and it starts to rain. You notice a blurry figure on the trek ahead; as you step closer, you realize that it's a bear possibly heading in your direction. You remember the old saying: "If it's brown, lay down. If it's black, fight back". Due to the poor light and rain, it is hard to decipher how far away the bear is, which exact direction it's heading in, let alone whether it has brown or black fur. However, you will eventually commit to an action: lay down on the ground or make loud noises to scare the bear away. Importantly, as the bear approaches you, there is an increasing urgency to commit to a choice. How much information do you need to make such a perceptual decision and how sure do you have to be to act upon it? The process by which the available sensory information is gathered and used to influence how we behave in the world is commonly referred to as "perceptual decision-making" (Heekeren et al., 2008; Shadlen & Kiani, 2013). On the one hand, making the decision too slowly runs the risk of being mauled by the bear. On the other hand, acting prematurely before collecting enough information for your decision also runs the risk of being mauled by the bear. Though this is an oversimplified example of perceptual decisions, it exemplifies the need for the brain to coordinate between perception and action to yield a rapid yet accurate behavioural response.

Over the past two decades, understanding how perceptual decisions are made has become a central theme in neuroscientific research. Both neurophysiological studies in monkeys and functional neuroimaging methods in humans have contributed to our further understanding of the neurobiology underpinning decisions. More recently, advances in the range of available methodologies, paradigms, and computational tools have dramatically broadened and a number of studies – including the original research in this thesis – have attempted to exploit these approaches to better understand how perceptual decisions are shaped and formed.

1.1. Studying Perceptual Decision-Making

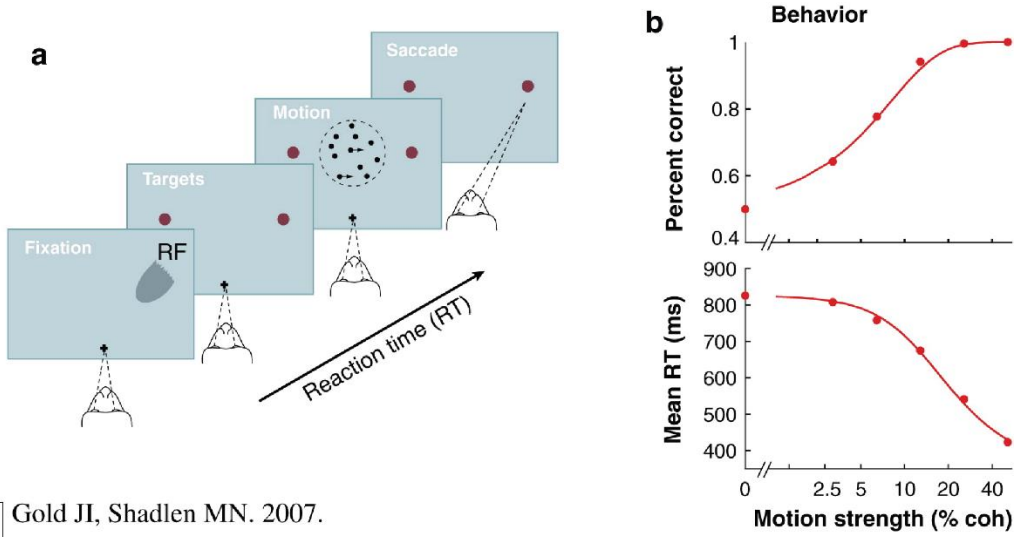

Gold JI, Shadlen MN. 2007.
Annu. Rev. Neurosci. 30:535–74

Fig. 1.1. *Random dot motion task.* ***(a)*** *Overview of the random dot motion task. Subjects view a patch of random dots and decides the net direction of motion; decision is indicated by a saccade to a peripheral.* ***(b)*** *Effect of motion strength (i.e., percentage of dots moving in a coherent direction) on accuracy and reaction time (RT). Original figure adapted with permission from Gold and Shadlen (2007).*

Much of what we have learned about perceptual decisions comes from laboratory tasks in which subjects are asked to make fast two-choice decisions. These tasks allow researchers to control the nature and quality of sensory input variables in the decision environment, and to reward the animal for specific sensorimotor behaviours. In particular, the random dot motion task (Fig 1.1A) has served as a cornerstone for how we understand neural contributions to perceptual decision-making (Newsome et al., 1989). In a given trial, monkeys are presented a random pattern of moving dots where most, but not necessarily all, of the dots move coherently in one direction. The monkey is then typically rewarded for making a saccade to a target corresponding to the direction of the coherent motion. The percentage of coherently moving dots can be adjusted to manipulate the amount of sensory noise in the decision environment, and consequently, manipulate the task difficulty. When information quality is low (for example, when most dots move randomly and only some move in a coherent direction), decisions can be optimized by repeatedly sampling sensory information and

integrating the resulting direction estimates over time. Although this task is a severe reduction of the complexity of how our brain performs in a naturalistic and dynamic environment, it has provided an avenue for researchers to investigate the neural mechanisms of perceptual decision-making, resulting in a wealth of insights (Gold & Shadlen, 2007).

Progress in our understanding of the neural mechanisms underlying decision-making comes, in large part, from the development of computational models of decision-making. These models provide a framework to infer latent psychological processes underlying the decision process, and to link them to neural mechanisms. They are based on the notion that observed behaviour, such as reaction time (RT) and accuracy, can be decomposed into latent processes that can not be directly observed. One family of models – here referred to with the umbrella term "evidence accumulation models" – has emerged as canon in describing choice behaviour (Ratcliff et al., 2016). Though many variations are available today (for review: Evans & Wagenmakers, 2019; Ratcliff et al., 2016), they all share the common assumption that a decision between two alternatives is based on an integrative mechanism in which information supporting each alternative accumulates over time until an internal decision bound is reached by a "decision variable". This decision variable is a level of representation that can be dissociated from sensory processing of evidence and motor planning. It is thought to integrate sensory evidence, as well as potentially incorporating other signals related to value, time, and prior probability. The decision variable is used by neurons that sense thresholds and calculate certainty to then trigger a decision that is usually executed through movement (Shadlen & Kiani, 2013). In this thesis, we will focus on the standard evidence accumulation model, namely the drift diffusion model (DDM).

1.2. The Drift Diffusion Model

The DDM (Fig. 1.1B) is a parsimonious model that posits the difference in evidence accrued for two choice alternatives is represented by a biased random walk process, the speed of which is captured by the drift rate (v) parameter. Decisions are made once the random walk hits one of

two critical decision thresholds (*a*). The starting point of this random walk may be biased (*z*) towards one choice alternative and begins after a period of non-decision time (*t*) for stimulus encoding and response execution latencies. The observed response time results from a combination of these four parameters. How the different decision parameters are adjusted is dependent on the shape of the RT distribution (Ratcliff et al., 2016). The DDM has had much success in describing and predicting choice behaviour in paradigms such as the random dot motion task (Ratcliff et al., 2016). Moreover, the DDM has been adopted by the neuroscientific community as an intermediary level between the observed behavioural data and its underlying neuronal substrate (Fig. 1.2A). For example, the mean firing patterns of single neurons in the lateral intraparietal cortex (LIP) of non-human primates, has been shown to mirror the drift rate estimated by the DDM (e.g., Gold & Shadlen, 2007; Roitman & Shadlen, 2002).

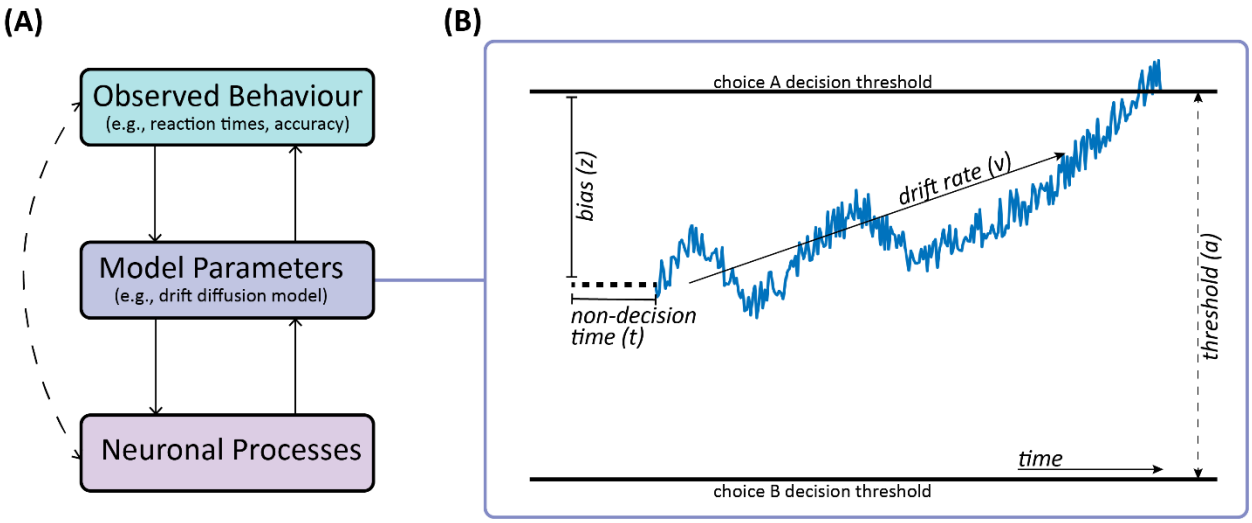

Fig. 1.2. *Computational models as a middle ground in observations.* ***(A)*** *Model parameters from computational models can serve as an intermediary level to help bridge observed behaviour with neuronal processes.* ***(B)*** *Overview of the drift diffusion model. The model is one of the most commonly used evidence accumulation model that decomposes behavioural data into four parameters: non-decision time (t) for stimulus encoding and response execution latencies, bias (z) towards one choice alternative, drift rate (v) for speed of evidence accumulation, and decision threshold (a) which determines how much evidence is needed before a decision is reached.*

1.2.1. Bayesian Estimation of the Drift Diffusion Model

One issue with computational models, such as the DDM, is that it can require a high number of trials to accurately estimate model parameters. While this is less problematic in non-human primates where animals can be incentivized to partake in thousands of repeated trials, this is difficult to achieve with human participants where there are typically substantial constraints on the duration of the task. As such, there is a need for an efficient and reliable estimation method despite the relatively small number of trials. Hierarchical Bayesian data analytic methods may provide a potential remedy to this problem.

Bayesian analytics are quickly gaining popularity in the cognitive sciences (Lee & Wagenmakers, 2013). In brief, the general principle of Bayesian analysis is that observed data are used to update the *prior* information to become *posterior* information. Uncertainty, or "degree of belief", of the value of a parameter is expressed as a probability distribution called the "prior distribution". Without any knowledge about what the value of the parameter might be, equal probability is assigned to every possible value of the parameter. Observed data can then be used to update the prior belief. This is described by the "posterior distribution" which quantifies the relative probability that each possible value of the parameter is the true value. With more sampling and new information provided by the observed data, uncertainty of the parameter's value can be reduced and the posterior distribution narrows.

There are three main advantages motivating the use of Bayesian estimation. First, compared to traditional frequentist approaches, Bayesian methods provide inference for the full posterior distribution of each parameter by quantifying uncertainty in their estimation, rather than simply providing the one most likely value of each parameter. Second, Bayesian analytics allows for the natural implementation of hierarchical models. Traditionally, psychological experimenters either fit models separately to each individual, thus assuming that subjects are completely independent of one another, or fit one model to the group, thus assuming all subjects are the same. Both approaches are sub-optimal in model parameter estimation: the former fails to capitalize on the statistical strength shared across individuals should one or more parameter be similar among subjects, whereas the latter approach fails to account for

individual differences and can result in situations where the estimated model cannot accurately fit any one subject. Hierarchical Bayesian methods circumvent these problems by allowing both group and subject parameters to be estimated simultaneously in a hierarchical manner (Kruschke, 2010), with the posterior distribution for any given subject constrained by the group distribution, and *vice versa*. Third, and perhaps most importantly, the statistical power gained by implementing a hierarchical Bayesian model can help overcome limitations of low number of trials. Hierarchical Bayesian estimations of the DDM have been shown to more robustly estimate DDM parameters, including regression effects of trial-by-trial variations of neural signals on decision parameters (Matzke & Wagenmakers, 2009; Wiecki et al., 2013).

Bayesian analysis, however, remains intensively computationally demanding. The fundamental reason for this is that models associated with coalescent data must integrate over trees of high complexity to form a convergent model. Though Bayesian estimations can still take days of computer time to execute, rapid growth in computation power and the availability of packages implementing approximation tools at higher efficiency (e.g., Markov Chain Monte Carlo approximation using PyMC in Python (Salvatier et al., 2016)) have helped improved usability.

1.3. Putative Neural Correlates of a Decision Variable

An important question remains: where in the brain should we look to find a decision variable? To understand how decisions are made in the brain requires some familiarity with the brain structures involved in decision-making and their organization; the details of this are the subject of entire textbooks. Here, I provide a brief and highly selective review of the putative neural basis of perceptual decisions most relevant to the original research presented later in this thesis.

In brief, the neural architecture for perceptual decision-making can be thought of as four distinct, but interacting, processing modules that contribute to forming a decision variable (for review: Heekeren et al., 2008). The first is a *sensory system* that computes, accumulates, and compares sensory evidence. The second is a *decision system* that integrates stimulus

representation, detects perceptual uncertainty or difficulty, and signals when additional resources are required to accurately process a task. The third is the *motor system* which prepares and executes an action based on the decision variable. The fourth involves the *performance monitoring system*, which updates future decisions strategies when it detects errors have occurred. Brain regions related to these four systems are thought to constantly interact as information moves from occipital to motor areas, with decisions emerging from a competition between relevant motor outputs (Cisek, 2007; however, see Tversky & Kahneman, 1981 for competing view). In particular, regions of the sensory and decision system have been targeted in attempts to decode a decision variable.

Our understanding of perceptual decisions comes, in large part, from neurophysiological studies in non-human primates using paradigms like the random dot motion task. The use of such visual discrimination tasks are apt choices given that the neural circuits underlying the visual system are among the best understood in the primate brain. According to the "affordance competition hypothesis" (Cisek, 2007), action specification begins in the visual cortex and proceeds toward the parietal lobe, transforming visual information into representation of potential actions (Fig. 1.3). This follows the conventional "dorsal stream" of the visual processing pathway involved with spatial information, as opposed to the parallel "ventral stream" involved in object identification (Ungerleider et al., 1982). Neural populations along the dorsal stream are thought to reflect a mixture of sensory, motor, and cognitive information – thus resembling a decision variable. They are subject to modulation by attentional selection, whereby information from certain regions of interest is enhanced while information from other regions is suppressed.

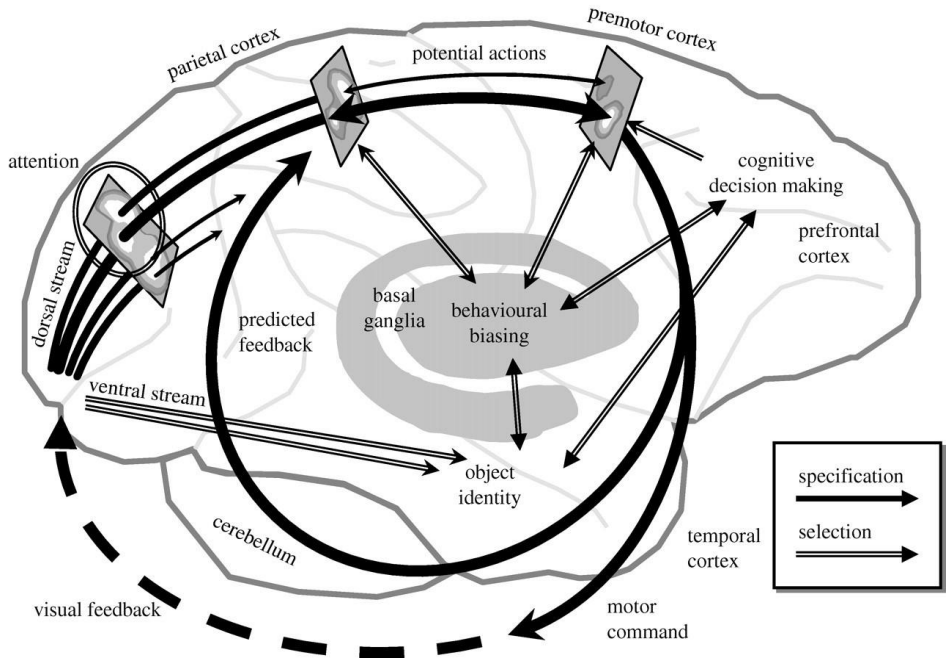

Fig. 1.3. *Sketch of the proposed neural substrates in the primate brain underpinning goal-directed, visually guided behaviours. Solid-lined arrows reflect pathways of action specification (i.e., how to do it) whereas double-lined arrows reflect pathways of action selection (i.e., what to do). Original figure reproduced with permission from Cisek (2007).*

Building on the computational framework for understanding decision-making, the neural mechanisms underlying perceptual choices have been extensively studied in the macaque monkey using extracellular recordings from single neurons. It is commonly assumed that firing rates of suspected accumulator-neurons reach a fixed threshold near the time of behavioural response, suggesting that the critical level needed for decision commitment is close to the peak firing rate. There have been attempts to locate "accumulator regions" where neurons may present this type of firing pattern, with research focused on cortical neurons that encode task-relevant sensory signals. In non-human primates, one part of the parietal cortex, namely the LIP, has received particular interest due to its direct projections to eye movement-related areas (Andersen et al., 1990) and connections to visual cortical areas of the dorsal and ventral visual stream (Lewis & Van Essen, 2000). The LIP has spatially-defined receptive fields that receive inputs from the middle temporal visual (MT) area where motion direction in the random dot motion task is encoded (Britten et al., 1993). Single-cell recordings found that populations of neurons in the LIP exhibit a gradual modulation of their firing rates – depending on the

direction and strength of the sensory evidence – in advance of a response. Thus, LIP neurons are thought to integrate signals from direction-selective neurons in lower visual areas (e.g., area MT) (Hanks et al., 2006; Shadlen & Newsome, 2001), and may therefore compute an integrating decision variable. Such neuronal activity is not purely motor-related since its time course varies systemically with the signal to noise ratio (i.e., coherency of the dots) even though the saccadic motor output remains the same. This line of work from non-human primates has provided compelling evidence that LIP neurons – or at least a subset of them – encode the cumulative sum of sensory information, in close correspondence to the DDM's drift rate parameter. This information is then used to promote a saccade towards a given spatial target.

It must be noted that recent work has challenged the notion that neuronal firing in the LIP directly encodes a decision variable posited to govern perceptual decisions. Katz et al. (2016) found that pharmacological inactivation of the LIP in rhesus macaques had no measurable impact on decision-making performance during the random dot motion task. Moreover, it is likely that LIP is one of many areas that represent a decision variable and that where such a signal might arise in the brain may depend upon the sensory stimuli used (e.g., motion direction, color, object) and the type of response executed (e.g., saccades, button-press). For example, the medial intraparietal area has been implicated in arm-reaching actions (de Lafuente et al., 2015; Swaminathan et al., 2013) and the premotor cortex in manual choices (Cisek & Kalaska, 2005). Nonetheless, convergent lines of evidence broadly suggest that decision variables can be detected in the monkey brain, primarily in the frontal and parietal cortex, provoking attempts to find human analogues.

Regions of the fronto-parietal network are not the only ones involved in perceptual decision-making. The competition between potential actions is thought to be biased by a multitude of regions that collect information for action selection, including input from regions of the ventral stream encoding stimulus features, as well as the basal ganglia and prefrontal cortex. Since action selection is a fundamental problem across vertebrates, the neural structures involved are likely conserved in evolution with the basal ganglia having emerged as a potential

candidate. The basal ganglia are a collection of subcortical nuclei that, as a whole, are thought to be involved in a central gating mechanism. While the cortex generates ensembles of possible choice alternatives, the basal ganglia selects among these alternatives by activating specific downstream circuits either promoting or suppressing behavioral response for each choice (Frank et al., 2007; Lo & Wang, 2006). This has motivated recent neuro-computational models to test the role of the basal ganglia in perceptual decisions, and their results lend credence to the basal ganglia's involvement in shaping the decision variable (Bogacz & Gurney, 2007; Ding & Gold, 2012; Thura & Cisek, 2017). Other brain structures, such as the prefrontal cortex of primates, are also likely involved in action selection. For example, neurons in the dorsolateral prefrontal cortex are sensitive to various combinations of stimulus features, and this sensitivity relates to the difficulty of task demands (Bechara et al., 1998; Heekeren et al., 2004; Kim & Shadlen, 1999). The dorsolateral prefrontal cortex is thought to establish the task set or the current goal, to link the sensory evidence accrued to a behavioural plan for action execution, and to signal the need for additional resources when sensory information is noisy. This is, of course, a very simplified account of how action selection is achieved but nonetheless provides us with a foundation to understand how and where decisions may be formed in the brain.

1.4. An Alternative: The Urgency Gating Model

Inspired by a marriage of computational modelling and neural recording (predominantly in non-human primates), the theory that neurons in the sensorimotor areas contribute to perceptual decisions by optimizing input signals through repeated sequential sampling and linear integration to a fixed decision threshold has been canonized in how cognitive neuroscientists view perception decisions. This line of work exemplifies the benefits of convergent mathematical and biological approaches in understanding brain function. However, outstanding issues with the DDM must be addressed. While pioneering studies and their subsequent work have largely been based on manipulating the reliability of sensory signals (e.g., level of motion coherence) by means of simple, well-controlled experimental designs

(e.g., random dot motion task), our natural interactive environment can change without warning. Decisions made in these unpredictable environments often do not allow one to stop, think, and collect a complete picture of one's surroundings. Even without time constraints, when sensory information is low, further sampling is unlikely to be informative for choice commitment. Despite this, we still observe individuals making a decision (i.e., a guess) in such settings, albeit taking longer to do it. This challenges the notion that an integrating decision variable can achieve a fixed critical threshold for decisions based solely on sensory evidence. Optimal models thus predict that the height of the decision threshold should "collapse" over time, such that less sensory evidence is required for decision commitment as elapsed decision time increases (Bowman et al., 2012; Drugowitsch et al., 2012; for opposing view: Hawkins et al., 2015). However, the empirical question of whether decisions about signals with unknown reliability respect a collapsing bounding algorithmically, and how this might be implemented by neurons, remains unknown.

One emerging view is that decisions may be driven to the critical threshold by an evidence-independent quantity referred to as an "urgency" signal. This signal is thought to ubiquitously elevate activity towards unchanged thresholds, which effectively implements a collapsing bound by inflating later accumulators states away from the starting baseline (Cisek et al., 2009; Murphy et al., 2016; Thura & Cisek, 2014). One line of evidence for such a signal can be observed by analyzing trials on which sensory evidence is entirely ambiguous (e.g., 0% motion coherence), where firing rates in LIP nevertheless grow towards the threshold associated with the eventual response (Churchland et al., 2008). Moreover, fitting a computational model (i.e., urgency gating model) with an evidence-independent, time-variant influence on the decision variable appears to better reflect the firing rate of LIP neurons at different levels of coherency in the random dot motion task (Ditterich, 2006; Standage et al., 2011). This urgency signal may be particularly enhanced when subjects are asked to emphasize speed over accuracy (Hanks et al., 2014; Heitz & Schall, 2012).

Carland et al. (2019) argue that urgency provides a central underlying mechanism by which multiple aspects of behaviour are jointly coordinated. Individual variability in the baseline level

of this signal may constitute an individual trait. This is driven by the notion that baseline urgency appears to be stable across time and context (Berret et al., 2018; Reppert et al., 2018). They argue that individual variability in urgency may provide a mechanistic link between decision-making and the behavioural manifestations of broader personality traits, such as impulsivity. Conceptually, the behavioural profile of an individual with relatively high "trait" level of urgency is broadly consistent with the behavioural trait of impulsivity, defined as tendency to act rapidly with undue consideration of consequence (Voon, 2014) or to exhibit disinhibition of prepotent responses (Choi et al., 2014). The trait of impulsivity itself has strong etiological ties to a variety of clinical psychopathologies, including substance use disorders, gambling disorder, attention deficit hyperactivity disorder, and disordered eating (Chamberlain & Sahakian, 2007; Fineberg et al., 2014; Schag et al., 2013). By extension, deviations from a "normative" trait urgency may confer increased vulnerabilities to these conditions. Moreover, the DDM has been used to infer disrupted cognitive mechanisms in a host of neurological and psychiatric disorders (Banca et al., 2015; Pedersen et al., 2017; White et al., 2010). If urgency is indeed a closer representation of the ground-truth in how decisions are formed, we must revisit the interpretations of these previous findings.

Where in the brain may an urgency signal arise? The notion of urgency ties closely to action selection during decision formation. The dynamic nature of action selection and speed-accuracy trade-off has been tested using the "tokens task" (Cisek et al., 2009; Thura et al., 2012). In each trial, tokens gradually move from a center circle to another circle on either the left or right. Subjects must decide based on these constantly changing sensory evidence which circle will ultimately have the greatest number of tokens. The timing of how the tokens moved was manipulated between different blocks of trials to encourage either slow and accurate or fast and risky decisions. It was found that as time passed, less evidence was needed to commit to a choice, in agreement with the proposed urgency gating hypothesis. Moreover, early decisions (typically made on the basis of strong evidence) were associated with reduced vigour in the movement the animals used to make their decisions, whereas later decisions (relying on weak sensory evidence but high urgency) were associated with greater vigour (Thura & Cisek, 2014). The authors interpreted this as resulting from a global influence of the urgency signal

during both decision and action. They argue this link between decision urgency and movement vigour points to the potential involvement of the basal ganglia, a region known to be involved in motor control (Jueptner & Weiller, 1998; Maia & Frank, 2011).

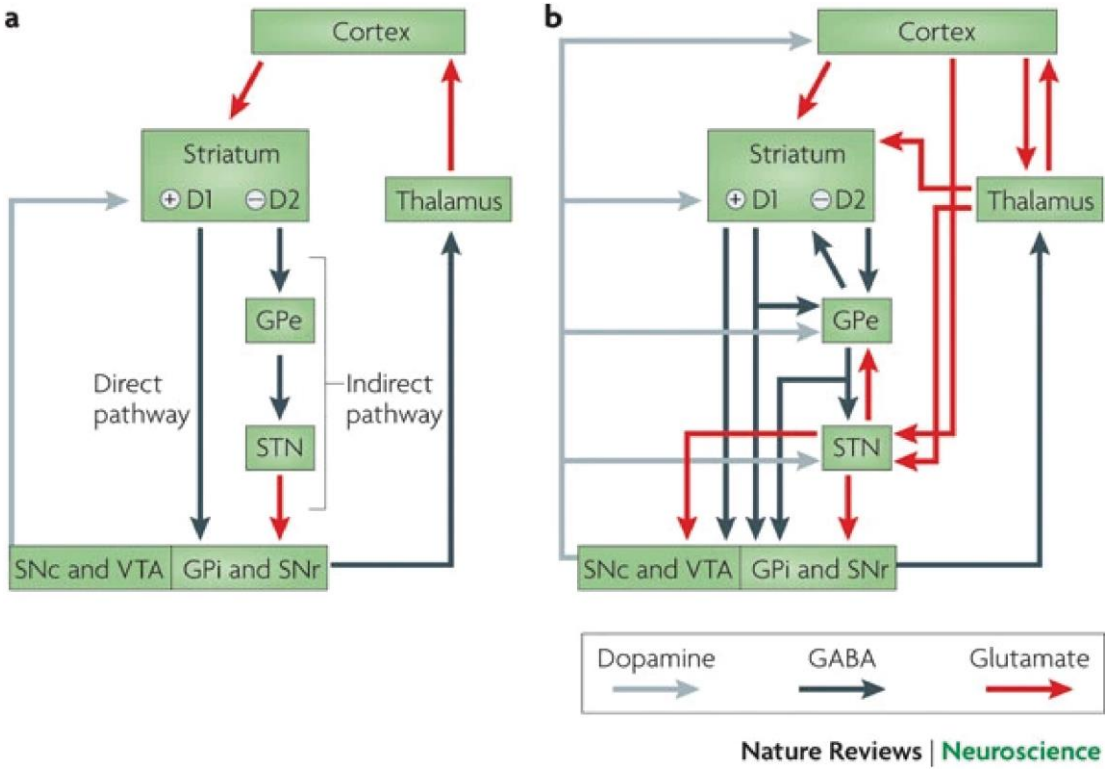

Fig. 1.4. *Overview of basal ganglia's pathways.* ***(a)*** *Output of the basal ganglia is determined by the balance between the direct and indirect pathway.* ***(b)*** *Anatomical investigations suggest a more complex organization. GPe: globus pallidus pars externa; GPi: globus pallidus pars interna; SNr : substantia nigra pars reticular; SNc : substantia nigra pars compacta; STN : subthalamic nucleus. Original figure reproducted with permission from Redgrave et al. (2010)*

The basal ganglia are a collection of subcortical nuclei that are interconnected with the cerebral cortex through a series of loops (Fig. 1.4). The input structures are together called the striatum (including the caudate, putamen, and ventral striatum), and receive direct projections from the cerebral cortex. The output structures are together called the pallidum (including global pallidus pars interna, substantia nigra pars reticulata, and ventral pallidum), which project to the brainstem movement generators, as well as back to the cerebral cortex via the thalamus. Intrinsic nuclei (including globus pallidus pars externa, the substantia nigra pars compacta, and subthalamic nucleus) activate and regulate these input-output regions. The model of action

selection in the basal ganglia proposes that the cortex generates ensembles of possible actions, and the striatum selects among these actions by activating specific downstream circuits that either promote or suppress movements. More specifically, Bogacz and Gurney (2007) proposed that the striatum is involved in estimating the conditional probabilities of multiple hypotheses being true given the sensory stimuli. According to this model, these probabilities are relayed by the direct dopaminergic pathway from the striatum to the pallidal output neurons. The indirect dopaminergic pathway, in which cortical inputs are further processed in the interconnected intrinsic nuclei, gathers information related to all alternatives and inhibits the output to the thalamus until enough information is accumulated. In sum, the basal ganglia are proposed to be involved in encoding certain actions, and facilitating the appropriate behavioural response for the choice alternative with the most supporting evidence by suppressing alternative signals via its dopaminergic projections to the indirect pathway (Frank et al., 2007; Lo & Wang, 2006).

Though the basal ganglia are perhaps best known for their role in motor output, they are also involved in sensory information processing (Ding & Gold, 2012; Forstmann et al., 2010; Nagano-Saito et al., 2012). They provide an indirect link between cortical (e.g., LIP and frontal eye field) and brainstem (e.g., superior colliculus) structures that encode evidence accumulation for saccadic decisions, thus influencing evidence accumulation, evaluation, and choice bias during the random dot motion task (Ding & Gold, 2010). The basal ganglia's influence likely extends beyond saccadic movements: a meta-analysis of fMRI studies investigating an array of simple perceptual decision-making tasks concluded that the basal ganglia broadcasts widely throughout the cortex, and complements the fronto-parietal network involved in general perceptual decision-making by serving as a gating mechanism (Keuken et al., 2014). Thura and Cisek (2017) recorded pallidal activity in monkeys, and found that pallidal firing rate did not contribute to evidence accumulation, and instead reflected a temporally growing urgency signal to commit to a choice. Other studies argue for the involvement of the subthalamic nucleus in task-switching or in mediating the decision threshold under stimulus conflict (Cavanagh et al., 2011a; Mansfield et al., 2011). Taken together, these results points towards the involvement of subcortical brain structures in several aspects of perceptual decision-making and perhaps in urgency; however, this latter relationship is debated and has yet to be established in humans.

While the interesting notion of an urgency neural signal controlling the timing of decisions may better explain observed behaviour, it remains controversial and is challenged on numerous grounds (Voskuilen et al., 2016; Winkel et al., 2014). For example, the performance of highly trained monkeys was better captured by a dynamic collapsing bound, whereas humans performing a limited number of trials were best described by a fixed decision threshold (Hawkins et al., 2015). Conversely, Thura et al. (2012) argue that standard psychophysiological tasks, such as the random dot motion task, where evidence is constant, cannot disambiguate drift rate or threshold from urgency. To tease these parameters apart, one must manipulate the dynamics of information presented. If one were to gradually raise the amount of sensory information available over time, a pure evidence accumulation model would predict that the decision variable should almost perfectly track the slope of this increase. An urgency gating model would instead predict that the decision variable should rise above and beyond the sensory information available, with signals deviating further from the raw sensory information and more towards threshold as time goes by, resulting in a non-linear decision variable. Further testing with these dynamic tasks is needed in order to conclude whether an evidence-independent urgency signal exists and to expose its potential neural underpinnings; this line of work in naïve (i.e., untrained) human subjects is particularly lacking and we attempt to bridge this gap with the research conducted in this thesis.

1.5. Of Monkeys and Men? Neural Decision Signals in Humans

Perceptual decisions have largely been probed by neurophysiological studies in non-human primates. However, the often-cited evidence from single-cell recordings is not unequivocal and complimentary data from human subjects are largely missing. Studying decision-making in humans is important because: (i) the neural underpinnings may differ between humans and over-trained animals, (ii) complex decision-making behaviour can be examined more feasibly in humans, and (iii) the advances in animal neurophysiology need to be bridged to humans in order to improve understanding of cognitive disruptions in psychiatric and neurological disorders. Here, I will briefly discuss some of the recent functional neuroimaging studies that

shed light into how decisions may unfold in the human brain. Of note, most studies have primarily focused on action specification and fronto-parietal regions that may demonstrate a decision variable, or on lower-level sensory processing regions that may encode sensory information, and have largely neglected the role of action selection in decision-making.

1.5.1. Finding a Decision Variable using Functional Magnetic Resonance Imaging

Functional magnetic resonance imaging (fMRI) is a key non-invasive neuroimaging methodology that allows for the localization of discrete brain structures involved in decision-making with millimetre-level precision. fMRI analysis is based on the assumption that neuronal activity is reflected by the blood oxygen level-dependent (BOLD) signal (Kwong et al., 1992; Ogawa et al., 1990a; Ogawa et al., 1990b). Neurons do not have internal energy reserves (i.e., sugar and oxygen) and thus require energy to be conveyed to them when active. Through a process called the haemodynamic response, blood carries and releases oxygen to active neurons at a greater rate than to inactive neurons. Importantly, neuronal activity leads to increased cerebral blood flow that exceeds the needs of the active neurons; therefore, blood oxygen level (carried by oxyhaemoglobin) goes up when neurons are more active. This changes the relative level of oxy- and deoxy-haemoglobin, of which the former is diamagnetic and the latter paramagnetic. The difference in magnetic susceptibility can then be detected using MRI. The onset of stimulus-induced haemodynamic response is typically delayed by roughly 2 seconds due to the time it takes blood to travel from arteries to capillaries and draining veins (Kwong et al., 1992). The signal then reaches a plateau 6-12 seconds after stimulus onset, returning to baseline with a similar ramp, and is followed by a post-stimulus undershoot (Logothetis et al., 1999). Algorithms can be used to convolve raw BOLD signals to this haemodynamic response, regressing out its effect, thus allowing researchers to examine task-dependent changes in the BOLD signal (Friston et al., 1994; Henson & Friston, 2007). Nonetheless, due partly to the nature of blood flow and partly to methodological constraints, fMRI BOLD responses generally have a relatively poor temporal resolution with sampling or repetition time often in the order of seconds.

Typically, researchers have looked for correlations between BOLD signal within certain voxels and fitted values of drift rate or other model parameters of the DDM. However, a single voxel in fMRI can reflect the aggregated activity of tens of thousands of neurons. Unlike the aforementioned animal neurophysiology studies, neural selectivity to sensory decision variables (e.g., motion direction) in paradigms such as the random dot motion task is indistinguishable by fMRI. Moreover, the sluggish nature of BOLD response makes it difficult to distinguish neural signals that occur before, during, or after a decision. Consequently, previous studies have often failed to dissociate sensory evidence from decision variables (Braunlich & Seger, 2016; Gluth et al., 2012; Nagano-Saito et al., 2012; Wheeler et al., 2015b) unless they artificially elongate task design to tens of seconds long (Ploran et al., 2007). A potential solution has been to devise visual discrimination tasks where choice stimuli preferentially activate different clusters of voxels along the ventral stream of the visual pathway using stimuli like faces and houses for example (e.g., Heekeren et al., 2004). Akin to firing rate in sensory regions (e.g., MT area in non-human primates), BOLD signal in these regions is thought to scale with the relative strength of evidence for each choice alternative. It is argued that the decision variable represents the temporal integration of the sensory evidence and should therefore highly correlate with the evidence itself. Thus, one approach has been to search for brain regions whose BOLD activity covary with the difference in relative BOLD signal in these extrastriate areas, in line with the assumption that the decision variable is a cumulative differential of sensory inputs. Moreover, studies often use conditions of high versus low sensory evidence to conclude, based on this contrast, where a decision variable might be formed in the brain (Fig. 1.5).

There is yet to be a consensus about how perceptual evidence accumulation is expressed in fMRI signal (for review: Mulder et al., 2014). On the one hand, it is hypothesized that evidence accumulation models should predict a *positive* correlation between sensory evidence and BOLD activity: the larger the discriminability between stimuli (likely reflecting higher drift rate), the larger the BOLD response. This hypothesis is derived from the idea that the computation of a decision variable requires a comparison of two or more neuronal populations whose activity reflects the accumulated sensory evidence in support of different options. Thus, on easier

trials, where there is clearer sensory evidence in support of one option, the activity in a decision-making area is predicted to demonstrate greater integrated activity and reach threshold faster. This fits with what is observed in the LIP area of non-human primates (Gold & Shadlen, 2007; Shadlen & Newsome, 1996). Indeed, in one of the first studies to interpret their fMRI findings in light of the DDM, Heekeren et al. (2004) reported that BOLD response in the dorsolateral prefrontal cortex not only covaried with the difference between signals of face- and house-selective regions, but also demonstrated greater activity for trials with high compared to low sensory evidence (Fig. 1.5). Similar findings have been observed in several other higher-level, fronto-parietal brain regions in subsequent work (Tosoni et al., 2008; White et al., 2012). These findings are contingent on the assumption that a decision variable remains elevated after reaching threshold until some fixed post-stimulus time, thus spending longer time at a high level for an earlier threshold crossing. If BOLD activity mirrors the decision variable, heightened BOLD activity should be maintained temporarily post-decision before subsiding, resulting in a greater overall BOLD signal for easier trials despite their faster reaction time.

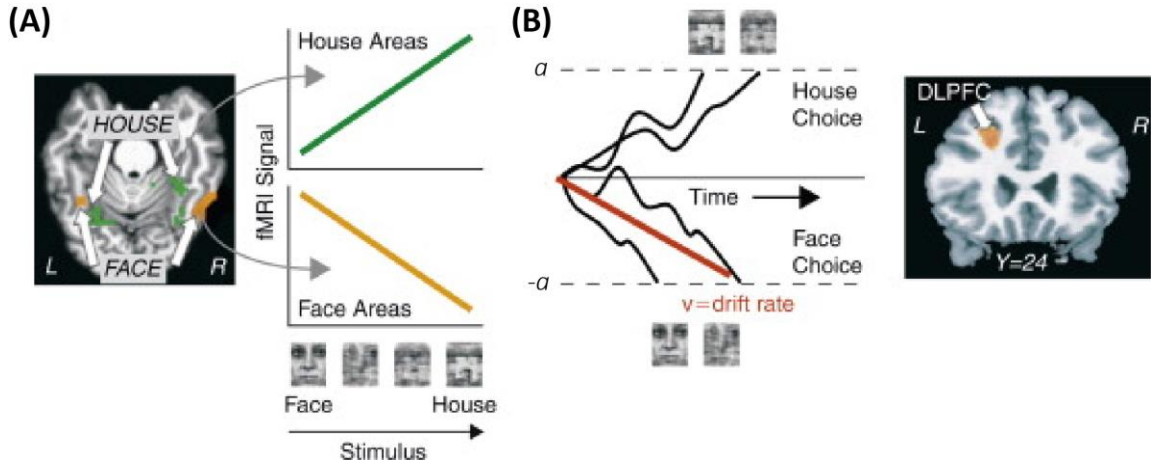

Fig. 1.5. *Example of a fMRI study of perceptual decisions.* ***(A)*** *BOLD activity in face- and house-selective brain regions is thought to scale with the level of sensory evidence.* ***(B)*** *It is argued that a higher-level brain region (i.e., dorsolateral prefrontal cortex) may represent a decision variable that integrates sensory evidence from lower-level sensory processing areas as (i) BOLD signal in this region covaried with the difference between signals of face- and house-selective regions, and (ii) demonstrated greater activity with clearer images of faces/houses when*

comparing high versus low sensory evidence. Original figure adapted with permission from Philiastides and Heekeren (2009); results based on work from Heekeren et al. (2004).

On the other hand, a competing hypothesis is that evidence accumulation models should predict a *negative* correlation between sensory evidence and BOLD activity. It is assumed the decision variable falls immediately to baseline upon reaching threshold, and the buildup in neuronal firing (although shallower) is more prolonged for slower responses. Thus, BOLD signal is summed across multiple samples or repetition times, and results in a greater overall signal. Moreover, during difficult decisions with low sensory information, there is thought to be a greater need to amplify choice-relevant information to overcome competing noise/information for successful computation of a decision variable. Findings in line with this hypothesis also implicated fronto-parietal brain regions, along with regions of the ventral stream that are thought to be involved in encoding sensory information, such as the fusiform gyrus (Ho et al., 2009; Liu & Pleskac, 2011; Noppeney et al., 2010).

A fundamental question in cognitive neuroscience deals with the issue of representation: what, how, and where in the brain is different information represented? How is this information transformed at different stages of processing? Though most fMRI studies have broadly concluded that the fronto-parietal network is likely *where* the decision variable is computed, there is conflicting accounts as to *how* a decision variable driving perceptual decisions in humans should relate to the BOLD response. Moreover, we may not be accurately measuring *what* is accumulated in the brain. Most studies assume that activations scaling with discrimination difficulty in sensory areas appropriate to the modality of discrimination (e.g., face or house) equate to sensory evidence. However, not all neural signals that appear to vary as a function of task-relevant stimulus features are necessarily read out by downstream systems controlling behaviour (Williams et al., 2007). As such, we cannot definitively conclude that the BOLD signal detected in these studies constitute the sensory evidence that the brain then exploits to form a decision variable. Taken together, fMRI can help elucidate neural mechanisms underpinning human perceptual decisions and early work has shown promising results, but many questions remain.

1.5.2. Decoding Sensory Evidence using Multivariate Pattern Analysis

Here, I will briefly detail an alternative approach to disentangling sensory accumulation from decision variable using fMRI. We have discussed above how exploiting extrastriate regions demonstrating face- and house-selectivity may be a potential way to circumvent issues associated with detecting sensory information representation in the brain by fMRI. Though this approach has been productive, it is nevertheless limited by univariate analysis that links cognitive variables to individual brain voxels. Rather than examining voxels in isolation, one can instead use powerful pattern-classification algorithms applied to multi-voxel/multivariate patterns of activity to decode the information that is represented in the pattern of activity. This multivariate pattern analysis (MVPA) can help elucidate more precisely *what* is accumulated and *where*, giving us a better understanding of how processes predicted by the DDM may be represented in the human brain.

Animal neurophysiology has long interpreted the selectivity of neurons as serving to represent various kinds of sensory or decision information. For example, the firing rate of neurons belonging to different receptive fields of the LIP in non-human primates has been used as evidence of an integrating decision variable for different motion directions in the random dot motion task (Hanks et al., 2006; Shadlen & Newsome, 2001). The population of neurons within an area is thought to jointly represent the information in what is called a neuronal population code (Averbeck et al., 2006) and may be reflected by patterns of activity across many spatially distributed neurons within a functional region (Norman et al., 2006). This idea, along with the realization that development for pattern classification in other domains (e.g., image recognition) can be productively applied to fMRI data analysis, has motivated studies to exploit MVPA with fMRI (Haxby et al., 2001; Kriegeskorte & Kievit, 2013).

MVPA commonly employs machine learning classifiers (Fig. 1.6), which treat each element (e.g., each voxel) of the patterns of interest as a separate dimension, or “feature”, in a high-dimensional space. Each trial-wise stimulus presentation elicits a pattern that occupies a point

in a *N*-dimensional neural activation space with *N* defined as the number of voxels within the region of interest. The classifier's goal is to find a way to transform this high-dimensional space into one where the voxel patterns associated with each condition are separable by a decision boundary or "hyperplane". Although a rich variety of classifiers are available, simple linear classifiers (e.g., support vector classifier with a linear kernel) are most commonly used as they provide a principled means of estimating a linear hyperplane between classes in activation space and have higher interpretability (James et al., 2013). To avoid overfitting, the classifier must be cross-validated; the hyperplane is estimated for a subset of the data designated as "training" data, and the classifier subsequently "tested" on the remaining data. The classifier assigns condition labels for the training data based on the position of the activity patterns relative to the hyperplane – this gives a weighting to each voxel in the pattern that determines their relative predicted contribution to the condition. Training and testing are done multiple times, with data partitioning shifted at each iteration (e.g., k-fold cross-validation) to ensure a random subset of data is used for validating. The performance of the classifier is then a function of the accuracy of its label assignment, averaged across iterations. If the mean classifier performance is statistically better than chance (e.g., > 50% for a two-condition classifier, or >25% for a four-condition classifier), the patterns for the different conditions are considered discriminable. This is a simplification of how machine-learning is applied for MVPA, but the same general principles can be applied to all decoding analyses. Note that the same methodologies can be applied to other neuroimaging modalities (e.g., electrodes as features).

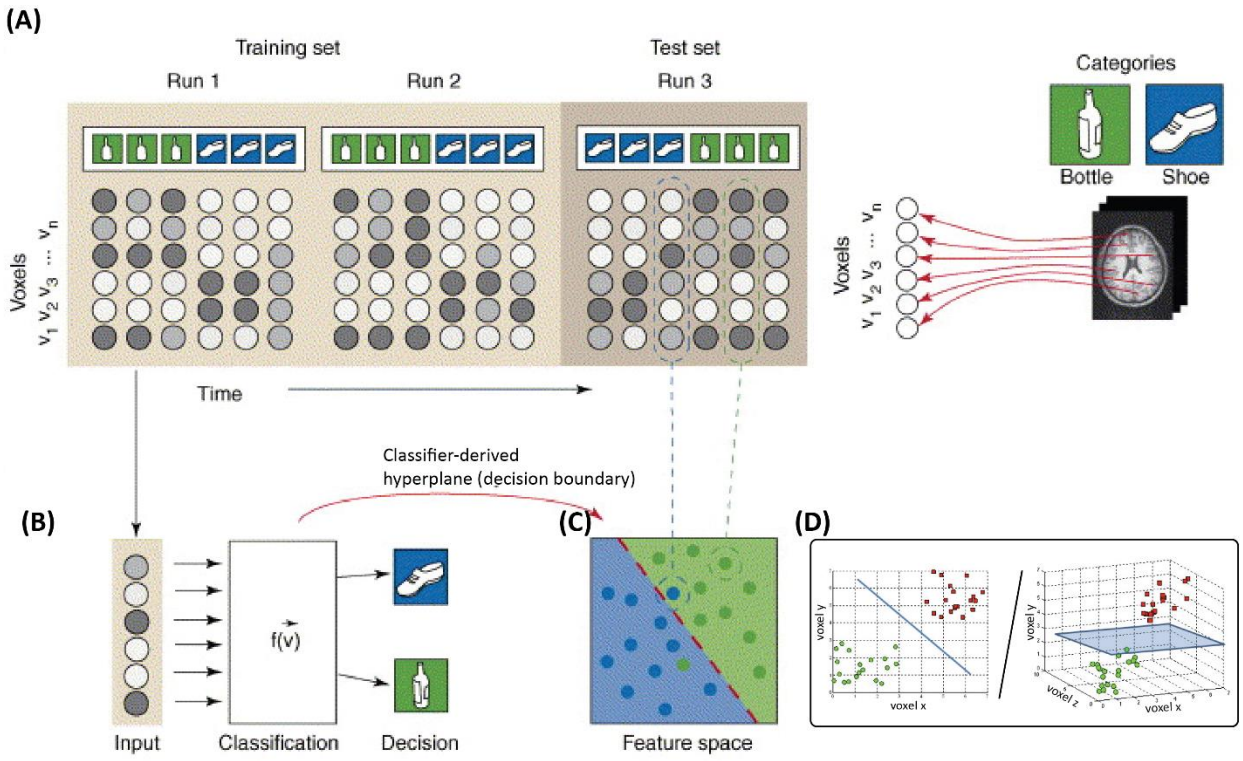

Fig. 1.6. *Overview of MVPA.* ***(A)*** *Hypothetical experiment where subjects view stimuli from two object categories (i.e., bottles and shoes). The fMRI time series is decomposed into discrete brain patterns that correspond to a spatial pattern of activity across voxels at a particular point in time.* ***(B)*** *A subset of the dataset is used to train a classifier, which is then tested on unseen data to test accuracy of predicted category labels.* ***(C)*** *After repeated cross-validation, the classifier defines the hyperplane (or decision boundary) that best discriminates between the two object categories. Each dot corresponds to a pattern and the color indicates its category (i.e., green for bottles, blue for shoes). Depending on the parameters set, the classifier can tolerate a certain level of misclassification.* ***(D)*** *An illustration of how patterns of activity can be portrayed in a higher-dimensional space of voxel patterns. On the left, a hyperplane between two hypothetical voxels can be visualized in a 2-D plot as a line. On the right, a hyperplane between three hypothetical voxels can be visualized in a 3-D plot as plane. The hyperplane becomes difficult to visualize once there are more than three features/voxels. Original figure adapted with permission from Norman et al. (2006).*

The primary advantage of MVPA methods over individual-voxel-based methods is increased sensitivity in detecting the presence of a particular mental representation in the brain. Conventional univariate fMRI analysis methods (e.g., Heekeren et al., 2004; Liu & Pleskac, 2011) try to find voxels that show a statistically significant response to experimental conditions (e.g., face versus house stimuli). These methods spatially average across voxels that respond

significantly to one condition, while subtracting away the other, to help increase sensitivity to a particular condition. Although this approach reduces noise, it also reduces signal in two important ways: (i) voxels with weak (i.e., non-significant) responses to a particular condition that may still carry some pertinent information are excluded from consideration based on statistical thresholds, and (ii) spatial averaging blurs out fine-grained spatial patterns that might discriminate between experimental conditions. Multivariate analysis overcomes these limitation by searching for the optimal combination of (distributed) voxels and assessing their contribution to stimulus discriminability (Davis et al., 2014; Kriegeskorte et al., 2006). Pioneering work by Haxby et al. (2001) illustrated how multi-voxel patterns of activity can be used to distinguish between faces, houses, and a variety of object categories (e.g., shoes, bottles, chairs, animals). Using MVPA, they showed that each category was associated with a reliable (i.e., cross-validated) and distinct pattern of activity in the ventral temporal cortex. Their results suggested that regions such as the "parahippocampal place" or the "fusiform face area" are not dedicated to representing only spatial arrangements or human faces, respectively. Rather, they are part of a more extended representation of *all* objects – or at least the extensive list of categories tested – to differing extents. Though previous fMRI work has employed univariate analyses to differentiate activity in face/house brain regions to infer sensory evidence, decoding information from patterns of neural activity using MVPA can provide stronger evidence about what information those patterns represent (for opposing view: Ritchie et al., 2017). Importantly, the increased sensitivity afforded by MVPA methods make it feasible to discriminate patterns of activity with less data – using only a few seconds' worth of BOLD activity (Haynes & Rees, 2005; LaConte et al., 2005; O'Toole et al., 2005). Though the temporal resolution of fMRI is inherently limited, MVPA allows for researchers to relate brain activity to behaviour on a trial-by-trial basis in the order of seconds with relative confidence (Haynes & Rees, 2005; Polyn et al., 2005).

Despite its potential benefits, the multivariate approach remains relatively under-utilized in cognitive neuroscience. One interesting approach developed here is the use of facial emotion detection as an example of sensory evidence accumulation in examining perceptual decisions. Facial expressions have been studied in great detail, likely because they are apparent in

everyday life and their controlled presentation in an experimental setting is relatively easy (Duchaine & Yovel, 2015; Haxby et al., 2000). The face-processing system is thought to include a core system wherein outputs from the inferior occipital gyrus, which engages in the early stages of face processing, are sent to the fusiform gyrus and the superior temporal sulcus for detecting aspects of faces including identity and emotional expressions. These core face-processing regions are linked to the extended system (e.g., intraparietal sulcus, auditory cortex, anterior temporal, and regions of the limbic system), which are not dedicated to the processing of visual information *per se* but extract different types of information from faces. fMRI BOLD activity from regions of the core and extended system can be accurately decoded by MVPA techniques to distinguish between emotional facial features (Wegrzyn et al., 2015). In the context of perceptual decisions, this decoded activity may carry sensory representations in the brain that vary with decision parameters from evidence accumulation models. As an added benefit, we can generate natural transitions in facial emotion to use as a dynamic stimulus to test predictions from different computational models (e.g., DDM vs urgency gating model, reviewed in Chapter 1.4). We exploit this well characterized face-processing system in the studies presented in this thesis to test perceptual decisions. Moreover, one of our studies (Chapter 2) is, to our knowledge, the first to exploit multivariate techniques to decode sensory information using fMRI in the context of an evidence accumulation model.

1.5.3. Finding a Decision Variable using Electroencephalography

Electroencephalography (EEG) may be more suited to test perceptual decisions in humans as it samples neural activity at millisecond temporal resolution. EEG recording measures the electrical activity generated by similarly orientated groups of cerebral cortical neurons near the scalp where the recording electrodes are placed. Each scalp electrode collects synchronous inhibitory or excitatory postsynaptic potential from hundreds of thousands of pyramidal neurons near each recording site. This summated activity, or "local field potential", can be represented as an electric field with positive and negative poles (i.e., dipoles) that are typically parallel to the orientation of their source pyramidal cells (Jackson & Bolger, 2014). Despite

having high temporal resolution, it is important to note that EEG signal is limited by the size of the electric field produced by neurons. Although reconstruction of the neural current (i.e., source localization) that produce a given EEG signal can be done, it requires the assumption of additional constraints to obtain a unique solution.

There is a rich history of using EEG techniques to explore and isolate distinct processing stages intervening between stimulus and response, and disentangling their individual contributions to a decision variable (Hillyard & Kutas, 1983; Woodworth et al., 1954). One prominent sensory-evoked event-related potential (ERP), the classic "P300", has been repeatedly linked with decision-making. For example, early-work on P300 found it to be evoked exclusively by task-relevant events requiring decisions (Rohrbaugh et al., 1974; Sutton et al., 1965) and that its amplitude was larger for detected versus undetected stimuli (Hillyard et al., 1971; Parasuraman & Beatty, 1980). However, a consensus regarding the precise role played by P300 in decision formation has failed to emerge (Nieuwenhuis et al., 2011; Nieuwenhuis et al., 2005; Polich, 2007; Twomey et al., 2015). This is in large part due to the discrete, sudden-onset ERP paradigms often employed, which result in temporally overlapping sensory, decision, and motor signals summed in a global signal, making it difficult to disentangle each distinct stage.

As with fMRI, innovative approaches have been taken in attempt to dissociate relevant decision parameters at the macroscopic level. Visual discrimination tasks, such as between faces and cars, have been used to test which signals can discriminate between the two conditions at trial-level (Philiastides et al., 2006; Philiastides & Sajda, 2006; Vanrullen & Thorpe, 2001). Employing machine-learning techniques (described above), a linear classifier was computed to differentiate the two conditions and construct discriminate component maps. These studies found two signal kernels (Fig. 1.7A): (i) an early frontal potential at ~170ms post stimulus-onset (i.e., N170) was selective for faces and only weakly predictive of errors, thus a possible correlate of sensory evidence, and (ii) a later centroparietal potential at ~300-450ms post stimulus-onset appeared to reflect task difficulty, and was thus argued to be a decision variable. In a follow-up study, trials were split into two groups based on the mean amplitude of the components. Trial bins with higher late component amplitudes within each stimulus coherence

level were associated with higher drift rates in the DDM (Ratcliff et al., 2009). This relationship was not observed when dividing the data on the basis of the early component, or on the latency (i.e., peak times) of either components. The authors thus concluded that while the early component may relate to the quality of incoming sensory evidence, the late component indexed decision-relevant evidence and constituted the decision variable. Furthermore, situated somewhere between the early and late components (~220ms post-stimulus onset) there was yet a third component that systematically increased with task difficulty/lower coherence. This third component was also detected at centroparietal electrode sites and was found to be strongly correlated with the onset time of the late component (Philiastides et al., 2006), with the authors suggesting that it is a top-down influence on decision-making, perhaps relating to a "caution" signal or decision threshold of the DDM, though this was never formally tested.

Rather than focusing on a component's peak amplitude alone, perhaps a better strategy is to characterize the temporal evolution of an EEG signal, which would track more closely with the predicted trajectory of a decision variable. More recently, a positive potential recorded over midline parietal electrodes has been shown to grow as sensory evidence accumulates (Fig. 1.7B) (Kelly & O'Connell, 2013; O'Connell et al., 2012; van Vugt et al., 2019), perhaps relating to the late component described in earlier work (Philiastides et al., 2006). This centroparietal positivity (CPP) potential reaches a peak before motor response, mirroring the firing rate acceleration observed in LIP neurons. By manipulating the task paradigm such that stimuli are presented in a smooth and gradual manner, the authors were able track the sensory information available, as well as eliminate transient sensory-evoked ERP signals and observe neural decision formation over a longer timescale. The same dynamics can be observed during detection of deviant stimuli that typically elicit the classic P300 potential, with which the CPP shares a scalp topography. This has led to the notion that the P300 and CPP may be the same under different names, and are common manifestations of a dynamically growing decision variable (Twomey et al., 2015). However, the short trial times in these studies means that these two signals cannot be disentangled temporally and, as such, cannot be definitively concluded as being identical. This is an issue we address in one of our studies (Chapter 3).

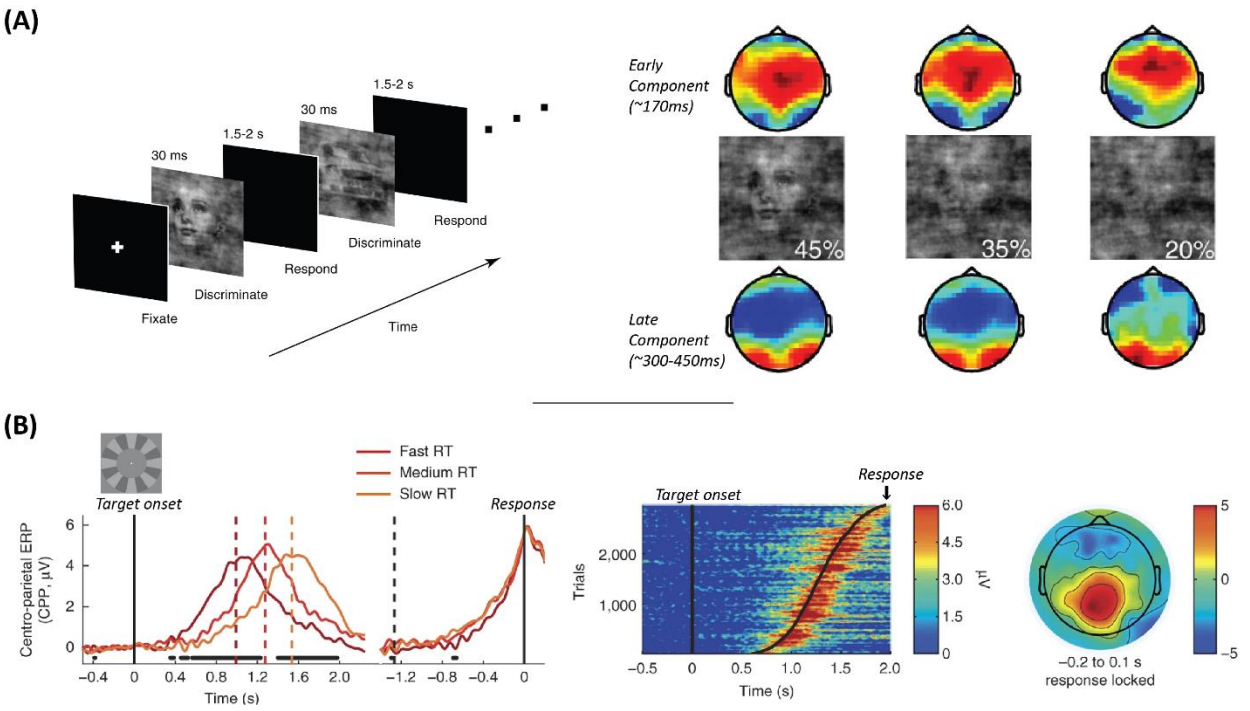

Fig. 1.7. *Examples of EEG studies investigating perceptual decisions.* ***(A)*** *Participants partook in a visual discrimination task between face and cars. Differences between the two categories revealed an early and late component whose activity scaled with the task difficulty/phase coherency of images. Original figure adapted with permissions from Philiastides and Sajda (2006).* ***(B)*** *CPP scales with dynamically changing sensory information and peaks close to the time of response. Original figure adapted with permission from O'Connell et al. (2012).*

Alternatively, the continuous sinusoidal rhythmic activity in EEG signal is thought to represent oscillatory cortico-cortical and cortico-subcortical communications. These communication loops occur spontaneously when the brain is at rest and not engaged in any specific task. When confronted with a task, the electrical activity of the cortex desynchronizes and changes in specific frequency bands of oscillatory activity are attributed to various cognitive functions (Başar et al., 2001; Klimesch, 1999; Sauseng et al., 2010). For example, when opposing perceptual decisions involve lateralized hand responses, the power of high-frequency, EEG beta band activity over motor regions diverges steadily between hemisphere that are contra- and ipsi-lateral to the hand responsible for the targeted response. This beta signal arguably reflects a gradual response preparation signal downstream to the encoding of decision information in the parietal EEG signals (Gould et al., 2012; Kubanek et al., 2013; Wyart et al., 2012). Theta band oscillations have also been implicated in perceptual decisions, with their power shown to

covary with decision certainty (Cavanagh et al., 2011a; Jacobs et al., 2006) and prediction errors (Cavanagh et al., 2010). Simultaneous fMRI and EEG recording revealed the decision threshold predicted by the DDM was not fixed across trials, but varied as a function of task difficulty (in this case, conflict), mid-frontal EEG theta oscillations, and subthalamic nucleus fMRI activity (Frank et al., 2015). While studying patients having undergone therapeutic deep brain stimulation, this group further demonstrated that mid-frontal theta oscillations are closely linked with subthalamic nucleus activity which gates behavioural outputs by raising the threshold required to arrive at a decision (Cavanagh et al., 2011b). However, other groups have also proposed that theta oscillations instead reflect the drift rate of the DDM (van Vugt et al., 2012).

1.5.4. Brain Networks as the Backbone to Behaviour

A unique contribution of macroscopic neuroimaging techniques is their ability to probe the interaction between different brain systems, helping reveal the wider brain networks involved in making perceptual decisions. While we have discussed some models of how the brain may arrive at a decision elicited by state-dependent activation in response to cognitive tasks, less is known about the quality and quantity of individual variation that occurs atop this blueprint (Van Horn et al., 2008). Typically, neuroimaging studies collapse data from many subjects and ignore the possibility that brain functional organization may vary between individuals. There may be meaningful idiosyncrasies in this organization across individuals that can reveal: (i) crucial variability in relating brain activity to behavioural phenotypes, and (ii) biomarkers with potential real-world utility for clinical conditions.

The fMRI community, and more recently the EEG community, have embraced resting state or intrinsic functional connectivity (FC) approaches to mapping brain organization (Kelly et al., 2012). FC charts spontaneous temporal coactivation between disparate brain regions: the more in sync (i.e., correlated) two regions are in their activity, the stronger they are thought to be connected functionally. There is mounting evidence that suggest FC reflects the connectivity

between brain regions and is more than just a spurious signal resulting from stochastic noise (Deco et al., 2011; Handwerker et al., 2012; Tagliazucchi et al., 2012; Thompson et al., 2013). Assuming FC reflects anatomical connectivity, a functional topography can unfold on a relatively fixed structural scaffold (Shen et al., 2015) in various intrinsic configurations termed resting-state networks (RSNs) over extended periods that are task-free ("resting") (Laird et al., 2011; Yeo et al., 2011). These RSNs have been variably named after the functional characteristics of the networks or according to the core brain regions comprising them (e.g., default mode, fronto-parietal, motor-visual, and dorsal attention network). Having demonstrated FC's utility for charting the large-scale functional architecture of the brain, there is now a growing momentum to leverage task-independent methods for investigation of phenotypic variations.

RSN dynamics are arguably a reflection of the array of cognitive architectures that the brain has available. Variations within and between RSNs are thought to "fingerprint" individual differences in a variety of traits and behaviour related to cognitive function, age, and mental health (Finn et al., 2015; Geerligs et al., 2015a; Geerligs et al., 2015b; Li et al., 2013; Sanz-Arigita et al., 2010; van den Heuvel et al., 2009). Recent neuroimaging studies have shown that the RSN architecture is largely preserved during rest and cognitive task (Cao et al., 2014; Cole et al., 2014; Krienen et al., 2014). In general, external tasks are thought to perturb the baseline network configuration observed at rest, and the extent to which the RSNs change between rest and task is a function of task difficulty (Gießing et al., 2013; Power & Petersen, 2013; Shine et al., 2016). More cognitively demanding tasks may benefit from a less modular and more integrated connectivity between RSNs (Cohen & D'Esposito, 2016). The emergence of momentary neural coalitions form the basis of complex cognitive functions (Bassett et al., 2015; Cole et al., 2014). A more globally integrated network architecture is thought to give rise to faster, more effective information processing during task performance. However, this integrated state is theorized to be metabolically costly to maintain, being present only when essential for the task at hand, in order to balance between efficient information-processing and metabolic expenditure (Bullmore & Sporns, 2012).

In tandem, there has been recognition in recent years that FC itself is not static, with connection strengths varying during a single resting-state scan (Chang & Glover, 2010; Hutchison et al., 2013; Lurie et al., 2018) and within various cognitive tasks (Cole et al., 2013; Gonzalez-Castillo et al., 2015; Shine et al., 2016). This has led to the conceptualization of a dynamic or time-varying FC that argues averaging over an extended period of rest may lead to a useful but oversimplified characterization of the brain's functional networks. Instead, different analytical techniques (e.g., k-mean clustering with sliding windows) can be used to identify transient "brain states" that may be present in the population tested. To this end, recent experiments using fMRI have demonstrated that the global brain signals at rest transition between states of high and low modularity over time (Zalesky et al., 2014). However, the psychological relevance of these fluctuations remains poorly understood. Emerging evidence suggests that more dynamic connectivity between specific networks (e.g., fronto-parietal and default-mode) (Douw et al., 2016), or the propensity to transition between certain brain states of high and low modularity at rest (Nomi et al., 2017), may relate to better cognitive performance. Although literature is accumulating about the time-varying FC of brain networks during resting state and, to a lesser extent, during task performance, there is a need to better understand the link between the two and how this may shape decisions – we attempt to bridge this gap in Chapter 4.

1.6. Summary

In the previous sections we reviewed the current knowledge of perceptual decisions, particularly as it pertains to humans. Decision-making underlies a wide range of human behaviour (e.g., economics and social interactions) and disruptions in this process are commonly noted in many neurological and psychiatric conditions (e.g., major depressive disorder, schizophrenia, substance-use disorders, and post-traumatic stress disorder (Aupperle et al., 2012; Rock et al., 2014; Stevens et al., 2014)). Understanding how the mind produces behaviour and the decision processes made prior to executing an action can shed light on what happens when this process is disrupted and help identify potential ways to ameliorate this

cognitive disruption. The challenge lies in the logistics of studying a highly flexible and dynamic system that is constantly evolving in a dynamic environment. Several computational models have been proposed in recent years in an attempt to account for how people arrive at a decision when presented with perceptual information. One school of thought posits that people gather information from the environment until they reach a decision threshold. This model (i.e., DDM) has received much support and is backed by a multitude of behavioural and neurological evidence. However, the DDM may not be applicable to real-world scenarios where dynamic and changing stimuli are present. Experimental tasks we use to understand this process often involve a constant stimulus that may not be representative of the true nature of our environment. Specifically, an alternative school of thought argues that evidence accumulation models are lacking in that they do not consider the aspect of time which may impose an "urgency" factor to the decision-making process.

At present, important knowledge gaps in human perceptual decision-making remains: Where are the neural origins of the hypothesized sensory encoding and decision variable in the human brain? How may different decision parameters unfold temporally and relate to different neural signals? What is the influence and meaning of individual variability in functional organization of the brain on perceptual decisions? Finally, can accounting for an endogenous, time-variant urgency signal improve our understanding of perceptual decisions and if so, where may this signal arise in the brain? This thesis consists of three studies that attempt to address these interrelated research questions as well as testing a series of specific experimental aims. Chapter 2 addresses how decision parameters are encoded in the human brain. We aimed to identify brain regions involved in the accumulation of sensory evidence and the pathways by which this information is relayed across the brain to inform decisions. We additionally tested the theory that the traditional DDM may fail to explain decisions in the face of ambiguous or low signal-to-noise decision environments. Chapter 3 examines perceptual decisions at a faster time-scale, disentangling neural signals within a trial that may relate to different decision parameters. We tested whether an urgency gating model may better explain the dynamics of the captured neural signals. Chapter 4 focuses on how the propensity to express different configurations of brain connectivity at rest may modulate and shape perceptual decisions in

task. We compare and contrast brain connectivity at rest to that in task and ask how this relationship may be affected by task demands. With these findings, we hope to provide a more comprehensive and valid understanding of how the brain deliberates in a dynamic environment.

CHAPTER 2. Neural correlates of evidence and urgency during human perceptual decision-making in dynamically changing conditions

2.1. Preface

There have been many successful studies of perceptual decision-making in monkeys usually employing visual discrimination tasks between two choice alternatives. These studies show that one can fit computational evidence accumulation models to behaviour and extract model signals from microelectrode recordings in various parts of the brain. This approach, however, has proven more difficult in humans. In this chapter, we developed a task consisting of smooth, continuously changing stimuli – a neutral face that morphs towards happy or sad expression – that allows us to track the amount of sensory information available in the decision environment at any given time within a trial. Participants underwent this task while inside the fMRI scanner. We used MVPA to extract the neuronal code for happy and sad facial expressions from the fusiform gyrus, and showed that this neural information is related to sensory encoding in the evidence accumulation model. Furthermore, we tested the theory that the traditional DDM may fail to explain decisions in the face of ambiguous or changing information. We provide evidence for an urgency signal from the caudate nucleus that can modulate the timing of decisions. This endogenous urgency signal varies between individuals and can potentially account for why certain individuals are prone to faster and erroneous decisions, particularly when the sensory information is ambiguous. This study aimed to characterize decision parameters underlying human perceptual decision-making in the setting of dynamic, changing environments by combining model-driven machine-learning fMRI techniques, psychophysics, and computational modelling. Our results reveal how decision parameters are encoded in the human brain and indicate that machine-learning techniques can be used to probe and disentangle the biological underpinnings of the decision process. This work has been published in *Cerebral Cortex*.

2.2. Abstract

Current models of decision-making assume that the brain gradually accumulates evidence and drifts towards a threshold which, once crossed, results in a choice selection. These models have been especially successful in primate research, however transposing them to human fMRI paradigms has proved challenging. Here, we exploit the face-selective visual system and test whether decoded emotional facial features from multivariate fMRI signals during a dynamic perceptual decision-making task are related to the parameters of computational models of decision-making. We show that trial-by-trial variations in the pattern of neural activity in the fusiform gyrus reflect facial emotional information and modulate drift rates during deliberation. We also observed an inverse-urgency signal based in the caudate nucleus that was independent of sensory information but appeared to slow decisions, particularly when information in the task was ambiguous. Taken together, our results characterize how decision parameters from a computational model (i.e., drift rate and urgency signal) are involved in perceptual decision-making and reflected in the activity of the human brain.

2.3. Introduction

Decisions are often made based on noisy or changing information. A prominent theory in decision-neuroscience, referred to as the evidence-accumulation or drift-diffusion model (Smith & Ratcliff, 2004), posits that deliberation is an integrative mechanism in which sensory information supporting different options accumulates over time until a boundary is reached, at which point the decision is made (Glaze et al., 2015; Gold & Shadlen, 2007; Yang & Shadlen, 2007). Neuroscientific support for the drift-diffusion model comes principally from single-unit recordings in non-human primates. “Accumulator regions” – where neurons exhibit ramp-like increases or drift in their firing towards a decision threshold – have been located in several brain areas in a widely-studied dot motion perceptual decision paradigm (Gold & Shadlen, 2007; Hanks et al., 2015; Roitman & Shadlen, 2002; Scott et al., 2017; Shadlen & Newsome, 1996, 2001). This work suggests that different pools of selectively tuned, lower-level sensory

neurons could feed information to higher-level cortical regions to compute perceptual decisions. However, single-unit recordings provide a spatially narrow view of the brain mechanisms underlying decision-making. Functional magnetic resonance imaging (fMRI) studies, though comparatively limited in spatial resolution, have begun to explore the neural substrates of evidence accumulation during perceptual decision-making in humans in attempt to provide a more holistic view (Heekeren et al., 2004; Ploran et al., 2007; Tremel & Wheeler, 2015).

Also, some decisions need to be made promptly despite incomplete or changing evidence. Simple drift-diffusion models have difficulty accounting for these situations. A recent theoretical approach suggests that decision-making incorporates an "urgency" signal, independent of the sensory evidence, which grows over time to bring neural activity closer to a decision threshold (Cisek et al., 2009; Mormann et al., 2010; Murphy et al., 2016; Thura et al., 2012). Single-unit recordings in monkeys have implicated the basal ganglia as the neural driver of this postulated urgency signal (Thura & Cisek, 2017). Urgency signals are of interest in human behaviour as they may relate to the trait of impulsivity (Carland et al., 2019; Thura & Cisek, 2014, 2016). However, the few studies to date that have employed fMRI to differentiate evidence accumulation and urgency parameters are limited by relatively small sample sizes (Mulder et al., 2014). Moreover, the univariate BOLD response analysis typically employed may fail to differentiate relevant neuronal populations that encode stimulus features used for making the decision as they ignore the possibility that information may be represented in a distributed manner across voxels (Braunlich & Seger, 2016; Gluth et al., 2012). Multivariate analysis overcomes this limitation by searching for the optimal combination of (distributed) voxels and assessing their contribution to stimulus discriminability (Davis et al., 2014; Kriegeskorte et al., 2006).

We designed a novel fMRI task to identify neural substrates of the time-dependent processes that occur during deliberation in a simple sensory decision-making task. We took advantage of the fact that it is possible to reliably decode brain activity related to facial emotion detection. Subjects decided whether a short video of a face presented on screen was transitioning to a

happy or sad emotion. Previous work suggests that not only is it possible to decode representation of faces from fMRI signal in extrastriate visual areas (Haxby et al., 2001), but that distinct emotional facial features are uniquely represented in the brain and can be decoded (Kassam et al., 2013; Wager et al., 2015). Our task allowed identification of multivariate patterns indicative of happy or sad faces, which we took to represent the sensory evidence upon which the decision was made. According to evidence accumulator models, information on the upcoming choice decoded from the population of neurons participating in facial processing should increase towards a decision threshold, reflecting the gradual accumulation of evidence in support of the upcoming choice. Analogous to results from single-unit recording studies in non-human primates, we hypothesize that decision-making parameters will covary with decoded fMRI activity related to detection of facial emotion. To test the urgency-gating model (Cisek et al., 2009), we included ambiguous trials in the study design. We examined the extent to which neural representation of evidence accumulation contributed to decisions in ambiguous conditions, and whether an urgency parameter improved model fit.

2.4. Methods

2.4.1. Participants

53 right-handed young, healthy adults (23 males; age mean 24.02yr±5.49 standard deviation [SD]) participated in the present study. Exclusion criteria included current or past diagnosis of a psychiatric disorder, neurological disorder, or concussion, and moderate to severe depression (score >5 on the Beck Depression Inventory (Beck et al., 1961)). All participants gave written informed consent prior to data acquisition and received monetary compensation for their participation. The study was approved by the Montreal Neurological Institute Research Ethics Board.

2.4.2. Task Design

Face stimuli were derived from the NimStim database (Tottenham et al., 2009). Photographs of six (3 males) out of 43 models with closed-mouth happy and sad expressions were selected as stimuli for the task because they had the highest identification accuracy in both Tottenham et al. (2009)'s initial validation of the dataset and in our piloting. Face stimuli were made achromatic in MATLAB and presented on a grey background. In order to manipulate the intensity of the emotional expressions, 18 intermediate face stimuli were also generated from the NimStim faces using STOIK MorphMan software (http://www.stoik.com/) to create different emotion levels that gradually transitioned between a model's neutral and happy or sad face. Thus, emotion levels varied from 0 to 19 in both directions. Two independent tasks were conducted using these stimuli: (1) a training task and (2) a dynamic task.

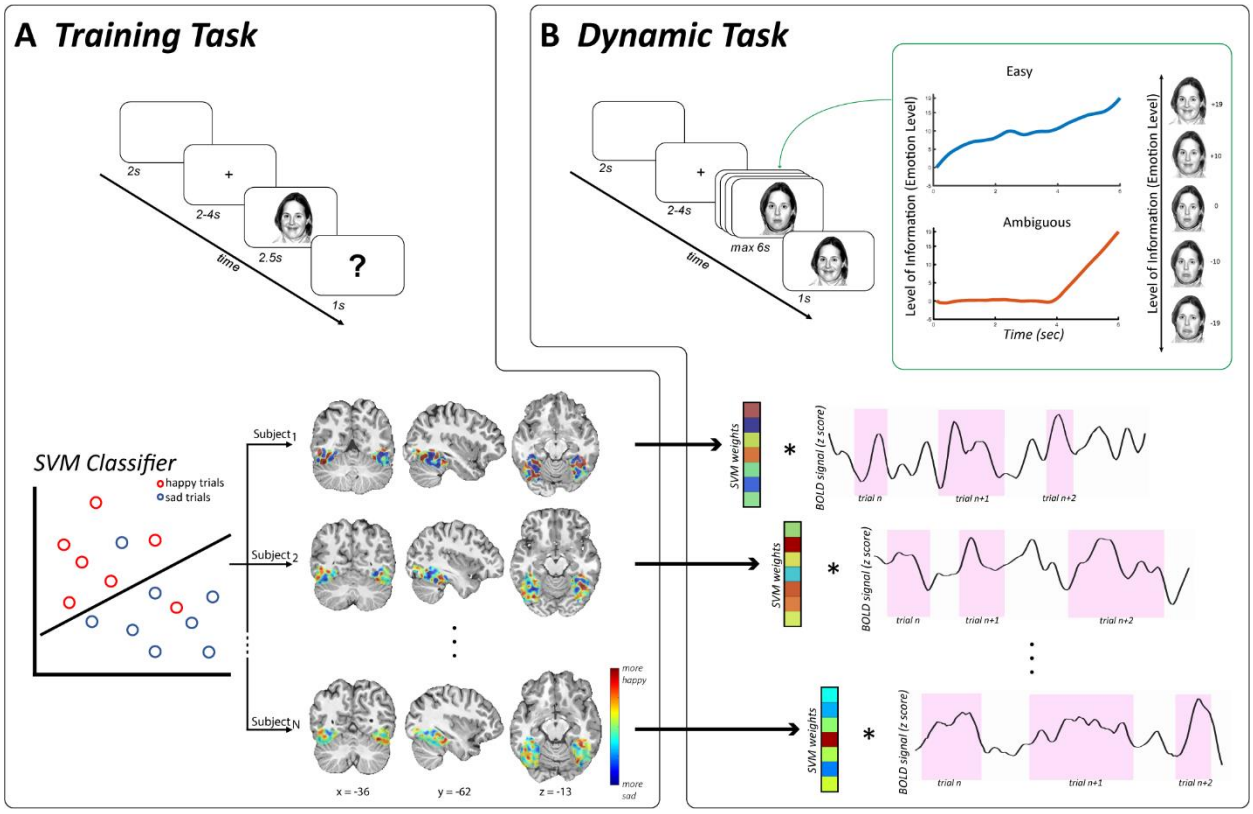

Fig. 2.1. *Experiment overview.* ***(A)*** *Training task was used to decode BOLD activity in response to viewing of static happy or sad faces. One classifier was generated for each of 7 bilateral regions of interest, per subject. The classifiers were then used to determine support vector machine-learning (SVM) weights, or distance from hyperplane, which were in turn projected to*

*the BOLD effect size values while viewing faces in the **(B)** dynamic task. This yielded a neural "code" per trial, per region. Two trial types were used in the dynamic task: (i) easy trials where facial expression gradually morphed towards one of the two emotions and (ii) ambiguous trials where facial expression varied around neutral until two-thirds into the trial after which point emotion rapidly ramped up towards happy or sad.*

The static training task (Fig. 2.1A) served to localize patterns of brain activity related to happy and sad faces. Subjects viewed a face with an emotional level >15 for 2.5 secs; this fixed time of display ensured that we eclipsed at least one full repetition time (TR) of fMRI acquisition to allow for accurate parameter estimation. After this, a question mark appeared with a maximum time of 1 sec, during which the subject was instructed to respond with their evaluation of whether the face was happy or sad; if no response was made, "Too Slow" was displayed on the screen for 1 sec.

In the dynamic task (Fig. 2.1B), subjects viewed dynamic stimuli of faces "morphing" between expressions. In these trials, a maximum of 60 frames were presented over 6 secs (i.e. 10 frames per second), plus a final image of the correct emotion (with the emotion level > 15) for 1 sec either after a response was made or at the end of a trial if the subject had not yet made a response. Participants were instructed to predict whether the face would be happy or sad by the end of the trial and to respond whenever they felt confident enough to do so. Subjects were asked to respond both as quickly and as accurately as possible. Within the dynamic task, there were two types of trials, namely "easy" and "ambiguous", which were modelled after previous work (Thura et al., 2012). In both trial types, the first image presented was the model's neutral face.

In easy trials, all faces presented were of the correct emotion (e.g., in a trial in which the correct answer is happy, no sad images are ever presented). Each successive frame had a 65% chance of being one level higher than the previous frame in the direction of the correct emotion. By the final frame, all trials had an emotion level >16. The final frame was presented for 1 sec as soon as the subject made a response, or it was presented as a 1 sec long additional

frame if they had not yet responded. Subjects could respond during this final frame only if they had not yet done so.

In ambiguous trials, the probability of each frame during the first two-thirds of the trials (i.e., up to the 40th frame) had a 50% chance of being one level higher than the previous in the direction of the correct emotion, such that the images generally hovered around a neutral valence. To prevent, for example, many slightly happy images and a few very sad images being presented, the maximum levels presented in the correct and incorrect direction before the 40th frame were kept within two levels of each other. Furthermore, the maximum level reached in either direction before the 40th frame was limited to 7. In the final third of the trial, there was a steep increase of level in favour of the correct emotion, with a 95% chance that a given frame would be exactly one level higher in favour of the correction emotion than the previous frame. All trials had a final emotion level > 16. As with the easy trials, this final frame was presented for a duration of 1 sec as soon as a response was made, or as a 1 sec long 61st frame during which subjects could respond if they had not yet done so.

In both tasks (i.e., static training and dynamic), a pause followed by a time-jittered fixation cross preceded each trial. The trials were evenly split between happy and sad (determined by the emotion at the final frame for the dynamic task), with the order of trials randomized in every block. Participants took part in 4 runs for the localizer task and 3 runs for the dynamic task. Both tasks had a total of 120 trials each, divided equally among the runs.

2.4.3. MRI Acquisition

Neuroimaging was carried out with a Siemens Magnetom Prisma 3T MRI scanner equipped with a 64-channel head coil at the Montreal Neurological Institute (MNI). High-resolution MPRAGE T1-weighted structural images were first obtained for anatomical localization (TR=2.3s; TE=2.3ms; FOV=240mm; scan matrix=192x256x256; voxel size=0.9mm isotropic). Functional data were then acquired with an echo-planar T2*weighted sequence for blood oxygenation level-dependent (BOLD) contrast (TR=0.719s; TE=30ms; scan matrix=104x108x72; flip angle=44°; FOV=208mm; voxel size=2mm isotropic, multiband acceleration factor=8). Here, we

capitalized on multi-band acquisition to help improve temporal resolution, allowing for the potential of multiple data points per trial to better characterize signal change during the decision process

2.4.4. MRI Preprocessing

Preprocessing and beta extraction were performed using SPM12 (http://www.fil.ion.ucl.ac.uk/spm/) and Matlab. Signals with >4% intensity change were despiked and corrected using ArtRepair Toolbox (Mazaika et al., 2007). Images were corrected for motion, realigned, normalized to the MNI ICBM152 template (Fonov et al., 2009), and minimally smoothed (6mm FWHM Gaussian kernel). Spatial filtering techniques (such as Gaussian smoothing) have been shown to increase the signal-to-noise ratio (Brants et al., 2011; Hendriks et al., 2017), as well as classification performance in multivariate pattern analysis (MVPA) (Op de Beeck, 2010). One subject was excluded from further analysis after quality control due to excessive motion.

2.4.5. Generation of Regions of Interest

We generated bilateral region of interest masks for 7 brain areas previously shown to be involved in the detection of facial expression (Haxby et al., 2000; Wegrzyn et al., 2015) and one for the caudate thought to play a role in urgency. An association test (FDR-corrected, <0.01) for the terms “amygdala”, “anterior temporal”, “fusiform gyrus”, “inferior occipital”, “insula”, “intraparietal”, “superior temporal”, and “caudate” on the Neurosynth meta-analytical database was conducted yielding one brain map per term indicating the probability of that term being used in a study given the reported activation (i.e., P(Term|Activation)) (Yarkoni et al., 2011). To avoid overlaps between our regional masks, voxels in overlapping regions were assigned to the region with the greatest z-score from the reverse inference map derived the Neurosynth search terms. These spatially unique maps were then binarized.

2.4.6. Multivariate Pattern Analysis & Fusiform Code

Preprocessed functional data were used as input for run-wise GLM first-level designs yielding one regressor for the event of interest, a second for all other events, and six motion regressors (Mumford et al., 2012), creating one GLM per event. This approach is thought to lead to more representative trial-by-trial estimates of the true activation magnitude. Only the beta value (i.e., parameter estimates or coefficients representing effect size from linear regression) for the event of interest was used for all further analysis in generating a classifier in the localizer task. For the dynamic task, fMRI signal extracted through the canonical GLM (i.e., one GLM per run with regressors for the duration of face presentation, intertrial interval, button press, six additional motion regressors as nuisance regressors, and a constant) implemented by SPM was used for statistical analysis.

A linear support vector machine-learning (SVM) algorithm (C=1.0, L2 penalty, square hinged loss, tolerance=0.0001, max iterations=1,000) was implemented using the scikit-learn package in Python (Pedregosa et al., 2011) to classify happy and sad stimuli from the preprocessed beta images after data normalization. Features were extracted within each of the regional masks, without additional voxel selection. A feature's (i.e., BOLD signal) distance away from hyperplane determined the SVM weight. A k-fold cross validation (k=10) was conducted to test the accuracy of the classifier and reveal voxels where local patterns of activation reliably discriminated between happy and sad faces. After subtracting the activity in the preceding inter-trial period and normalization, the SVM weights from the classifier derived from the localizer task were then projected to each trial's BOLD effect size in the dynamic task to calculate the fusiform "code" during viewing of the morphing video.

Statistical significance of the decoder's accuracy was tested using permutation of the original data per subject with randomly shuffled class labels of the training and testing data sets before supplying them to the classifier (Mahmoudi et al., 2012; Pereira & Botvinick, 2011). This procedure was done 1,000 times in order to generate a null distribution and was used to test how likely a certain classifier accuracy was to occur by pure chance. Due to exchangeability issues between run – that is the risk of predicting runs rather than class label – labels were only

permuted within, rather than across data splits (i.e., within each subject, within each run). P-values were calculated as the proportion of instances where permutated data had equal or higher accuracy than the original decoder accuracy divided by the number of all permutations. Eight subjects with classifiers that did not perform better than chance in any of the regions investigated were excluded from further analysis.

2.4.7. Fitting the Hierarchical Drift Diffusion Model (HDDM)

The drift diffusion model (DDM), an established dynamic model of two-choice decision processes (Ratcliff et al., 2016), was fitted to subjects' reaction time (RT) distributions. The DDM simulates two-alternative forced choices as a noisy process of evidence accumulation through time. The mode implies a single accumulator integrating the sample evidence according to a stochastic diffusion process until the evidence accumulated reaches one of two decision bounds, here for 'happy' or 'sad'. The model decomposes behavioural data into four parameters mapped on to the latent psychological process: drift rate (v) for speed of accumulation, starting point (z) for a response bias towards one choice, non-decision time (t) for stimulus encoding and response execution latencies, and critical decision threshold (a).

Here we used a hierarchical extension of the DDM (HDDM) (Wiecki et al., 2013) to estimate decision parameters. This method assumes that parameters for individual participants are random samples drawn from group-level distributions and uses Bayesian statistical methods to optimize all parameters at both the group and subject level. In other words, fits for individual subjects are constrained by the group distribution, but can vary from this distribution. This Bayesian approach for parameter estimation has distinct advantages over other methods in robustly recovering model parameters estimates for both individual and group levels, particularly when the number of trials is relatively small. Moreover, HDDM has been shown to reliably estimate DDM parameters, including regressing effects of trial-by-trial variations of neural signals on decision parameters (Matzke & Wagenmakers, 2009; Wiecki et al., 2013). Bayesian estimates allow for quantification of parameter estimates and uncertainty in the form of joint posterior distribution, given the observed experimental data (Gelman et al., 2013). To account for outliers in behaviour that cannot be captured by HDDM (e.g., slow responses due

to inattention or fast erroneous responses due to action slips), we removed 5% of the trials at each tail of the RT distribution. Markov chain Monte Carlo sample methods were used to accurately approximate the posterior distribution of the estimated parameters. 5,000 samples were drawn from the posterior to obtain smooth parameter estimates, the first 100 samples were discarded as burn-in. Convergence of Markov chains were assessed by inspecting traces of model parameters, their autocorrelation, and computing the Gelman-Ruben statistic (Gelman & Rubin, 1992) to ensure that the models had properly converged.

Two models were used: one without inclusion of any fMRI data and a second that allowed for trial-by-trial variations in neural activity to modulate decision parameters. To test our hypotheses relating neural activity to model parameters, we estimated posterior distributions not only for basic model parameters, but the degree to which these parameters are altered by variations in neural measures (i.e., facial emotion code from each region of interest, and caudate BOLD activity – see below). In these regressions, the coefficient weighs the slope of the parameters (defined by drift rate *v* and threshold *a*) by the value of the neural measure on this trial, with an intercept, for example: $v(t) = \beta_0 + \beta_1 condition + \beta_2 fusiform\ code(t) + \beta_3 condition(t) * fusiform\ code(t)$. The regression across trials allows us to infer the degree to which threshold changes with neural activity. Changes in drift rate relate to RT speed and accuracy.

Modulators, in this case the fMRI-derived neural parameters, were iteratively added in to our model to test whether successive additions improved model fit. Model fit was assessed by comparing each models' deviance information criterion (DIC) value (Spiegelhalter et al., 2002), with a lower value for a given model (for the whole group) indicating higher likelihood for that model compared to an alternative model, taking into account model complexity (degrees of freedom). A DIC difference of 10 is considered significant (Zhang & Rowe, 2014). DIC is widely used for comparisons of hierarchical models where other measures (e.g., Bayesian information criterion) are not appropriate (Frank et al., 2015; Ratcliff et al., 2016). Parameters of the best model were analyzed by Bayesian hypothesis testing, which examines the probability mass of the parameter region in question (i.e., percentage of posterior samples greater than zero).

Posterior probabilities ≥95% were considered significant. Note, this value is not equivalent to p-values estimated by frequentist methods but can be interpreted in a similar manner.

2.4.8. Psychophysiological-Interaction (PPI)

Generalized psychophysiological-interaction (gPPI) analysis (McLaren et al., 2012) was used to identify brain regions with activity that covaried with the activity of the fusiform "seed" voxels as parametrically modulated by the fusiform code. Two 6mm spheres centered at the peak voxel from the z-score map of the "fusiform gyrus" search term from Neurosynth – identical to the aforementioned search in the Generation of Regions of Interest section – in each hemisphere were used as seeds (left center: x=-42, y=-48, z=-20; right center: x=44, y=-48, z=-16). Our GLM included regressors accounting for periods corresponding to trials for each emotion (i.e., happy and sad) each parametrically modulated by the fusiform code, with intertrial interval duration, button press, six additional motion regressors as nuisance regressors, and a constant. gPPI regressors were created by deconvolving the seed to obtain an estimated neural signal during perceptual decisions using SPM's deconvolution algorithm, calculating the interaction with the task in the neural domain, and then re-convolved to create the final regressor. Participant effects were then used in a group-level analysis, treating participants as a random effect, using a one-sample t-test against a contrast value of zero at each voxel.

2.4.9. Fitting the Urgency Gating Model (UGM)

A filtered evidence variable x was derived using the following differential equation:

$$\tau \frac{dx(t)}{dt} = -x(t) + gE(t) + G(0, N) \qquad (1)$$

whereby at a given time *t*, the evidence *E,* which denotes the amount of information (i.e., facial emotion level) is multiplied by an attentional fixed gain term g. Further, an intra-trial Gaussian noise variable *G*(0,*N*) with a mean of 0 and a standard deviation of *N* was added. Here we chose *N*=6, because it gave a range of simulated RTs with similar variability as the observed data (but see Supplementary Table A2.4 for evidence that the model is robust to the choice of *N*). How

far back in time sensory information is considered by the model is determined by the time constant τ. We next computed the estimated neural activity y.

$$y(t) = x(t) * u(t) \qquad (2)$$

This was determined by multiplying the filtered evidence x with an urgency parameter u. A decision is made when the variable $y(t)$ reaches threshold *T*. A non-decision time of 200ms was added to yield the predicted RT.

Implementation of the non-hierarchical DDM (nDDM) and the urgency-gating model (UGM) differed in two key ways. First, there was no urgency parameter u added to the nDDM. In other words, the nDDM assumes that once the variable $x(t)$ reach the threshold T, a decision is made. Second, in the UGM, a low-pass filter of the sensory information in the first-order linear differential equation was applied. The time constant τ was set to 200ms for the UGM whereas the maximum trial duration of 6000ms was used as time constant for the DDM. We assumed a time constant of 200ms for the UGM on the basis previous behavioural and physiological studies (Cisek et al., 2009; Thura et al., 2012; Thura & Cisek, 2014). Evidence (*E*), gain (g), and noise (*N*) parameters were the same in both models.

In the nDDM, the *T* parameter was adjusted using an exhaustive search to find the variable that minimized the mean squared error between the model's predicted RT versus the real RT across all trials for each subject. In the UGM, the u parameter was similarly searched for using this criterion. Note that for each model, one parameter was adjusted to fit the data; both *T* and u influence the means of RT distributions. The models were used to simulate 5,000 trials, the mean of which was used to compare against the real RT distributions.

2.4.10. Statistical Analysis of Behavioural Data

Statistics for this study were conducted in R (R Core Team, 2015) and MatlabR2018b (MATLAB, 2018). Due to low sample size, which may increase vulnerability to spurious outliers, non-parametric tests were used to assess the following subject-level data. Mean RTs and accuracy were evaluated by a Friedman's test to compare the effect of trial type and emotion while accounting for runs in each instance. Spearman correlations were used to test for all

correlations between task performance (i.e., accuracy and RT) and other metrics of interest (e.g., HDDM decision threshold, UGM urgency signal, questionnaires). To test a possible two-way interaction effect of accuracy (i.e., correct and incorrect) and condition (i.e., easy and ambiguous) on neural activity, we ran a two-away Analysis of Variance as the non-parametric equivalent (i.e., Friedman's test) does not consider interaction effects. Wilcoxon Signed-Ranks tests were then used to compare neural activity between incorrect and correct trials whereas Wilcoxon Rank Sum tests were used compare between groups (i.e., early versus late responders – see below). In both cases, z-values refer to Wilcoxon's z (approximation).

2.4.11. Neural Correlates of Urgency

To look for neural correlates of urgency gating, we compared individuals who tended to wait for information in ambiguous trials to those who tended to respond early (*n*=24 and 21 participants respectively, see below). We compared BOLD activity during stimulus presentation in early vs late responders, using the fusiform MVPA code as a parametric modulator (see equation 2). Because there were no significant differences in the whole-brain analysis we focused on the caudate nucleus region of interest, based on previous work identifying this structure as a likely source of urgency signals (Ding & Gold, 2012; Nagano-Saito et al., 2012; Thura & Cisek, 2017).

2.5. Results

2.5.1. Multivariate Pattern Analysis of Facial Emotion Detection

First, the static task was used to localize patterns of brain activity related to the two facial emotions using linear support vector machine-learning (SVM) classifiers (Fig. 2.1). MVPA was applied to the beta values derived from a first-level GLM of the BOLD response from each trial (Mumford et al., 2012) for each of the 7 a priori face-processing regions of interest (Haxby et al., 2000; Wegrzyn et al., 2015), resulting in 7 classifiers per participant. Subjects who failed quality control or had classifiers that did not significantly decode above chance level were

removed from further analysis (*n*=8). In the remaining group, above-chance classification was possible in all 7 regions of interest (Fig. 2.2).

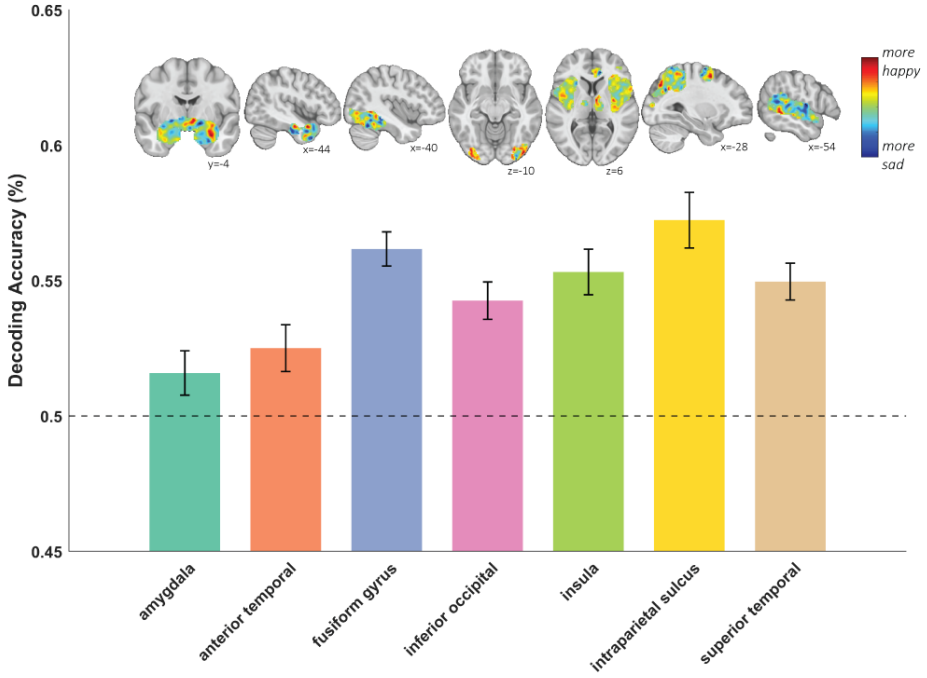

Fig. 2.2. *Decoding performance. Mean decoding accuracy (n=45) from each region of interest. Error bars depict standard error of the mean. Brain slices show SVC weights from a sample subject with warm and cold colors representing weighting towards happy and sad, respectively.*

2.5.2. Decision Making Task: Behavioural Results

Participants then engaged in the dynamic task, with easy and ambiguous trials. RTs on easy trials (with gradually increasing information) were significantly faster ($\chi^2_F(1,52)=138.77$, $p<.0001$) and responses more accurate ($\chi^2_F(1,52)=197.32$, $p<.0001$) relative to ambiguous trials (Fig. 2.3). RTs on ambiguous trials were bimodally distributed with responses tending to either be early or late. Overall, subjects also responded faster ($\chi^2_F(1,52)=46.30$, $p<.0001$) and more accurately ($\chi^2_F(1,52)=31.42$, $p<.0001$) to trials that were heading towards the happy than the sad direction.

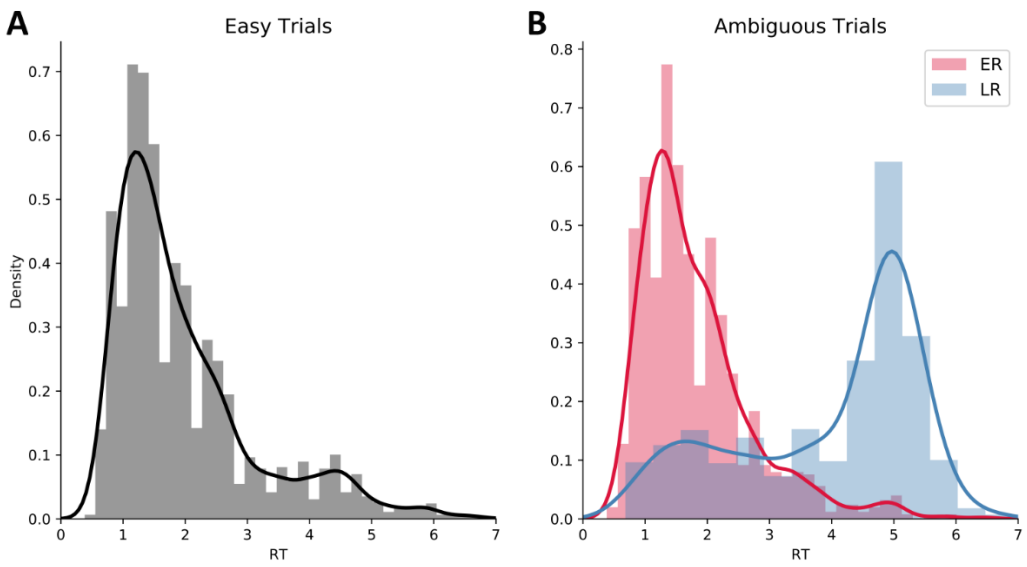

***Fig. 2.3**. Reaction time distributions. Histogram of reaction time for **(A)** easy and **(B)** ambiguous trials. Solid lines reflect the gaussian kernel density estimation. ER: early responders (n=21); LR: late responders (n=24).*

2.5.3. Fusiform Code Modulates Drift Rate on a Trial-By-Trial Level

SVM weights from the classifiers derived from the static task were projected to the BOLD effect size maps in each trial of the dynamic task to determine the regional MVPA "code" while viewing the morphing video. Two central hypotheses were tested using HDDM (Wiecki et al., 2013).

First, we assessed basic assumptions of the model without inclusion of any fMRI data. This involved modulating drift rate by differences in the information available as determined by trial type (analogous to motion coherence in random dot motion tasks (Ratcliff & McKoon, 2008)). High (absolute) drift rates result in faster responses and fewer errors, whereas a drift around zero indicates chance performance with long RT. The drift rate parameter calculated using this basic model was correlated with participants' overall accuracy in predicting the correct emotion at the end of a trial (r=.3331, p=.0271), even when RT was used as a covariate in a partial correlation (r=.302, p=.0463), suggesting that drift rate was a better reflection of behavioural performance than RT alone. Consistent with the behavioural data (above), there was a bias towards the happy decision threshold (z, mean=0.5606±0.0019).

Second, we tested whether drift rate reflected the regional fMRI MVPA code from our seven regions of interest on a trial-by-trial level (Fig. 2.4A). We estimated posterior distributions not only for basic model parameters, but the degree to which these parameters are altered by variations in neural measures. Compared to a base model, allowing fusiform MVPA code to modulate drift rate yielded an improved model fit (difference in DIC=26.29) whereas MVPA codes from the other 6 regions did not improve model fit (Fig. 2.4B). Thus, model selection provided strong evidence that trial-by-trial variations in drift rate are modulated by fusiform code as a measure of the evidence for facial emotion. Moreover, while facial emotion is reflected in the entire set of *a priori* regions, only information in the fusiform gyrus appeared to influence the decision.

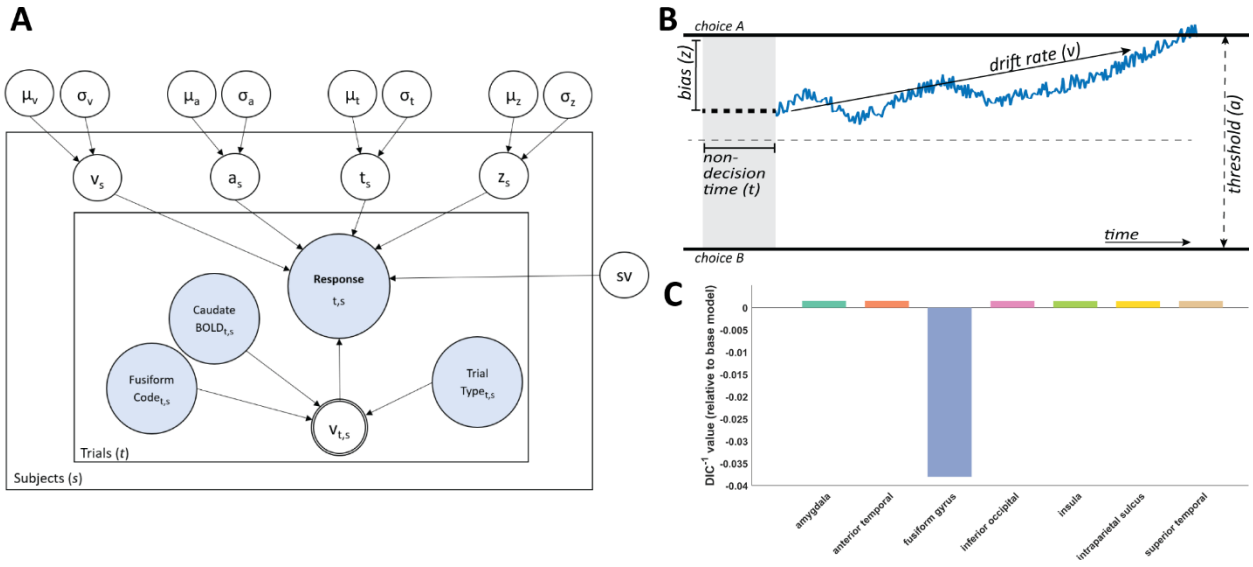

Fig. 2.4. *Hierarchical Drift Diffusion Model (HDDM). **(A)** Illustration of the model with trial-wise neural regressors. Decision parameters including drift rate (v), decision threshold (a), non-decision time (t), bias (z) and standard deviation of drift rate (sv) were estimated for the group (circles outside the plates with: group mean (μ) and variance (σ)) and subjects (s) (circles in outer plate). Blue nodes represent observed data, including trial-wise behavioural data (accuracy, RT) and neural measures (neural MVPA code from a region as determined by projected SVM weights). Trial-wise variations in v were modulated by neural measures as well as trial type (easy or ambiguous trials). **(B)** Schematic of the drift diffusion model and estimated decision parameters. Evidence is accumulated over time until one of two decision thresholds is reached at which point a response is made. **(C)** Model comparison of the seven neural HDDMs.*

Inverse function of DIC values relative to DIC of the HDDM not containing any neural data are shown (raw DIC values can be found in Supplementary Table A2.1).

2.5.4. Neural Circuitry Interacting with Fusiform Code

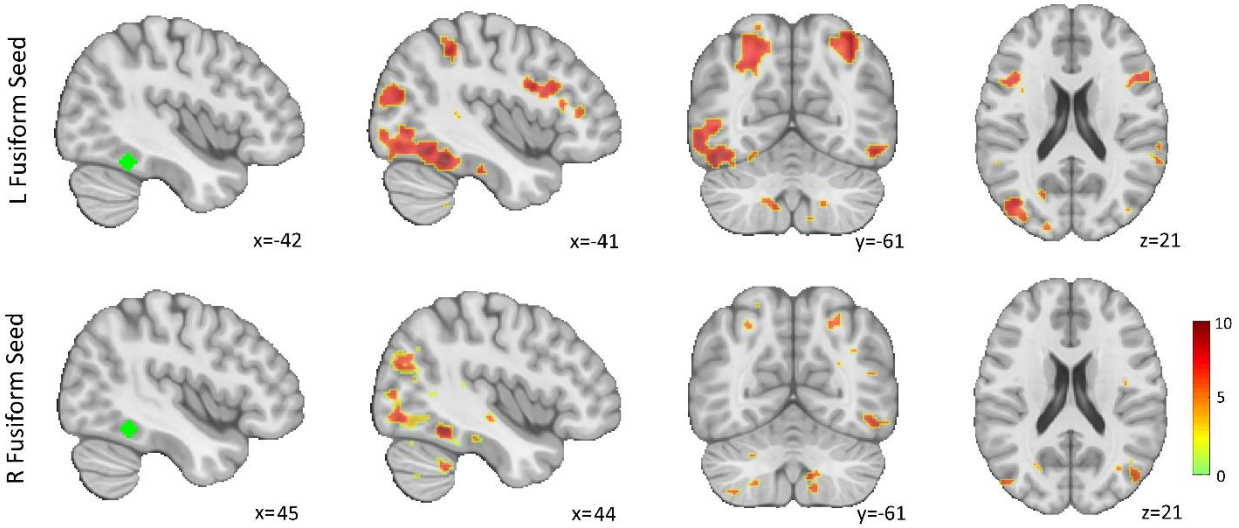

Fig. 2.5. *Information flow. Group psychophysiological interaction (gPPI) from a left (top row) and right (bottom row) fusiform seed as parametrically modulated by the multivariate fusiform code for emotion. Color bar represents t-values.*

We were interested in exploring the broader neural circuits that interact with the fusiform face area during perceptual decisions. We used a generalized psychophysiological-interaction (gPPI) analysis (McLaren et al., 2012) to identify brain regions with activity that covaried with the activity of fusiform "seed" voxels as parametrically modulated by the fusiform code. This allows us to identify putative downstream areas that receive the information decoded in the fusiform gyrus in the dynamic task. Two gPPI analyses were conducted with two 6mm spherical seeds: one in the left fusiform (center: x=-42, y=-48, z=20) and one in the right fusiform (center: x=44, y=-48, z=-16). We found significant increases in connectivity within the entire ventral face processing stream posterior and anterior to the fusiform seed, including multiple areas along the lateral occipital cortex and superior temporal sulcus (Fig. 2.5, Supplementary Table A2.2). There was also connectivity with several portions of the dorsal visual stream, namely the superior parietal lobule, inferior parietal sulcus, and supramarginal gyrus, moving anteriorly to premotor areas that encompass the frontal eye

fields. In addition, for the left fusiform seed alone, there was also connectivity with inferior frontal gyrus, dorsolateral prefrontal and orbitofrontal cortex.

2.5.5. Individual Differences in the Tendency to Wait

To further probe the role of fusiform MVPA code, we tested whether the magnitude of this code may differ in easy versus ambiguous trials. In easy trials, the absolute fusiform code significantly differed between correct and incorrect trials (z=2.212, p=.0269). This was the not the case in ambiguous trials with no difference in fusiform code observed between correct and incorrect trials (z=-0.103, p=.9179). Analysis of Variance revealed a significant interaction effect (F(1,43)=4.381, p=.042) but no main effect for either accuracy (p=.241) or condition (p=.086) on fusiform code. However, a proportion of participants tended to respond rapidly during ambiguous trials, before there was enough information to arrive at a decision (Fig. 2.3B). To disentangle these individual differences, we conducted a post-hoc analysis comparing subjects who tended to respond when no information was present in an ambiguous trial versus those who tended to wait for information to be available before responding. Subjects were split into two groups: (1) early responders who, on >=80% of ambiguous trials, responded during the first two-thirds of the trial before information ramped towards one direction (N=21) and (2) the rest, who were categorized as late responders (N=24). Across the three runs, early responders demonstrated no significant changes in RT (F(2,46)=0.433, p=.651) suggesting no learning effect (average RT for run 1=1.819s, run 2=1.835s, run 3=1.773s). Conversely, late responders seemingly learned to slow down over time (average RT for run 1=3.690s, run 2=4.019s, run 3=4.156s) (F(2,40)=5.920, p=.006). As expected, early responders had significantly lower decision thresholds (mean=2.671±0.724) than late responders (mean=5.067 ±0.1.114) in the non-neural HDDM model (t(43)=-8.661, p<.0001). Early responders were significantly less accurate in predicting trial outcome (mean=53.17%, stdev=0.05) than late responders (mean=77.22%, stdev=13.12) (z=-5.604, p<.0001) in ambiguous trials. Early responders had accuracy close to chance in ambiguous trials, suggesting that they were guessing based on partial information.

We next examined the regression coefficients to determine the relationship between trial-by-trial variations in fusiform code and drift rate in a post-hoc analysis (see methods). Our data was split three-ways to generate separate models in HDDM: (1) easy trials across all subjects, (2) ambiguous trials among late responders, and (3) ambiguous trials among early responders. This allowed us to compare drift rates of decisions made during periods of low versus high information. Greater fusiform code increased drift rates in easy trials (95.61% of posterior probability >0) and in ambiguous trials among late responders (97.86% of posterior probability >0). However, this effect was not observed in ambiguous trials among early responders (73.96% of posterior probability >0) (Fig. 2.6). A post-hoc independent samples Kolmogorov–Smirnov test indicates that the distributions of the posterior probability in early and late responders significantly differed from one another (D=0.688, p<.0001). Taken together, our results suggest that fusiform code does not simply drive increases in drift rate, but that this relationship depends on the quality of information as well as individual differences. Early responses during ambiguous trials are made before information is available, therefore the fusiform code cannot affect the response or the modeled drift rate. This further supports the interpretation that the fusiform code is a measure of the evidence that drives the response.

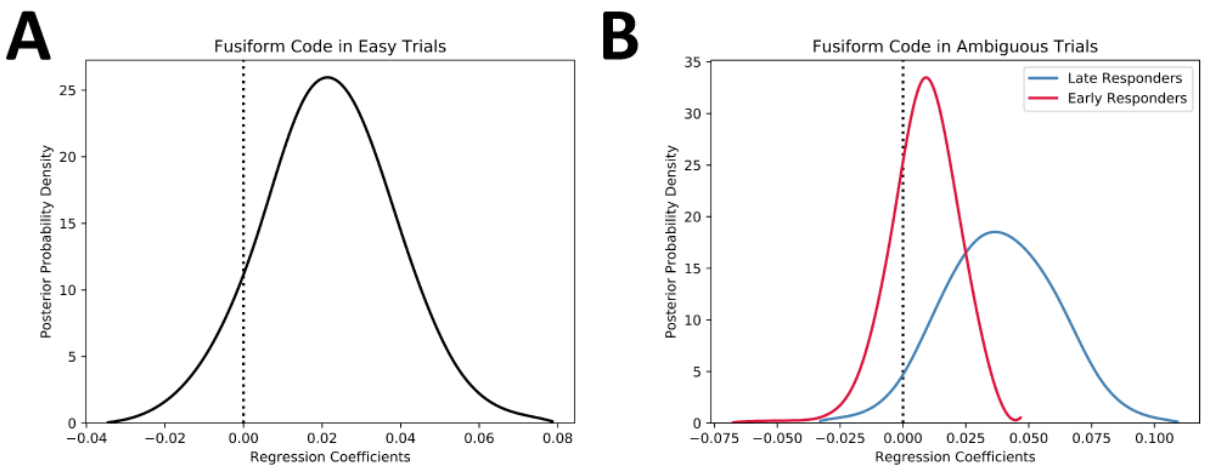

Fig. 2.6. *Posterior probability density for modulation of drift rate.* ***(A)*** *Easy trials,* ***(B)*** *ambiguous trials split by early (ER) and late (LR) responders. Peaks reflect the best estimates, while width represents uncertainty.*

2.5.6. Caudate BOLD Signal May Reflect Inhibition

We then tried to determine what neural signals differed between late and early responders. A whole-brain group-level GLM of late, versus early, responders revealed no significant differences. However, there was higher caudate activation in two clusters ((1) t=4.45; x=-8, y=4, z=18; (2) t=3.97; x=-8, y=18, z=2) after small volume correction using a structural caudate mask (alpha=.05) as an *a priori* region of interest (Ding & Gold, 2012; Thura & Cisek, 2017) when comparing ambiguous versus easy trails, taking into account the parametric modulation of the fusiform (Fig. 2.7B). This suggests that caudate activity plays a role and may serve to slow down decision in favor of a more accurate choice. Conversely, lower caudate BOLD activity among early responders potentially reflects disinhibition resulting in response prior to having accrued enough evidence.

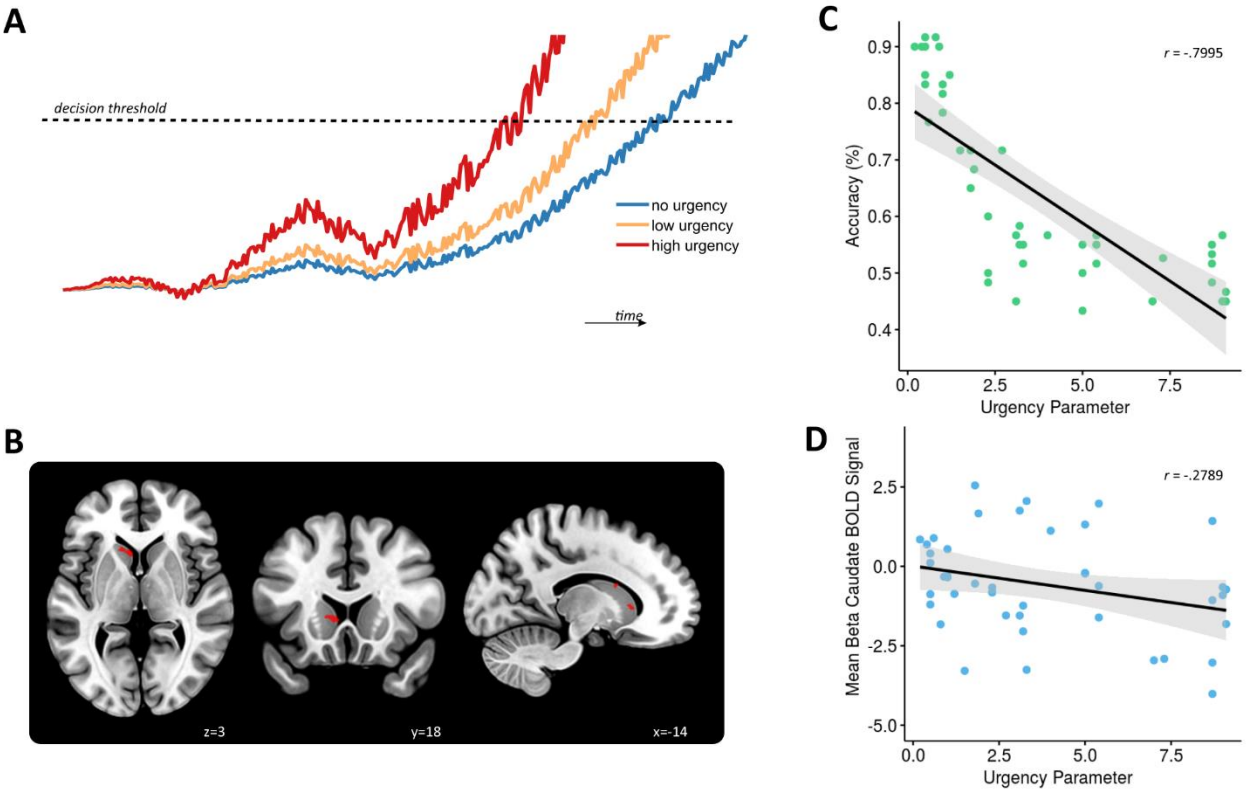

Fig. 2.7. *Urgency gating.* ***(A)*** *Predicted neural activity y for a sample trial as estimated per the urgency gating model ($y(t) = x(t) * u(t)$) across time t. This is determined by multiplying a filtered evidence variable x with no (mirroring the drift diffusion model), low, or high urgency u. Both x and u change across time, with u growing as a linear function of time. Once*

$y(t)$ crosses the decision threshold, a decision is made. ***(B)*** *A whole-brain group-level general linear model (GLM) revealed that early, versus late, responders had lower caudate activation in two clusters ((1) t=4.45; x=-8, y=4, z=18; (2) t=3.97; x=-8, y=18, z=2), highlighted in red, after small volume correction using a structural caudate mask (alpha=.05) when comparing BOLD activity, that was parametrically modulated by the fusiform code, between ambiguous versus easy trails. An estimated urgency parameter was negatively correlated with* ***(C)*** *performance accuracy among ambiguous trials (r=-.80, p<0001) and* ***(D)*** *mean beta of caudate BOLD signal from within the two significant clusters from our GLM analysis (r=-.28, p=.06).*

2.5.7. Testing the Caudate Signal with the Urgency Gating Model

The caudate is not typically implicated in facial processing (Haxby et al., 2000). Therefore, we sought to test whether its involvement here reflected a not previously described role in facial emotion processing or whether it may be involved in another aspect of decision-making that is independent of the sensory information content, as hypothesized by the urgency gating model. We ran an SVM classifier per participant restricted to the caudate to decode happy and sad faces in the training task. We found that, as opposed to the fusiform and other face processing areas, caudate activity did not decode facial emotions better than chance (mean=50.08%±0.06). Furthermore, we found that adding the trial-by-trial caudate BOLD signal extracted from the aforementioned clusters to the HDDM model did not improve model fit nor did it significantly modulate the drift rate (Supplementary Fig. A2.1). Taken together, this suggests that the caudate did not decode facial information in this task, but rather, perhaps reflects another decision variable untested by the HDDM.

Given the growing literature in support of an "urgency" gating signal (Cisek et al., 2009)(Fig. 2.7A) and the hypothesized role for the basal ganglia in this gating, we tested whether the caudate BOLD may reflect this decision parameter. We used a second model (see methods) that directly tested whether an additional urgency parameter may multiplicatively add to the evidence accumulated, driving it towards a decision threshold, as described by Thura et al. (2012). First, we validated that parameter fits by a non-hierarchical DDM (nDDM) model without urgency corroborated the non-neural basic HDDM results. The estimated decision threshold parameter per participant generated from these two models were highly correlated (r=.9461, p<.0001). Next, we tested whether a fitted urgency parameter added to

this nDDM model may relate to the caudate BOLD signal from our clusters. We found that the mean caudate BOLD activity per subject negatively correlated with participants' urgency parameter with marginal significance (r=-.2789, p=.0636) (Fig. 2.7D). Urgency was strongly related to decreased accuracy among ambiguous trials (r=-.7995, p=<.0001) (Fig. 2.7C). We did not find any significant correlation between urgency and any of our questionnaire measures of impulsivity (i.e., BIS-11, BIS/BAS) (p>.05) (Supplementary Table A2.3).

2.6. Discussion

Much research on decision making has used simple choice paradigms based on visual evidence, such as dot motion tasks. When used in non-human primates, these tasks allow accurate characterization of the properties of sensory inputs, fitting of computational models to behaviour, and identification of neural activity that reflects the underlying sensory evidence or decision variables (Gold & Shadlen, 2007). However, these paradigms are difficult to use in human participants, where trial numbers are usually smaller, and the ability to accurately measure neural activity limited. Here, we took advantage of the large body of knowledge on face processing studied with fMRI, combined with MVPA and hierarchical Bayesian modelling, to overcome these limitations.

We used a dynamic task in which participants had to identify the correct emotion from face pictures that gradually transitioned from neutral to happy or sad. Applying machine learning to fMRI data from a training task, we identified patterns of neural activity that encode facial emotion information. We then applied the individual decoders to the dynamic task and showed that the MVPA code in the fusiform gyrus reflected the evidence used to make a choice, as suggested by its relation to computational modelling parameters (drift rate) and by connectivity patterns to areas implicated in sensory decoding, decision-making, and motor control. This suggests that the neural MVPA code was driving decision in our task.

Multivariate encoding of sensory information was found to reflect adjustments of decision parameters in our evidence accumulation model. We confirmed previous MVPA studies by

showing that facial emotion can be decoded from each of 7 brain regions hypothesized to form a distributed system for facial emotion processing (Haxby et al., 2000; Wegrzyn et al., 2015). However, only the MVPA code from the fusiform gyrus contributed to the drift diffusion model. There was a clear distinction between it and the other 6 regions in terms of DIC (Fig. 2.4C). This suggests that, while emotional facial features lead to recoverable neuronal activity in the entire face processing network, the fusiform gyrus is central to decoding and feeding the information forward in this decision-making task. These results are in keeping with recent evidence that the fusiform gyrus is especially involved in emotion processing (Harry et al., 2013; Wegrzyn et al., 2015). On the other hand, the amygdala, sometimes postulated to specifically decode facial emotion (Haxby et al., 2000), did not influence evidence accumulation in our model. Further support for the role of the fusiform comes from the fact that the strength of the emotional code derived from MVPA was correlated with the estimated drift rate. Single cell recordings in monkeys have shown that drift rate is proportional to the signal-to-noise or coherence of the stimulus (Gold & Shadlen, 2007), implying that better sensory evidence is associated with faster accumulation. Note that the relationship between fusiform code and drift rate was contingent on the trial type and on individual differences in participants' tendency to wait for more information before deliberation: it only influenced drift rate in easy trials and for late responders on ambiguous trials. In early responders on ambiguous trials, fusiform code did not contribute to evidence accumulation; this is expected, as there is insufficient evidence in the early portion of ambiguous trials. In sum, our results point to the fusiform gyrus as the key node in decoding facial information and accumulating evidence for the purpose decision-making in this experiment.

The fusiform gyrus decodes the sensory information, but does it feed this information forward for the purpose of computing a decision variable (Gold & Shadlen, 2007)? We used generalized PPI to identify brain regions where functional connectivity with a seed in the fusiform gyrus was modulated by the fusiform MVPA code. This approach attempts to go beyond simple connectivity to map the actual flow of information used in the task. It has a similar goal to other multivariate pattern covariance methods proposed previously sometimes referred to as Informational Connectivity (Anzellotti et al., 2017; Coutanche & Thompson-Schill, 2013). While

these analyses do not reveal directionality, they suggest possible pathways by which information flows to a series of regions belonging to the ventral and dorsal visual streams as well as premotor and cerebellar regions. Informational connectivity with fusiform was found along several more posterior areas of the visual system, likely representing visual information streaming from occipital cortex to fusiform. In the forward direction, the observed connectivity pattern suggests that face information flows to ventral stream regions implicated in object identification (Mishkin et al., 1983), such as the superior temporal sulcus, and dorsal stream areas involved in action specification (Goodale & Milner, 1992). The latter regions included the inferior parietal sulcus, superior parietal lobule, supramarginal gyrus, and frontal eye fields. All of these regions have been previously implicated in sensory evidence accumulation in monkeys and humans (Gold & Shadlen, 2007; Mulder et al., 2014). The inferior parietal sulcus, which corresponds to the lateral intraparietal area in monkeys, is thought to receive sensory evidence information from relevant sensory areas (motion sensitive areas in the case of moving-dot tasks, the fusiform in the current study), and to convert this into a decision variable that is then passed on to premotor areas (Gold & Shadlen, 2007; Hanks et al., 2006). Our results support this model, by demonstrating (1) that sensory evidence is computed in the fusiform, and (2) that the fusiform exhibits informational connectivity with inferior parietal sulcus and premotor areas. This informational connectivity pattern can be interpreted in the light of the affordance competition model (Cisek, 2007), in which information related to sensory representations and action selection constantly interacts as it moves from occipital to motor areas, and where decisions emerge from a competition between relevant motor outputs. This model predicts that sensory decoding should feed information forward to the medial temporal, parietal and premotor areas involved in converting sensory information into action, as shown here.

Previous fMRI studies have attempted to image regions involved in evidence accumulation (reveiwed in: Mulder et al., 2014). Typically, researchers look for correlations between BOLD signal and fitted values of drift rate or computed evidence variables. However, in studies to date, it has not been possible to use fMRI to discriminate between neural representations of sensory evidence as opposed to decision variables. For example, Wheeler et al. (2015a) designed a paradigm in which shapes appeared successively to indicate cumulative probability

in favour of a left or right hand response. Thus, at each time point it was possible to relate BOLD to an evidence variable. They were able to identify brain regions involved in evidence accumulation independent of action preparation, but because the visual stimuli were similar, sensory evidence accumulation could not be imaged. Braunlich and Seger (2016), using a similar paradigm, found that evidence thus defined correlated with BOLD in motor regions (contralateral motor cortex and putamen, ipsilateral cerebellum), suggesting that a motor decision rather than a sensory evidence correlate, was being imaged. Using a stock-picking paradigm with sequential probabilistic information, Gluth et al. (2012) found that a calculated decision variable was reflected in value-coding brain areas (ventromedial prefrontal cortex and ventral striatum) while a response variable was tracked in motor areas. Another study using a moving-dot paradigm identified correlates of the accumulation rate in the inferior parietal sulcus, but once again this likely reflected a decision variable rather than sensory evidence (Nagano-Saito et al., 2012). In sum, previous fMRI studies imaged decision variables or value signals related to different choice options rather than the accumulating sensory evidence that guides these choices. By using MVPA, we were able to distinguish neural responses to the two choice stimuli used here and show that this response reflected evidence accumulation since it modulated the drift rate in our Bayesian model.

The basal ganglia did not display PPI connectivity to fusiform, nor did they appear to encode face information, however they did emerge in our analysis of group differences, albeit only after small volume correction. Specifically, there was greater caudate activation during ambiguous stimulus viewing in late versus early responders. In the affordance competition model the basal ganglia are thought to bias decisions via cortico-striatal connections (Cisek, 2007; Thura & Cisek, 2017). One type of response bias is to slow down in ambiguous situations, which one could call “negative urgency”. Indeed, Cisek et al. (2009) have suggested that the pure evidence accumulation models do not fully account for observed behaviour when speed-accuracy trade-offs are present or information is ambiguous. They suggest the presence of an additional model parameter, termed urgency, that is independent of the sensory evidence, but multiplies the drift rate to hasten or slow down decisions when the context demands it. Fortuitously, approximately half our subjects slowed down during ambiguous trials, waiting for

the stimuli to morph towards the final emotion, and the others did not. One way for race models to accommodate slower responses is to raise the decision threshold, but because easy and ambiguous trials were intermixed, participants did not have *a priori* knowledge of which type of stimulus would be displayed in any given trial. Another way to account for slower responses on ambiguous trials is lower urgency. Our findings implicate the caudate in slowing down decisions when the evidence is ambiguous. Moreover, there was a weak negative correlation between caudate BOLD effect size during ambiguous trials and the fitted urgency parameter; therefore, caudate BOLD may reflect negative urgency. These results are consistent with microelectrode recordings in the basal ganglia of monkeys in which neuronal firing was insensitive to evolving sensory evidence but could influence the response speed by modulating activity in sensory processing regions (Thura & Cisek, 2017). The observed caudate activity in our study may reflect the indirect pathway of the basal ganglia – originating from a striatal population of projection neurons thought to generate a net inhibition resulting in a "stopping signal" (Frank & Claus, 2006). For example, in a fMRI study with a dot-motion task, we found that participants slowed their responses when offered the possibility of monetary reward, and that caudate activation during these trials correlated with a raising of the decision threshold (Nagano-Saito et al., 2012). Dopamine signaling was shown to underpin this effect. It should be noted that evidence-independent urgency signals could end up being modeled as drift rate or threshold in pure evidence accumulation models; to disambiguate urgency from pure evidence accumulation, one needs to dynamically manipulate the amount of information presented, as in the present study (Cisek et al., 2009). It must be noted however that the caudate effect only emerged after small-volume correction of the neuroimaging data, meaning that it should be confirmed in future studies.

Findings from our study should be considered in light of its limitations. First, both the evidence accumulation and urgency signal are hypothesized to grow in time. Though we used multiband fMRI acquisition to reduce repetition time below 1 second, without the ability to record at millisecond resolution, the estimated neural parameters of each model may lack in precision. Second, we used facial emotion as an exemplar of sensory information for perceptual decision-making. Future studies should test whether MVPA decoding can also be applied to other forms

of sensory information, and whether the relationship to decision parameters holds. Third, though we observed caudate activity thought to reflect a dopaminergic stopping signal, our study does not measure dopamine nor the indirect pathway *per se*. The implications of this pathway in human decision-making in ambiguous environments merits further research.

2.7. Conclusion

By combining model-driven multivariate fMRI analysis, psychophysics, and computational modelling, we characterized two decision parameters underlying human perceptual decision-making processes (drift rate and urgency signal) in the setting of dynamic, changing environments. Our results reveal how these decision parameters are encoded in the human brain and indicate that MVPA techniques can be used to probe and disentangle the biological underpinnings of the decision process. This may be of particular relevance to characterizing brain phenotypes related to disorders of decision-making (e.g., addictions, impulse control disorders, and obsessive-compulsive disorder).

CHAPTER 3. Disentangling the neural decision parameters involved in perceptual decisions in humans.

3.1. Preface

EEG may be better suited to parse the temporal characteristics of decision parameters and differentiate how neural signals may evolve and devolve with time. As a continuation from Chapter 2, we tested the same dynamic perceptual decision-making task in a relatively large cohort of subjects while they underwent EEG. In this chapter, we replicated previous work that demonstrated a domain-general neural correlate of the decision variable, namely the CPP, which gradually builds throughout the trial and ramps steeply close to the time of response. We provide evidence that the CPP signal reflects the combined influence of sensory evidence as well as an urgency signal. To our knowledge, this study is the first to directly test the trial-by-trial influence of urgency on a decision variable in naïve human subjects. Furthermore, we were able to dissociate this decision variable signal from an ERP that was evoked earlier in the trial, contradicting previous findings that suggest these two signals are one and the same. This highlights the importance of having high temporal resolution and sufficiently long trial times to properly tease apart neural signals temporally. Our results reveal how neural correlates of decision parameters may unfold in time and provide further evidence for the role of an urgency signal in perceptual decisions. This work is currently in preparation for submission.

3.2. Abstract

Conventional models of perceptual decision-making posit that noisy sensory evidence is integrated and determines choice based on the decision threshold reached. Neural signals bearing these properties (i.e., decision variables) have been characterized in non-human primates but complimentary data in humans is largely missing. Moreover, recent findings suggest an additional evidence-independent, time-variant urgency signal is in play and decreases the amount of sensory evidence needed to commit to a choice as time elapses. Our

findings provide evidence that activity of a previously identified neural decision variable, namely the centroparietal positivity (CPP), reflects the combined influence of sensory evidence and an endogenous urgency signal. We demonstrate that the predicted neural signal from a urgency gating model fitted with the observed CPP activity over time. Inter-individual variability in this urgency signal potentially accounted for why certain individuals are prone to fast and erroneous decisions, especially when signal-to-noise ratio of the decision environment is low. These findings highlight potential determinants of perceptual decisions in human perceptual decision-making and reveal how neural signal dynamics may unfold throughout the decision formation.

3.3. Introduction

Imagine you are arriving at a stop light and as you approach, the light turns yellow. You must consider the relevant information at your disposal: your distance from the stop, the speed of your vehicle, the traffic condition etc. Importantly, as the stop is getting closer, there is an increasing urgency to commit to a choice and your decision is expressed through a movement – a step on either the gas or the brake. Studies of decision-making conventionally assume a stochastic accumulation of sensory evidence and a decision is made once the accrued evidence passes a criterion level, termed the decision threshold (Gold & Shadlen, 2007; Ratcliff & McKoon, 2008). Decision parameters from this class of drift diffusion models (DDMs) have predominantly received support from studies in non-human primates that have successfully identified neuronal signals encoding these ingredients (Kiani & Shadlen, 2009; Shadlen & Newsome, 2001).

While pioneering studies on the neural correlates of decision-making by proxy of the DDM in non-human/human primates have been conducted by means of simple, well-controlled experimental paradigms (e.g., random dot motion task) (Ratcliff et al., 2016), natural actions during interactive behaviour in the wild are determined by constantly changing and unpredictable environment. The notion that sensory evidence must achieve a critical threshold

before decision is difficult to reconcile with when choices are made based on little or no sensory evidence – what then drives choice commitment when there lacks sensory input to be integrated? Convergent lines of research now support the notion of an additional "urgency" signal which non-selectively elevates activity towards unchanged action thresholds, such that less sensory evidence is required for decision commitment as elapsed decision time increases (Cisek et al., 2009; Murphy et al., 2016; Thura & Cisek, 2014). While the traditional DDM models would predict the neuronal firing in evidence accumulation regions (e.g., lateral intraparietal area) to scale with sensory evidence, a model with an urgency parameter would predict such firing would additionally ramp more rapidly towards a decision threshold as time elapses. Indeed, primate single-cell recording studies indicate that this evidence-independent influence on the decision process is observable in the activity of neurons that reflect evolving decision formation (Ditterich, 2006; Hanks et al., 2014; Heitz & Schall, 2012; Standage et al., 2011; Thura & Cisek, 2016). Recently, this line of work has been extended to human decision-making using scalp electroencephalography (EEG) which characterized a centroparietal positivity (CPP) in the event-related potentials (ERPs) that traces evidence accumulation, irrespective of the feature being evaluated (O'Connell et al., 2012). Speed pressure was found to enhance representations of sensory evidence, rendering the alternatives more distinguishable, and may have a knock-on impact on steepening the CPP (Steinemann et al., 2018). However, to our knowledge, no EEG study has formally tested an urgency signal and how it may affect a neural decision variable. Moreover, the sudden-onset and discrete trial presentation coupled with short trial times often favoured in ERP research has a key shortcoming: stimuli elicit strong early sensory-evoked components that may partly obscure the dynamics of an unfolding decision process.

While previous work has illuminated the mechanistic basis of decision formation in non-human primates, complimentary data on the neural decision variables in humans remains understudied. Moreover, the influence an additional urgency signal may have on this neural evidence accumulation signal is, to our knowledge, untested. In the present study, we aim to address these outstanding issues. As a mean to disambiguate evidence accumulation and urgency processes, we designed a dynamic decision-making task more closely resembling

naturalistic settings while also allowing us to track the amount of information available in the environment (Thura et al., 2012; Yau et al., 2020). We exploited EEG's high temporal resolution to tease apart neural determinants of human decision formation. First, we hypothesized that a neural signal (i.e., N170 or P300) close to the start of the trial likely reflects the setting/adjusting of decision threshold whereas a neural signal (i.e., CPP) that ramps up in time with peak close to response reflects the evidence accrued. Second, we tested whether the predicted neural signal from our candidate models matched the actual observed data. We predict a model incorporating an urgency signal would provide a better fit with the neural decision variable. Finally, with a relatively large sample of subjects, we investigated whether individuals may exhibit differing latent levels of the endogenous urgency signal, and if this may affect the relation between neural signals and decision parameters.

3.4. Methods

3.4.1. Participants

74 right-handed young healthy adults (34 males; age mean 23.4years±5.17 standard deviation) participated in the experiment for monetary compensation. All subjects gave informed consent prior to data acquisition and were screened for current or past diagnosis of a psychiatric disorder, neurological disorder, or concussion, and moderate to severe depression (score >5 on the Beck Depression Inventory (Beck et al., 1961)). The study was approved by the Montreal Neurological Institute Research Ethics Board.

3.4.2. Experimental Design

Participants were presented short videos of a face "morphing" between expressions (Fig. 3.1). Each trial was preceded by a time-jittered fixation cross. Trials always began with a neutral expression and gradually transitioned into either a happy or sad emotion. Participants were instructed to predict whether the facial expression would be happy or sad by the end of the trial via a button box in their right hand, and to respond whenever they felt confident enough

to do so. Subjects were asked to respond both as quickly and as accurately as possible. Face stimuli were derived from the NimStim database (Tottenham et al., 2009) and manipulated to generate 18 intermediary faces that gradually transitioned in intensity of emotional expressions between a model's neutral and happy or sad emotion. Thus, emotion levels varied from 0 to 19 in both directions. Trials lasted for a maximum of 60 frames over 6secs (i.e., 10 frames per sec), plus a final image of the correct emotion (with the emotion level >15) for 1sec either immediately after a response was made or at the end of the trial if the participant had not yet made a response. In the latter case, subjects could still respond during the final frame (i.e., 61st frame) only if they had not yet done so earlier in the trial. Responses during this period were recorded but the frame would not change and continue to persist until the original 1sec window was over.

The current study consisted of two trial types (or conditions), namely "easy" and "ambiguous", which were modelled after previous work (Thura et al., 2012). These two trial types were interleaved throughout the runs and subjects did not know, at the start of the trial, which trial type will proceed. In easy trials, all intermediary faces presented were of the correct emotion (e.g., in a trial in which the correct answer is happy, no sad images are ever presented). Each successive frame had a 65% chance of being one level higher than the previous frame in the direction of the correct emotion. By the final frame, all trials had an emotion level >16. In ambiguous trials, frames within the first two-thirds of the trial (i.e., up to the 40th frame) generally hovered around a neutral valence. Each successive frame had a 50% chance of being one level higher than the previous in the direction of the correct emotion and could only reach a maximum of emotion level 7. To prevent, for example, many slightly happy and a few very sad images being presented, the maximum emotion levels presented in the correct and incorrection directions were kept within two levels of each other. In the final third of the trial, there was a steep increase of emotion level in favour of the correct emotion, with a 95% chance that a given frame would be exactly one level higher than its predecessor. As with the easy condition, all trials had an emotion level >16 by the final frame.

Each subject partook in 120 trials total, divided equally across 3 blocks. Trials were evenly split between happy and sad (determined by the emotion at the frame frame), and between easy and ambiguous. Trial order was randomized in every block.

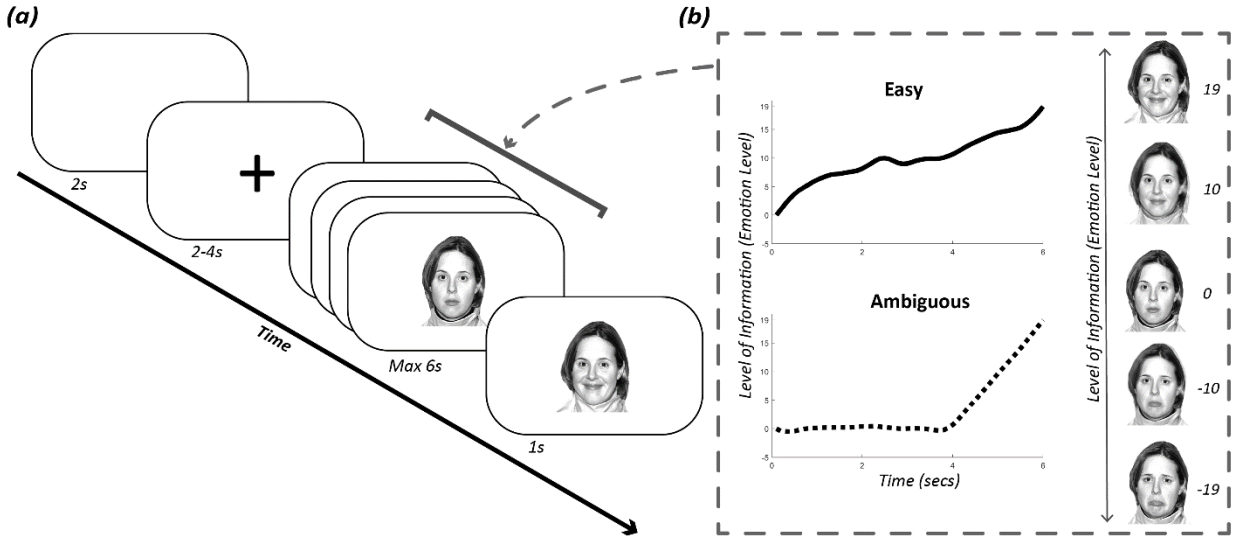

Fig. 3.1. *Schematic of task design.* ***(a)*** *Progression of a single trial begins with a blank image followed by a time-jittered fixation cross. A short video that start at a neutral facial expression which transitions into a happy or sad emotion is then presented. Participants are asked to respond what they think the final emotion will be and to do so whenever they felt confident in their prediction. If either a response is made or 6secs have elapsed, an image of the correct emotion is presented.* ***(b)*** *Two types of trials were employed: "easy" and "ambiguous". In easy trials, facial expressions gradually morphed towards one of the two emotions. In ambiguous trials, facial expressions remain relatively neural until two-thirds of the trial has elapsed, after which point emotion rapidly ramped up towards happy or sad.*

3.4.3. EEG Acquisition and Preprocessing

EEG was recorded continuously using a 256-channel high-impedance HydroCel Geodesic Sensory Net (Electrical Geodesic, Inc., Eurgene, OR) using the NetStation 5 acquisition software (Electrical Geodesic). As per manufacturer standard recommendations, electrode impedance levels were kept below 50Ω during acquisition. Data were collected with a sampling rate of 1000Hz using the electrode Cz as reference with online visualization filters of 60Hz for Notch, 5Hz for high-pass, and 120Hz for low-pass.

Raw data were preprocessed offline using the Automagic pipeline (Pedroni et al., 2019). First, bad channels were identified using PREP (Bigdely-Shamlo et al., 2015) in which a 1Hz high-pass filter is applied, power-line noise removed, and robust average referencing iteratively implemented to detect and interpolate bad channels to arrive at an average reference that is not affected by artifacts. Bad channels were then excluded as to avoid contamination in later preprocessing steps. Second, continuous EEG recordings were filtered with a bandpass filter of 0.1-60Hz. Third, artifacts related to eye-blinks and muscle movement were corrected for using the Multiple Artifact Rejection Algorithm (MARA) – a supervised learning algorithm that classifies whether components identified by independent component analysis qualify as artifacts based on established expert ratings (Winkler et al., 2011). Finally, the previously excluded bad channels were interpolated and the data was down-sampled to 250Hz for computational efficiency. Data quality after preprocessing was assessed automatically by Automagic and confirmed by subsequent manual inspection. Further details regarding the Automagic pipeline can be found online (https://github.com/methlabUZH/automagic). After preprocessing and quality control, data from 57 participants were used for further analysis.

Preprocessed data files were imported into MNE-Python (Gramfort et al., 2013; Gramfort et al., 2014) for statistical analysis and visualization. Epochs were created around the stimulus onset (-1,000ms to 8,000ms time-window) and response (-1,000ms to 1,000ms time-window), with both baseline-corrected for the 500ms preceding stimulus onset. Epochs in which the activity exceeded ±150µV were excluded (average number of trials post-preprocessing: Easy=57.92±4.47, Ambiguous=57.74±4.64).

3.4.4. Event Related Potentials

Here we focused on three ERPs of interest: the N170, P300 and centroparietal positivity (CPP).

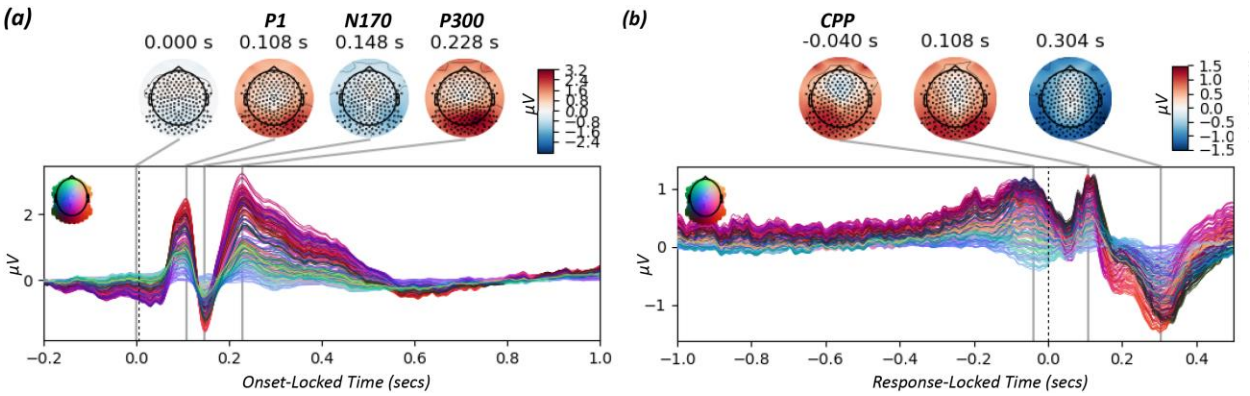

Fig. 3.2. *Grand average across all trials and subjects (N=57) for* ***(a)*** *onset-locked and* ***(b)*** *response-locked epochs. Topomaps for the timepoints of peak activity are depicted above the waveforms, with warmer and colder colors indexing higher and lower activity, respectively.*

The N170 is a face-sensitive visually evoked ERP elicited over posterior visual cortical areas. It's amplitude is thought to scale with how similar the stimuli is to a face (Eimer, 2011) but has recently also been cited as a domain-general response to unexpected perceptual events (Robinson et al., 2018). Previous work using a face-car visual discrimination task to test the drift diffusion model found that the N170 reflected an early perceptual event that is not directly related to the actual decision (Philiastides et al., 2006; Philiastides & Sajda, 2006). Based on the existing literature and on our grand-average waveform, we extracted the N170 as the peak amplitude between 120-200ms at two lateral occipital sites (E114 & E168) after stimulus onset (Supplementary Fig. A3.1).

The centroparietal "P300" or "P3b" has a long-established role in decision-making and is well defined in the literature, though its exact role in the decision process is debated (Polich, 2007; Sutton et al., 1965). We focused on the posterior P3b specifically, instead of the frontal P3a, as it has been previously linked with the CPP component (O'Connell et al., 2012; Twomey et al., 2015) and shown to modulate onset of a neural decision variable based on task difficulty (Philiastides et al., 2006). In keeping with the literature and on the maxima and time distributions observed in the grand-average waveform across our participants (Fig. 3.2), P300 was defined as the peak amplitude between 200-400ms at electrode site Pz after stimulus onset and the maximum amplitude reached has been previously implicated in decision-making (Picton, 1992).

More recently, a CPP component that spatially overlaps with the P300 has been also identified and is thought to index a developing decision variable in the decision-making process (Kelly & O'Connell, 2013; O'Connell et al., 2012; van Vugt et al., 2019). Unlike the traditional conception of ERP components as unitary processes, the CPP is thought to be a gradual signal that scales with the strength of sensory evidence, peaking close to the time of decision/action. This rise-to-threshold like activity is thought to be insensitive to sensory modality or target feature (O'Connell et al., 2012) and resembles the drift rate parameter of the DDM which indexes the speed of sensory evidence accumulated over time. Unlike the P300, there is no clear established time-window of interest for CPP with variations in the relative timing used likely reflecting differences in paradigms and design (O'Connell et al., 2012; van Vugt et al., 2019). As such, we took a data-driven approach to identify a time-window of interest over which we could observe CPP signal buildup. As with O'Connell et al. (2012), we calculated the temporal slope of the activity from each participant's average waveform at electrode site Pz in moving windows of 100ms length in 10ms steps, starting from -1,000ms to response execution (i.e., 0ms). Signal buildup rate was computed as the slope of a straight line fitted to the unfiltered signal within each sliding window. A one-tail permutation t-test implemented via *mne.stats.permutation_t_test* with 5,000 permutations was then used to identify signal buildup rates that significantly differed from 0 across all subjects in a positive direction – indicating CPP activity is ramping up – and are marked in black below the waveforms in Fig. 3.5. The cumulative sum of activity within this time-window of interest was then used to index CPP signal buildup for further analysis. An alternative to using the cumulative sum is to calculate the area under curve; however, these two signals are almost identical (Spearman's rho=.999, $p<.0001$) and did not affect our findings. We additionally compared our analysis to results from a larger cluster, centered on the Pz (5 electrodes: E101, E100, E129, E119, E110, E128) (Supplementary Fig. A3.1 & A3.2), to ensure our findings replicated.

3.4.5. Time-Frequency Analysis

In addition to standard ERP, different frequencies of oscillatory activity in the EEG signal has been linked to decision parameters of the DDM. The theta band power from mid-frontal

electrodes, for example, has been linked to decision threshold and is thought to reflect a gating mechanism (Cavanagh et al., 2011a; Cavanagh et al., 2011b; Frank et al., 2015). A harmonic posterior alpha signal has also been implicated (Klimesch, 2012; Kloosterman et al., 2019) as well a motor beta signal in the contralateral hemisphere to the hand for response execution (O'Connell et al., 2012). We were interested in testing whether our straight-forward, minimalistic processing analysis of ERPs was linked to these ongoing oscillatory fluctuations. To this end, we used the Morlet wavelet methods implemented via *mne.time_frequency.tfr_morlet* to assess spectral power across the trial period on our preprocessed epoch data. The trial's estimated power was then baseline-corrected for the 500ms preceding stimulus onset and resampled using *scipy.signal.resample* to match onset and response across all trials (i.e., all trials began at timepoint 0 and ended at timepoint 1 which stood for the maximum RT for the subject). Power was averaged across the frequency range for each band (alpha=0-4Hz, theta=4-8Hz, alpha=8-12Hz, beta=12-30Hz, gamma=30-45Hz). Each sample of EEG time course was z-scored and outliers (z>4.5) were replaced with the average EEG power (Frank et al., 2015). We then extracted the early (first 10% of trial time after onset) and late power (last 10% of trial time before response) for each frequency band to compared against ERPs of interest. Based on the literature, we focused on theta power from the FCz, alpha from the Pz, and beta from electrodes of the left hemisphere. We also repeated this analysis using the power for each frequency band averaged across all electrodes (Supplementary Fig. A3.3).

3.4.6. Tendency to Wait: Early versus Late Responders

As with our previous work (Yau et al., 2020), we observed two distinct groups of individuals based on their performance under the ambiguous condition (Fig. 3.3) : (1) early responders (n=32), who on >=80% of ambiguous trials, responded during the first two-thirds of the trial before information ramped towards one direction and (2) the rest, who were categorized as late responders (n=25). We hypothesized that one factor that may drive this group difference lies in differences in the endogenous urgency signal.

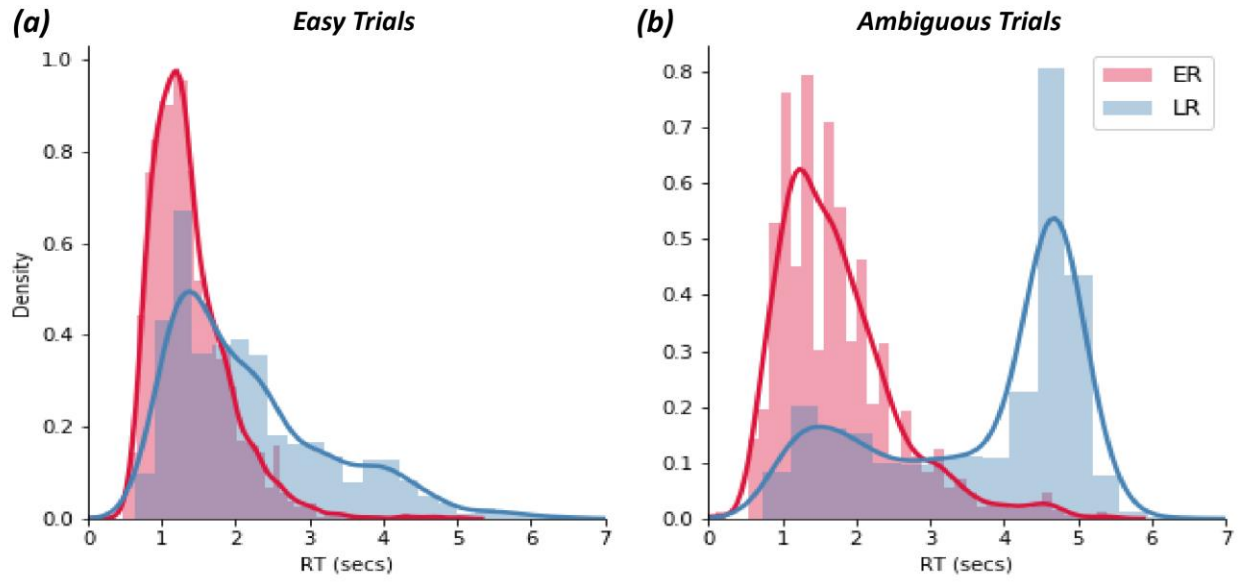

Fig. 3.3. *Histogram of reaction time distributions in* ***(a)*** *easy and* ***(b)*** *ambiguous trials. Solid lines reflect the gaussian kernel density estimation. ER: early responders (n=32); LR: late responders (n=25).*

One mixed-design ANOVA per neural signal (i.e., N170 maximum amplitude, P300 maximum amplitude, and CPP cumulative sum) were conducted to investigate the within-subject relationships of conditions (i.e., easy and ambiguous) and between-subject relationships for group affiliation (i.e., early and late responders) as well as their interaction. Given the unequal sample size, Levene's test was used to test and confirm equality of variance between the two groups. If sphericity was violated, Greenhouse-Geisser corrected degrees of freedom are reported.

In addition, given that CPP gradually ramps up in time, we tested whether CPP buildup/slope may differ between the two groups at specific time intervals within our larger time-window of interest. A two-tailed, two sample permutation t-test (*mlxtend.evaluate.permutation_test*) with 5,000 permutations was conducted per condition. Time windows where the two groups significantly differed are marked in purple below the waveforms in Fig. 3.5.

3.4.7. Hierarchical Drift Diffusion Model

Drift diffusion models (DDM) have been widely applied over the last decades and is commonly used to infer latent psychological processing underlying perceptual decision-making, and to link them to neural mechanisms (Ratcliff et al., 2016). In the DDM framework, decision-making between two alternatives is reflected by a continuous integration of relative sensory evidence over time until sufficient sensory evidence has been accumulated and a decision threshold for one of the choices is reached. The model decomposes behavioural data into four parameters: non-decision time (*t*) for stimulus encoding and response execution latencies, bias (*z*) towards one choice alternative, drift rate (*v*) for speed of evidence accumulation, and decision threshold (*a*) which determines how much evidence is needed before deliberation (Fig. 3.4a). The shape of the reaction time (RT) distribution determines which decision parameters are to be adjusted (Ratcliff et al., 2016).

Here, we applied a hierarchical estimation of the DDM (HDDM) (Wiecki et al., 2013), implemented in Python 2.7 (http://www.python.org), to calculate the decision parameters (Fig. 3.4b). The hierarchical design assumes that model parameters from individual participants, while varying, are not completely independent. Rather, individuals' parameters are drawn and constrained by the group distributions with group priors (Gelman et al., 2013). This Bayesian estimation is thought to be more robust in recovering model parameters, particularly when the number of trials are relatively small (Matzke & Wagenmakers, 2009; Wiecki et al., 2013). Trials that fell within 5% of each tail of the RT distribution were considered outliers that cannot be captured by HDDM (e.g., slow responses due to inaction or fast erroneous responses due to action slips) and removed from analysis (Wiecki et al., 2013). Markov chain Monte Carlo sampling was used for Bayesian approximation of the posterior distribution of model parameters. 5,000 samples were drawn from the posterior to obtain smooth parameter estimates, the first 100 samples were discarded as burn-in. Convergence of Markov chains were assessed by inspecting traces of model parameters, their autocorrelation, and computing the Gelman-Ruben statistic (Gelman & Rubin, 1992) to ensure that the models had properly converged.

As a first step, we constructed a base model whereby decision parameters are simply a function of RT and accuracy. In a second model, we expanded upon this base with a simple model that allowed drift rate and decision threshold to vary between condition (i.e., easy and ambiguous). Our third model further extended this by allowing for trial-by-trial variations in neural activity, in addition to condition, to modulate decision parameters. The estimated posterior distributions index the degree to which the decision threshold (a) are altered by variations in P300 and N170 as well as drift rate (v) by CPP buildup. Our comprehensive model is as follows: [$a(t) = \beta_0 + \beta_1 P300(t) * \beta_2 N170(t) * \beta_3 condition(t)$, $v(t) = \beta_4 + \beta_5 CPP(t) * \beta_6 condition(t)$]. In these regressions, a larger positive coefficient weight (β) indicates a stronger positive correlation between neural measure and decision parameter, and *vice versa*. Of note, distribution of the decision threshold and drift rate parameter were estimated separately for early and late responders for all models using the "*depends_on*" function in HDDM as group distributions are hypothesized to be different. Further, we iteratively added in modulators to test whether successive additions of these modulators improved model fit (described below).

Deviance information criterion (DIC), a widely used criterion for comparisons of hierarchical models, was used for model comparison (Spiegelhalter et al., 2002). A lower raw DIC value for a given model (for the whole group) favors models with highest likelihood and least number of parameters. A DIC difference of 10 is considered significant (Zhang & Rowe, 2014). All reported DIC values are relative to the base model (i.e., target model DIC minus base model DIC) – the more negative the value, the better the model fit compared to the base model. Parameters of the best fitting model were analyzed by Bayesian hypothesis testing which examines the probability mass of the parameter region in question (i.e., percentage of posterior samples greater/smaller than zero). For all HDDM analyses, we considered posterior probability ≥95% of the respective parameters being different than zero as significant.

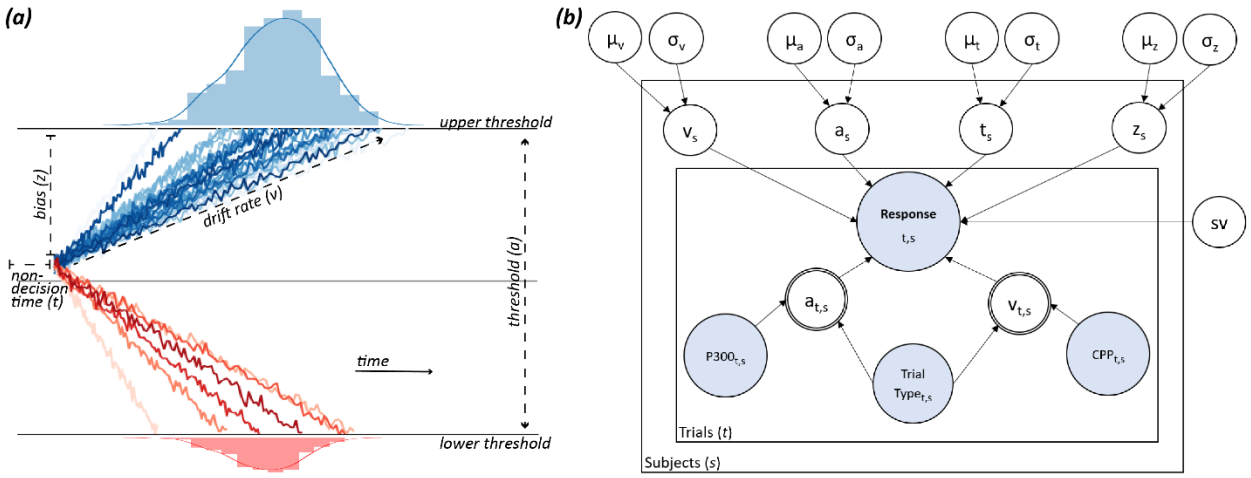

Fig. 3.4. *Overview of the drift diffusion model.* ***(a)*** *Schematic of the drift diffusion model.* ***(b)*** *Graphical illustration of the hierarchical drift diffusion model (HDDM) with trial-by-trial neural regressors. Round nodes represent continuous random variables and double-bordered nodes represent deterministic variables, defined in terms of other variables. Decision parameters including drift rate (v), decision threshold (a), non-decision time (t), bias(z), and standard deviation of drift rate (sv) were estimated for the group (nodes outside the plates with: group mean (μ) and variance (σ)) and subjects (s) (nodes in outer plate). Blue nodes represent observed data, including trial-wise behavioural data (accuracy, RT) and neural measures (P300 and CPP). Trial-by-trial variations of v and a were modulated by P300 and CPP, respectively, as well as by trial type (i.e., easy or ambiguous trials).*

3.4.8. Urgency Gating Model

Models of decision-making incorporating an endogenous urgency signal posits that choices result from a combination of signals that reflect the available sensory evidence as well as a level of urgency which grows in time (Cisek et al., 2009; Drugowitsch et al., 2012). We constructed a minimalistic urgency gating model (UGM) and a non-hierarchical drift diffusion model (nDDM) to compare against and to test whether accounting for an urgency signal may better fit our observed data.

In both models, a filtered evidence variable x was derived by the following differential equation:

$$\tau \frac{dx(t)}{dt} = -x(t) + gE(t) + G(0, N) \qquad (1)$$

At any given time *t*, the evidence *E* (i.e., level of information/facial emotion level) is multiplied by an attentional fixed gain term *g*. An intra-trial Gaussian noise variable *G*(0,*N*) with a mean of 0 and a standard deviation of *N* was added. A *N* of 6 was chosen based on previous work (Carland et al., 2019; Yau et al., 2020) and because it gave a range of simulated RTs with similar variability as the observed data in our current study. The time constant τ determines how far back in time sensory information is considered by the model. The UGM posits that only recent information is used to inform decision whereas nDDM does not; thus, τ was set to 200ms for the UGM on the basis of previous behavioural and physiological studies (Cisek et al., 2009; Thura et al., 2012; Thura & Cisek, 2014) while the maximum trial duration of 6sec was used as τ for the DDM. Evidence (*E*), gain (g), and noise (*N*) parameters were the same in both models.

Next, the filtered evidence x at a given time t was then used to compute the estimated neural activity y as follows:

$$y(t) = x(t) * u(t) \qquad (2)$$

A decision is made then the variable $y(t)$ reaches a critical decision threshold *T.* Importantly, the UGM assumes that evidence is multiplied by an urgency signal u that linearly increases with time (Cisek et al., 2009; Thura & Cisek, 2014; Yau et al., 2020). A core prediction of the UGM is that decisions made with low levels of filtered evidence x should be associated with high levels of urgency and *vice versa*. In other words, high urgency will push one to commit to a choice even if evidence for that choice is weak. On the other hand, the nDDM does not have an urgency signal u; once the variable $x(t)$ reaches threshold *T*, a decision is made. In both models, a non-decision time of 200ms was added to yield the predicted RT.

Each model adjusted for one parameter: for UGM, the u parameter and for nDDM, the *T* parameter. Both these parameters influence the means of RT distributions. An exhaustive search was implemented to find the parameter that minimized the mean squared error between each model's predicted RT versus the observed RT across all trials for a subject. The models were used to simulated 5,000 trials, the mean of which was used to compared against the real RT distributions.

Linear mixed effect models implemented via *statsmodels.mixedlm* were used to examine the relationship between the actual observed CPP signal compared to a neural code predicted by either the UGM or the nDDM at the trial-level. Subjects were included as a random variable with differing intercepts. For both the predicted and observed neural signal, buildup was determined as the cumulative sum of activity from 500ms post stimulus-onset to the time of response. This 500ms delay was to ensure that we did not confound our CPP activity with the P300 signal as they spatially overlap. The log-transformed absolute value of the predicted neural code was used for our analysis as this value had directionality towards the upper or lower bound, whereas CPP is thought to be a general evidence accumulation signal and positively ramp up regardless of the stimulus presented. As with the HDDM, trials that registered no response or with RT that fell within 5% of each tail of the RT distribution were considered outliers and discarded.

3.4.9. Statistical Analysis of Behavioural Data

Statistics for this study were conducted using packages including *pingouin (Vallat, 2018), statsmodels* (Seabold & Perktold, 2010), and *mlxtend* (Raschka, 2018) in Python 3.7 (http://www.python.org). To account for potential spurious outliers in our relatively low sample size, non-parametric tests were used to assess the following subject-level data. Mann-Whitney U tests were conducted to compare differences in behavioural performance (i.e., mean accuracy and RT) between emotion, groups, as well as neural signals between correct and incorrect trials. Spearman correlations were used to examine relationships between different neural signals (e.g., P300 and CPP) and other metrics of interest (e.g., HDDM decision threshold, nDDM decision threshold, and UGM urgency signal). An alpha of .05 was used as threshold for statistical significance and were corrected for multiple comparison using the FDR Benjamini-Hochberg correction as implemented by *statsmodels.stats.multitest.multipletests*.

3.5. Results

3.5.1. Behavioural Results

The early responder (ER) group were significantly less accurate on ambiguous trials (mean=53.76%±6.23) than the late responder (LR) group (mean=73.36±7.34) (U=629.5, p<.0001). ER individuals appear to be performing at chance level, suggesting that they were guessing rather than making informed judgements. Difference in accuracy performance was also observed on easy trials with the ER group (mean=94.86%±5.42) having lower accuracy than the LR group (mean=98.89%±1.2) (U=766.0, p<.0001) although both groups preformed near ceiling. Moreover, although group categorization was made based on RTs on ambiguous trials (see *Methods*), ER (mean=1.39s±0.28) tended to also respond earlier than LR (mean=2.16 ±0.61) on easy trials (U=718.0, p<.0001). Overall, subjects were neither faster (U=6165.5, p=.498) nor more accurate (U=5536.0, p=.107) to either happy or sad stimuli.

3.5.2. Comparing Neural Signals of Interest between Early and Late Responders

To examine endogenous determinants of decision RT, we began by identifying the neural correlates previously implicated in evidence accumulation during perceptual decision-making. In addition to a prominent sensory-evoked P300, we observed a CPP activity that increased over time and peaked close to the time of response – consistent with the build-to-threshold dynamics proposed by drift diffusion models. These two signals were significantly positively correlated (*rho*=.38, p<.0001). The grand-average waveforms indicate that CPP generally peaked before response suggesting that CPP encodes sensory information and not motor readiness. Crucially, the use of a gradual morphing stimuli eliminated sensory-evoked deflections (e.g., N170 and P300) from the ERP trace, making it possible to disentangle the two and finely trace the evolution of the CPP from its onset to its peak. Given the temporal evolution of the CPP, we probed with a permutation test whether there may be windows of time within which the buildup rate may differ between groups. For easy trials, we found that LRs had greater CPP signal buildup compared to ERs during the -280ms to -64ms preceding response (Fig. 3.5b). For ambiguous trials, we again observed greater CPP signal buildup among

LRs than ERs over two time-windows preceding response: -300ms to -204ms and -180ms to -84ms (Fig. 3.5d).

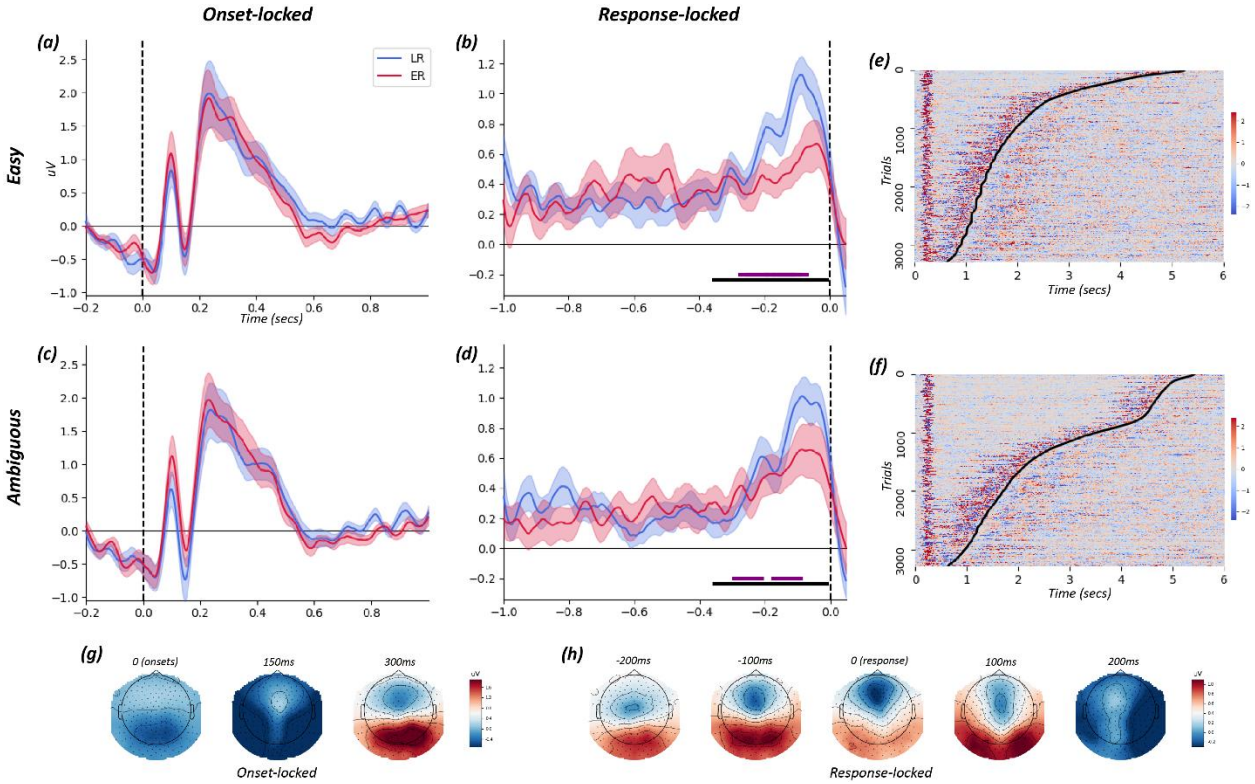

Fig. 3.5. *Grand average waveforms and topographical maps.* ***(a-d):*** *Grand average waveforms from electrode site Pz. The onset-locked P300 signal is depicted in the left-hand column for* ***(a)*** *easy and* ***(c)*** *ambiguous trials. The response-locked CPP signal is depicted in the right hand column for* ***(b)*** *easy and* ***(d)*** *ambiguous trials. In these CPP plots, the identified time window of interest where slopes differ from zero, indicating signal buildup, is marked by the solid black line at the bottom. Group differences in slope is marked by the solid purple line at the bottom. Blue and red lines relate to the late and early responders, respectively. Shading around the lines reflect the 95% confidence interval.* ***(e-f):*** *Single-trial plots for* ***(e)*** *easy and* ***(f)*** *ambiguous trials show the temporal relationship between the neural signal from the electrode site Pz (normalized relative to each individual's baseline average) and decision time (curved black line). P300 can be noted early in the trial whereas CPP can be observed preceding the time of decision.* ***(g-h):*** *Topographical maps for* ***(g)*** *onset- and* ***(h)*** *response-locked activity are depicted at various time points.*

We next sought to examine whether N170 amplitude, P300 amplitude, and CPP within a broader time window of interest (*see Methods*) may differ between our groups as well as between conditions (i.e., easy and ambiguous) (Fig. 3.5). Contrary to our hypothesis, no

significant main effect of group (F(1,55)=2.409, p=.126), condition (F(1,55)=.059, p=.809), or their interaction (F(1,55)=0.113, p=.738) was observed for the N170. For P300, no significant main effect of group (F(1,55)=0, p=.986), condition (F(1,55)=0, p=1.00), or their interaction (F(1,55)=0.718, p=.402) was observed. Similarly for the CPP, no main effect of group (F(1,55)=1.708, p=.197), condition (F(1,55)=1.611, p=.210), or their interaction (F(1,55)=2.399, p=.127) was statistically significant. Additionally, N170 amplitude (U=1631, p=.973), N170 latency (U=1794, p=.845), P300 amplitude (U=1646, p=.973), P300 latency (U=1649, p=.973), and CPP (U=1862, p=.845) did not differ between correct and incorrect trials. Taken together, this suggests that our neural signals of interest likely relate to subjective indexing, rather than actual evidence in the environment.

3.5.3. Trial-by-trial Variations in Neural Signals Modulates Decision Parameters

Though we did not observe discernable differences when examining our neural signals alone, one might nonetheless postulate that these neural signals may relate differently to decision parameters depending on group affiliation and condition. We thus assessed whether decision parameters are modulated by EEG neural signals and to estimate the regression coefficients determining their relationship while accounting for trial-by-trial variations. Non-neural HDDM models where both decision threshold and drift rate varied as a function of condition (difference in DIC=-1262.89) compared with just threshold (DIC=-86.1) or just drift rate (DIC=-1236.46) had improved model fit. Moreover, allowing the decision threshold and drift rate to vary parametrically with P300 amplitude and CPP buildup, respectively, yielded a better fitting model (DIC=-1272.87) compared to just P300 (DIC=-86.15), CPP (DIC=-1243.81), or no neural signal (DIC=-1236.46) (summarized in Supplementary Fig. A3.4). Allowing decision threshold to vary with N170 did not improve model fit (DIC=87.97), suggesting it is not used to inform perceptual decisions – at least in the context of the DDM. In sum, our best fitting model was one that allowed for decision threshold and drift to vary by condition, as well as by both P300 and CPP, respectively.

Trial-by-trial modulation of P300 amplitude were parametrically related to higher decision thresholds, but only in LRs and only for ambiguous trials (99.20% posterior probability > 0). This

is confirmed in the interaction analysis; P300 was significantly higher on ambiguous compared to easy trials among LRs (95.33% posterior probability > 0). Regression coefficients indicate all other relationships were not significant (Supplementary Table A3.1 & A3.2). Our results suggest that LRs are using P300 as a "caution" signal when the environment lacks abundant information for one choice over another, while ERs are not.

CPP on the other hand, is thought to index the amount of information in the environment and thereby the drift rate. Among ERs, CPP was related to lower drift rate on easy trials (99.99% posterior probability < 0), likely because they still tend to respond relatively early and at points of low level of information. However, on ambiguous trials, CPP was in fact related to higher drift rate in ERs (97.98% posterior probability > 0). Interaction analyses suggest that CPP was significantly related to greater increases in drift rate on ambiguous compared to easy trials among ERs (99.90% posterior probability > 0) and a similar trending effect was noted among LRs (91.41% posterior probability > 0). This contradicts the notion that CPP indexes only actual sensory evidence in the environment. Moreover, given that ERs perform around chance on ambiguous trials but still demonstrate high levels of CPP signal buildup suggests CPP may also index subjective perception of evidence and that perhaps another variable not considered by the HDDM may be at play.

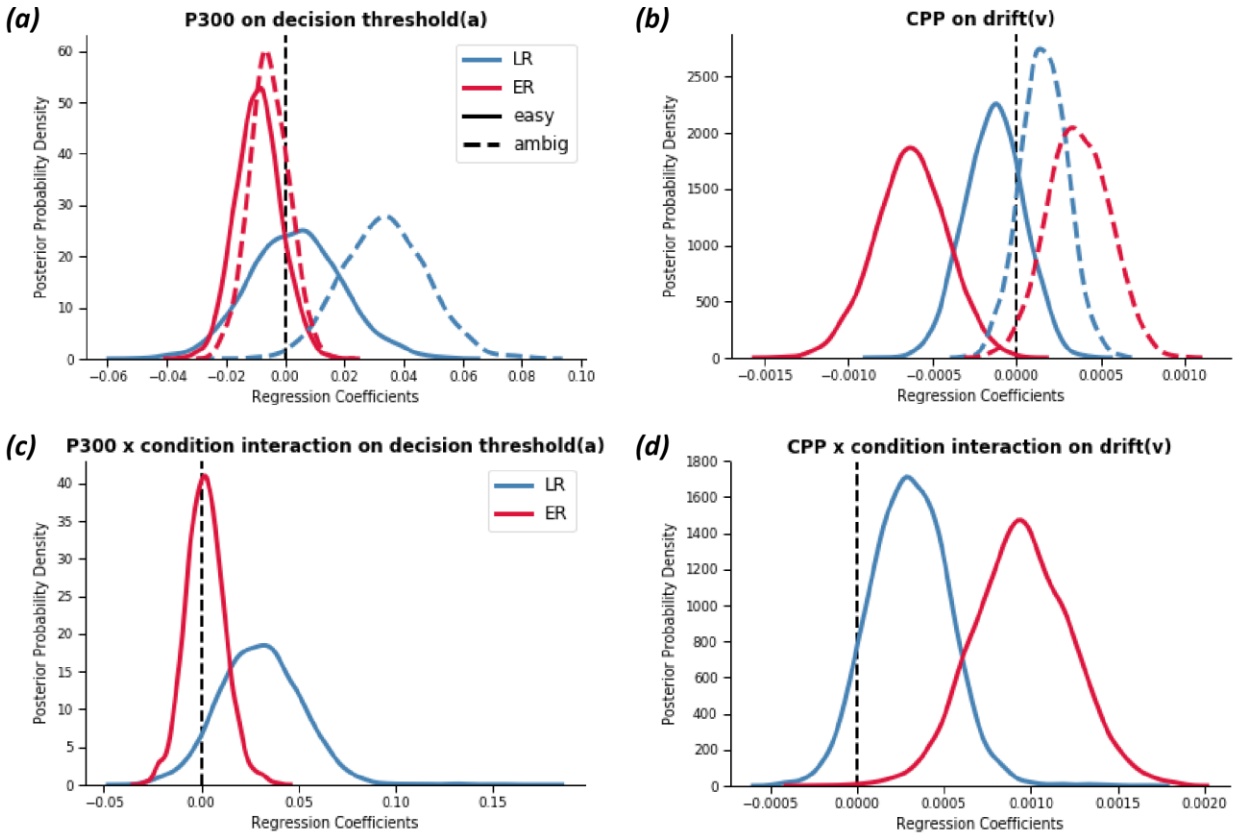

Fig. 3.6. *Bayesian posterior probability densities for modulation of decision parameters estimated from the hierarchical drift diffusion model by neural signals. Peaks reflect the best estimates, while width represent uncertainty. Simple effects of* ***(a)*** *P300 on decision threshold and* ***(b)*** *CPP on drift rate are depicted in the upper row. Interaction effect of* ***(c)*** *P300* ***(d)*** *and CPP on decision threshold and drift rate, respectively, with condition are depicted in the lower row. A more positive regression coefficient indicates ambiguous > easy.*

3.5.4. CPP Reflects a Combination of Evidence Accumulation and an Evidence-Independent Urgency Signal

We hypothesized that the CPP signal buildup across the entirety of a trial reflects a combination of both the sensory evidence available in the environment and an evidence-independent urgency signal. As discernable from the waveform plots (Fig. 3.5b & Fig. 3.5d), CPP does not linearly ramp in time but rather, the slope is steepest close to the time of response and resembles a dynamic signal that grows in time. We therefore tested a second model that accounts for this "urgency" signal (Fig. 3.7; described in *Methods*). As expected, the estimated

urgency signal was significantly lower for the LR (mean=1.73±1.27) compared to the ER (mean=6.60±3.39) group (U=26.5, p<.0001).

The predicted neural signal from a model that included the evidence-independent urgency signal significantly related to our actual recorded CPP signal (β=43.74, p=.023, 95%CI=[6.17, 81.33]). We did not observe this with the nDDM (β=7.155, p=.706, 95%CI=[-30.07, 44.38]). A pairwise Spearman correlation indicates that our nDDM and HDDM yielded highly similar decision threshold estimates (rho=.951, p<.0001) and are, therefore, comparable. Taken together, our findings confirm that the observed CPP signal buildup fitted with predictions of the dynamics that a neural decision variable signal should exhibit from a model that incorporated an urgency parameter.

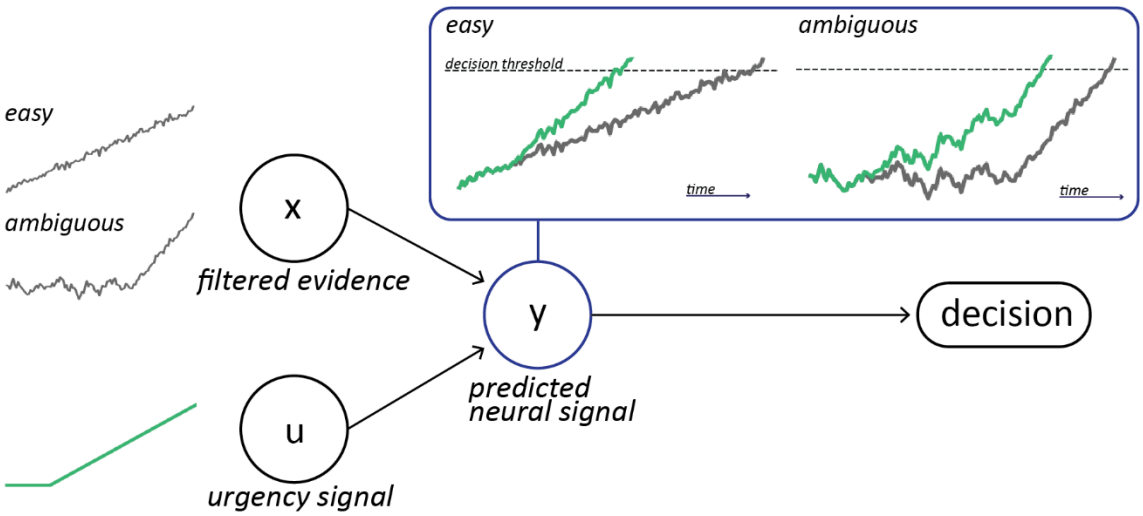

Fig. 3.7. *Schematic of the urgency gating model. Sensory evidence is first differentiated and filtered. The resulting signal (x) is then multiplied by a subject's evidence-independent urgency signal (u) that grows in time. The combined signal together forms the model's predicted neural signal (y). Green lines depict a neural signal that incorporates an urgency signal whereas grey lines do not. Once the predicted neural signal crosses a decision threshold, a decision is made.*

3.5.5. Relationship between ERPs and Oscillatory Fluctuations in EEG Signals

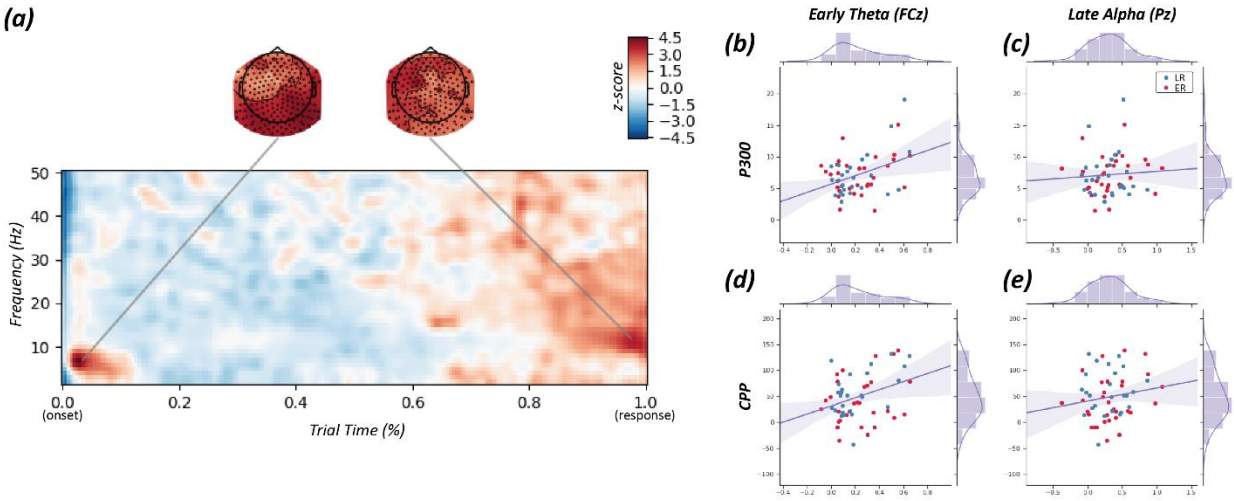

Fig. 3.8. *Time frequency analysis.* ***(a)*** *Average time-frequency power across all trials. Data is resampled to match onset (timepoint 0) and onset (timepoint 1). A strong early theta power and a late alpha power can be observed. Heatmap depicts strength of power, as compared to baseline (-500ms to onset), with warmer and colder colours reflecting higher or lower power, respectively.* ***(b-e)*** *Scatterplots with regression lines depicting correlation between ERPs of interest (i.e., P300 and CPP) and EEG oscillatory power (i.e., early theta and late alpha).*

Difference frequencies of EEG oscillations have been previous implicated in perceptual decisions (e.g., Cavanagh et al., 2011a; Klimesch, 2012). Here, we aimed to link our ERPs to these bands of EEG oscillations. Our paradigm allowed us to identify when in the decision-process this signal peaked. We observed an early theta power near stimulus onset and a late alpha power close to the time of response (Fig. 3.8, see Supplementary Fig. A3.3 for replication of finding with whole-sensor power). Pairwise Spearman correlations indicate that early mid-frontal theta power was related positively to both P300 maximum amplitude (*rho*=.329, *p*=.012) and CPP buildup (*rho*=.411, *p*=.001). However, late posterior alpha did not relate significantly to either P300 (*rho*=.116, *p*.389) or CPP (*rho*=.147, *p*=.274). No other significant correlation was observed between either the early or late power of other frequency bands and our ERPs of interest.

3.6. Discussion

The current study interrogates the neural determinants of perceptual decision-making in humans by isolating discrete neural signatures of decision caution and sensory evidence encoding. These signals are observable with minimum signal processing and the high temporal resolution of EEG allows for these signal dynamics to be observed throughout decision formation – akin to previous work with single-cell recordings in non-human primates. Our findings provide evidence contradicting the common assumption that timings of decision commitment are determined by a context-dependent, but time-invariant criterion, on accumulated evidence. Through analysis of observed behaviour, computational modelling, and scalp electrophysiology, we show that human decisions are made not solely based on the accumulated sensory evidence, but that an urgency signal can change the amount of evidence needed to commit to a choice. This endogenous urgency signal varies between individuals and can potentially account for why certain individuals are prone to fast and erroneous decisions, particularly when signal-to-noise ratio of the decision environment is low.

The information available in a natural environment can vary from one decision to the next and additionally, can change even within decisions. Estimating the drift rate as a static, linear, and time-invariant parameter is suboptimal because the occurrence of a weak signal would lead to prohibitively long decision times. This has motivated computational models to account for a dynamic decision criterion, namely the "urgency" signal (Churchland et al., 2008; Cisek et al., 2009), and have received support for its time-dependent influence on the decision process of highly-trained monkeys (Hanks et al., 2014; Thura & Cisek, 2014, 2016). However, little evidence for a time-dependent neural signal in mostly naïve human subjects exists; those that do often ask subjects to emphasize on either speed or accuracy and thereby artificially manipulate a sense of urgency (Murphy et al., 2016; Steinemann et al., 2018). Here, we formally tested an urgency parameter and demonstrated that individuals have natural tendencies to exhibit differing levels of urgency which influenced their decision time and accuracy.

In neurophysiology, the firing rate of neurons represent the accumulated evidence for one choice or another until a decision threshold is surpassed. Here, we found that the domain-general CPP signal gradually builds throughout the trial, ramping up steeply close to decision, and resembled characteristics of a neural signature of decision formation. As with previous studies (Kelly & O'Connell, 2013; van Vugt et al., 2019), the peak of CPP activity temporally preceded that of the response, suggesting it reflects an intermediate level in the decision hierarchy between stimulus onset and motor action. Further supporting the role of CPP in evidence accumulation, we found that CPP covaried with the drift rate parameter though this relationship was context-dependent and modulated by individual differences in tendencies to wait. Importantly, our results challenge the notion that CPP solely traces sensory evidence (O'Connell et al., 2012) in two key ways: (i) CPP was related to higher drift rate in situations of high, compared to low, ambiguity in the decision environment, and (ii) the group of subjects who tended to respond early in the trial when sensory evidence is low and performed around chance, still demonstrated CPP signal buildup. This dovetails with recent finding that CPP is mediated by subjective evidence and perceived decision confidence, over and above the sensory evidence (Herding et al., 2019; Tagliabue et al., 2019). Furthermore, it lends support to the consideration that CPP reflects a combinatory force of sensory evidence and an dynamic urgency signal that pushes one to commit to a choice even if evidence for that choice is weak (Cisek et al., 2009). It must be noted that the evidence-independent urgency signals could be misconstrued as drift rate or threshold in pure evidence accumulation models; to disambiguate the two, one needs to dynamically manipulate the amount of information presented (Thura et al., 2012), as in the present study. Indeed, neural signals predicted by a model that accounts for an individual's urgency signal fit better with our observed CPP signal than that predicted by the conventional drift diffusion model. Note that this urgency signal was estimated per subject and reflects a global mechanism affecting decision-making that is not specific to any one sensory input modality or effector. Such a global gain modulation may not only manifest in the firing rate of neurons tracking the evolving decision process; urgency may influence processes both early and late in the decision hierarchy such as in the gain of sensory inputs to decision

circuits (Heitz & Schall, 2013) and in downstream regions involved directly with motor execution (Thura & Cisek, 2016, 2017).

Finally, the use of relatively long trial times with smooth sensory transitions in the present study allowed us to temporally disentangle the CPP from it's spatially overlapping counterpart, the P300. This classic ERP has been frequently implicated in decision-making since it's discovery (Sutton et al., 1965) and several lines of evidence have converged to show that the amplitude of the P300 component lies at the interface between stimulus processing and response preparation (Donchin & Coles, 1988; Polich, 2007; San Martín et al., 2013) though there is little consensus regarding its precise functional role. Here, we demonstrated that P300 is used as a caution signal and relates to increased decision thresholds among individuals tending to wait, particularly when information in the environment is ambiguous. One prominent theory on the biological origins of P300 amplitude is that it is a cortical manifestation of the phasic locus-coeruleus-noradrenergic orientation response which potentiates information processing and prepares/facilitates a behavioural response to the eliciting stimulus (Nieuwenhuis et al., 2011; Swick et al., 1994). This may underpin the famous sensitivity of the P300 to stimulus probability (Lucci et al., 2016; Mars et al., 2008) and motor inhibition (Smith et al., 2008) – concepts which, in the terminology of the evidence accumulation framework, translates to changes in the decision threshold. Collectively, our findings suggest that the P300 and CPP play critically different roles in the decision process. The short trial time implemented in previous studies may have equivocated the two components and led to the misconception that they are one and the same (O'Connell et al., 2012; Twomey et al., 2015; Verleger et al., 2005).

Although the notion of urgency in decision-making has been gaining momentum, there remains debate how a hypothetical urgency signal is incorporated into the decision process and where it originates. One potential alternative interpretation of our findings is that decisions results from boundary adjustments over the course of a trial. Previous psychophysical studies in humans have found collapsing bound to improve model fit (Palestro et al., 2018; Tajima et al., 2016), though negative findings exists (Hawkins et al., 2015; Voskuilen et al., 2016). This may be a

matter of interpretation: an increasing urgency signal is mathematically equivalent to a symmetrically collapsing decision threshold. However, as with other studies investigating the neural signals of urgency (Cisek et al., 2009; Thura et al., 2012), results from our study indicates that urgency works via a dynamic gain in evidence accumulation in time. Nonetheless, open questions remain regarding where such urgency might be generated in the brain. According to the affordance competition model, the basal ganglia is thought to bias decisions via cortico-striatal connections (Cisek, 2007) and preliminary findings in humans point to the caudate as a potential root of the urgency signal (Yau et al., 2020). However, further study is warranted to better source the urgency signal in the brain.

3.7. Conclusion

Our results reveal how different decision parameters may be reflected in neural signals. In particular, we demonstrate that the CPP, which behaves as a developing decision variable, is a reflection of the sensory evidence available in the decision environment as well as an endogenous urgency signal that grows in time. By embedding these neural signals into a computational framework, it is possible to generate testable predictions about how different parameters should vary as a function of specific stimulus properties such as discriminability. These mechanisms expose principles of cognitive function in general and can pave a new and more precise understanding of how clinical brain disorders and experimental manipulations impact on decision-making in the human brain.

CHAPTER 4. Dynamics of brain connectivity at rest constrains performance in task.

4.1. Preface

The current understanding of how distinct brain regions coordinate perceptual decision-making across the brain is limited, with most research groups focusing exclusively on a limited number of recording sites, such as the LIP. Since decisions are formed across brain systems rather than individual brain regions, we questioned whether decision-making is influenced by individual variability in the functional organization of the brain. To this end, we took advantage of resting-state fMRI and examined FC during an extended task-independent, rest period. We tested whether fluctuations between and the propensity to occupy/dwell in certain network configurations at rest may relate to improved behavioural performance on the dynamic perceptual decision-making task. Given our knowledge of how a FC configuration of high modularity may help conserve metabolic expenditure, whereas low modularity may be more efficient in processing information, we hypothesized that longer dwell time at rest in a modular brain state may allow for better performance in task. Additionally, we tested whether variations between individuals in the urgency signal we observed in Chapter 2 and 3 relate to our observed findings. We found that individuals with a propensity to spend greater time in a more modular brain state at rest also demonstrated higher subcortical activity in task. Activity from these subcortical regions were related to the subject's estimated urgency level. Our results demonstrate the importance of network topology in shaping behavioural performance when confronted with external tasks. This work is currently in preparation for submission.

4.2. Abstract

Cognitive processes are thought to be coordinated across multiple brain regions organized in intrinsic networks. Recent studies suggest that the functional organization of networks is largely preserved between task and rest, suggesting the two are highly intertwined.

Understanding variabilities in the network profile at rest can give context to brain activity and performance in task. Here, we utilized a time-varying, dynamic approach to characterize fluctuations in functional connectivity at rest and identified four distinct brain states. Individuals with a propensity to more frequently express a state at rest with higher global modularity, especially between the transmodal default mode and unimodal visual and somatomotor networks, were also more likely to demonstrate increased thalamic and caudate activity in task. Activity from these subcortical regions served as a "braking" signal that slowed decision time and consequently, improved behavioural accuracy in task. Next, we show that network profile during more difficult trials in task resembled a more integrated brain state, and that this relationship correlated with behavioural performance. These results underscore the importance of brain network configuration dynamics in shaping behaviour.

4.3. Introduction

In the highly dynamic environment we inhabit, brain regions must communicate and relay information in a rapid manner to make accurate and timely decisions. These relay pathways conforms to intrinsic topographies, identifiable during extended periods of rest, known as resting-state networks (RSNs) (Laird et al., 2011; Yeo et al., 2011). The magnitude of correlation, or functional connectivity (FC), between different RSNs are thought to not merely reflect epiphenomenal activity at rest, but can reveal processes contributing to individual differences in a number of behavioural and cognitive domains in task (Stevens & Spreng, 2014). However, the conventional method that presumes these correlations are stable in time ignores the potential dynamic interplay within and between RSNs. There is now evidence that RSNs coalesce and dissolve in a "dynamic" or time-varying manner (for review: Cohen, 2018). A natural next step is to understand how individual differences in human behaviour and cognition may be driven not only by external task demands, but be constrained by one's propensity to express different latent brain connectivity patterns.

Brain activity continuously fluctuates at rest even in the absence of an explicit task. Topology of these fluctuations are thought to conform to an intrinsic network profile and are more stable than the synchrony of elicited activation by tasks (Cao et al., 2014; Cole et al., 2014; Krienen et al., 2014). Because FC at rest appears to be such a stable characteristic of the brain, it is often thought of as a trait measure and can "fingerprint" individual differences in cognition function, age, and mental health (Finn et al., 2015; Geerligs et al., 2015a; Geerligs et al., 2015b; Sanz-Arigita et al., 2010; van den Heuvel et al., 2009). These studies together suggest that a stable core network is necessary for healthy general cognitive function. On the other hand, humans demonstrate behavioural flexibility in response to their environment and must, therefore, be reconfiguring their brain networks to meet external task demands. This level of reconfiguration appears dependent on the level of attention and cognitive control required (Gießing et al., 2013; Power & Petersen, 2013) with more cognitively demanding tasks benefiting from a less modular and more integrated connectivity between RSNs (Cohen & D'Esposito, 2016). Thus, from a relatively stable core network configuration emerges a dynamical repertoire of large-scale, context-dependent functional networks that are critical for flexible cognition and behaviour.

In tandem, time-varying functional connectivity (tvFC) has received growing attention in recent years due to progress in acquisition techniques and computational tools to quantitatively characterize reoccurring brain patterns (i.e., "tvFC states") at a high temporal and spatial resolution (Allen et al., 2014; Calhoun et al., 2014; Lurie et al., 2018). This has altered the view of intrinsic network topographies – the conventional approach of averaging FC across scan time might obfuscate underlying dynamics in networks configuration and rather, individuals traverse in and out of different tvFC states across time. tvFC state metrics, such as state transition probabilities and dwell lifetime, calculated using functional magnetic resonance (fMRI) have shown promise and sensitivity to capturing brain communication in mental and vigilance states (Shirer et al., 2012) and in disentangling disease progression (Damaraju et al., 2014; Fiorenzato et al., 2019). The notion that FC between RSNs is a transient rather than stable phenomenon is supported by electrophysiological (Rabinovich et al., 2012; Tagliazucchi et al., 2012) and calcium imaging (Matsui et al., 2018) studies that demonstrate endogenous neural signals continuously

shift to form adaptive patterns of activity over various time scales. However, the behavioural relevance of FC dynamics remains poorly understood with most existing studies have only focused on specific brain regions (Braun et al., 2015; Douw et al., 2016).

Here, participants underwent fMRI while participating in a perceptual decision-making task and again while at rest. We first aimed to temporally decompose FC configurations at rest and identify latent brain states by means of tvFC. We take a data-driven approach to assess FC dynamics based on established techniques including: whole-brain group spatial independent component analysis parcellation to identify RSNs (Calhoun et al., 2001) and *k*-mean clustering of fixed-length sliding windowed correlation matrices to identify FC states (Allen et al., 2014) during resting state fMRI (i.e., rs-fMRI). Second, we test the hypothesis that differences in intrinsic FC signatures as indexed by tvFC state metrics derived from rest relates to behavioural performance in task. Finally, we examine whether different FC configurations in task may be expressed as a function of task difficulty and if this expression impacts behavioural performance.

4.4. Methods

4.4.1. Participants

53 right-handed young, healthy adults (23 males; age 24.02yr±5.49) participated in the present study. Participants with a current or past diagnosis of a psychiatric or neurological disorder were excluded. Informed consent was obtained from all participants and the study was approved by the Montreal Neurological Institute Research Ethics Board.

4.4.2. Perceptual Decision-Making Task

Participants were presented short videos of a face "morphing" between expressions (Fig. 4.3A). In a given trial, a face from the NimStim dataset (Tottenham et al., 2009) of neutral facial emotion was displayed in the center of the screen and gradually morphed into a happy or sad expression. The maximum trial time was six seconds with participants asked to press a

response button for either happy or sad in their right-hand, as quickly and as accurately as possible, once they felt confident they could predict the final emotion. Our paradigm consisted of two levels of task difficulty: easy and ambiguous. In easy trials, the faces morphed in a gradual manner towards the correct emotion. In ambiguous trials, the faces remained around neutral for two-thirds of the trial and then rapidly ramped towards the correct emotion. The task consisted of three blocks of 40 trials (i.e., 120 trials total), split evenly between happy and sad, and between easy and ambiguous. Importantly, trial types were interleaved within a block. Further task details have been described elsewhere (Yau et al., 2020).

4.4.3. Endogenous Urgency Signal

A particular inter-individual parameter of interest is the "urgency" signal. This endogenous signal is thought to modulate the deliberation process, continually pushing decision-related neural activity towards a decision threshold for choice commit as time elapses (Cisek et al., 2009). Variability in the baseline level of urgency is thought to be stable over time and across contexts (Berret et al., 2018; Reppert et al., 2018; Thura & Cisek, 2014) and may therefore be an individual trait. Moreover, the urgency signal is related to a variety of discretely quantifiable behaviour commonly related to decisions and actions, suggesting it may be a particularly useful construct for conceptualizing certain phenotypical personality traits (Carland et al., 2019). Here, as with our previous work (Yau et al., 2020), we estimated the urgency signal via a minimalistic urgency gating model. This model builds upon the tradition drift diffusion model of perceptual decision-making (Ratcliff et al., 2016) and assumes that an urgency signal is multiplied onto the evidence available in the decision environment (Cisek et al., 2009). Once this combined signal reaches a critical threshold, decision is then made. An exhaustive search was implemented to find the optimal urgency parameter that minimized the mean squared error between the model's predicted reaction time versus the observed reaction time across all trials acquired from our perceptual decision-making task for a given subject. This yielded one optimal urgency parameter per subject which was then used to test against tvFC measures.

4.4.4. MRI Acquisition and Preprocessing

Neuroimaging was carried out with a Siemens Magnetom Prisma 3T MRI scanner equipped with a 64-channel head coil at the Montreal Neurological Institute (MNI). High-resolution MPRAGE T1-weighted structural images were first obtained for anatomical localization (TR=2.3s; TE=2.3ms; FOV=240mm; scan matrix=192x256x256; voxel size=0.9mm isotropic). Functional data was then acquired with an echo-planar T2*weighted sequence for blood oxygenation level-dependent (BOLD) contrast using multi-band acquisition to help improve temporal resolution (TR=0.719s; TE=30ms; scan matrix=104x108x72; flip angle=44°; FOV=208mm; voxel size=2mm isotropic, multiband acceleration factor=8). First, participants completed a perceptual decision-making task in scanner (described above). Second, a task-free, eyes-open rs-fMRI was collected. Participants were instructed to relax and focus on a fixation cross – a design shown to maximize reliability (Zou et al., 2015). A total of 840 functional image volumes were collected (i.e., 10mins). The same parameters were used for task and resting-state data acquisition.

Task-data preprocessing was performed using SPM12 (http://www.fil.ion.ucl.ac.uk/spm/) and MATLAB (MATLAB, 2018). Signals with >4% intensity change were despiked and corrected using ArtRepair Toolbox (Mazaika et al., 2007). Images were corrected for motion, realigned, normalized to the MNI ICBM152 template (Fonov et al., 2009), and minimally smoothed (6mm FWHM Gaussian kernel). Spatial filtering techniques (such as Gaussian smoothing) have been shown to increase the signal-to-noise ratio (Brants et al., 2011; Hendriks et al., 2017). First-level analyses were conducted with each participant's preprocessed volumes.

Preprocessing for the rs-fMRI data was performed using FMRIPREP 1.4.1 (Esteban et al., 2019) including the following steps: skull stripping, estimation for head-motion parameters, co-registration to corresponding structural image (boundary-based registration with 9 degrees of freedom), and spatial normalization to MNI space (non-linear registration). For more details of the pipeline see https://fmriprep.readthedocs.io/en/1.4.1/workflows.html. Outputs from FMRIPREP were then treated for confound denoising using XCP Engine (Ciric et al., 2018). We implemented the 36P strategy which expands the 6 motion estimates and 2 physiological time

series with global signal regression to yield 9 regressors, their derivatives, quadratic terms, and square derivatives. Additionally, we implemented spike regression which flagged for volumes that exceeded 0.25mm root mean square displacement (Ciric et al., 2017; Satterthwaite et al., 2013). This strategy has been shown to most optimally attenuate resting-state confounds (Satterthwaite et al., 2013).

4.4.5. Independent Component analysis (ICA)

After preprocessing, rs-fMRI data were subject to spatial independent component analysis (ICA) implemented using the GIFT toolbox (http://mialab.mrn.org/software/gift/)(Calhoun et al., 2001). All participants' data were reduced with a two-step approach using principal components analysis: first to 120 components which was concatenated and further reduced to 100 components. We then decomposed the data into 100 independent components (ICs) using the infomax ICA algorithm (Bell & Sejnowski, 1995). The number of components chosen were based on previous research that demonstrate this decomposition sufficiently captures functional parcellation of major brain systems (Allen et al., 2014; Nomi et al., 2017). To determine the reliability of the ICA algorithm, we repeated the analysis 100 times using ICASSO (Himberg & Hyvarinen, 2003). Independent components were then back reconstructed to obtain individual-specific maps using the group-ICA approach (Erhardt et al., 2011). ICs were visually inspected by two independent reviewers for assignment to functional domains based on previously characterized RSNs (Laird et al., 2011). In addition to the manual inspection, our ICs were binarized (i.e., masked) and compared against templates from Laird et al. (2011) using Spearman's correlation. ICs were assigned to networks with which they showed highest correlation coefficients (mean r=.301). If this rating differed from raters' assignment, the components were again visually inspected until consensus was reached. 46 of the 100 ICs were matched to RSNs and the rest were deemed artifacts.

4.4.6. Time-varying Functional Connectivity (tvFC) at Rest

tvFC was computed across ICs using the sliding-window approach which extracts the dynamic interaction between brain areas by using a moving time-window along the BOLD time series

(Allen et al., 2014; Hutchison et al., 2013) using the GIFT toolbox (http://mialab.mrn.org/software/gift/). For each participant, 766 time-windowed domains were obtained for each of the ICA's time-course by convolving a window width of 63 TRs (45secs) with a Gaussian of sigma 3 TRs (to obtain a tapered edge) and sliding in 1 TR steps. The window size was chosen according to previous tvFC analysis that indicate optimal window sizes hover between 30-60sec and can discern cognitive states (Allen et al., 2014; Hutchison et al., 2013; Shirer et al., 2012). Within each time-windowed domain, 1035 (i.e., 46 ICs * (46 ICs-1)/2) unique functional connectivity pairwise correlations were obtained between windowed ICAs time-courses. Covariance matrices were calculated using L1 regularized inverse covariance matrices carried out by a graphical LASSO algorithm (Friedman et al., 2008; Smith et al., 2011) to account for potential effects of noise on covariance estimation due to sampling short time-windows. The regularization parameter (λ) was optimized for each participant independently. Finally, the tvFC matrices were Fisher-z-transformed to normalize variance before further analysis.

A discrete number of reoccurring tvFC patterns were detected by applying clustering analysis on the windowed correlation matrices concatenated across participants. We use *k*-means clustering with *k* (number of clusters) from 2 to 20, repeating each 20 times (Allen et al., 2014; Calhoun et al., 2014). Clustering was first conducted on a sub-sampled number of windows (i.e., windows with relative maxima of variance) for all time points in order to estimate initial cluster centroids (cluster medians). The sum of absolute distance or L1 distance method was used with a maximum of 150 iterations for *k*-means cluster computation. The optimal number of clusters $k=4$ was obtained using the elbow criterion of the ratio comparing within- versus between-cluster sum of squares distances. The resulting four centroid states from the clustering of sub-sampled data were subsequently used as initial clustering positions for clustering all data. These clusters are referred to as tvFC states and describe connectivity patterns that individual participants move between over time. It is important to note that not all individuals have tvFC in all states. Two clustering measure output metrics are derived per participant: dwell lifetime (i.e., average number of TR's spent in a given state) and number of transitions (i.e., frequency of changes between states). To test the relationship between

clustering measure outputs and behaviour (e.g., reaction time, accuracy, and urgency), Spearman partial correlations correcting for age was used. False discovery rate corrections (alpha=.05) were applied to account for multiple comparison.

4.4.7. Modularity of Different tvFC States

One key organizational principle in FC is the degree to which brain regions dissociate from each other. At the global level, this concept of modularity is widely measured by partitioning the network's nodes, or FC communities, to maximize the modularity quality function, *Q* (Newman & Girvan, 2004). Given that functional brain networks may contain negative edge weights, we adopted the asymmetric generalization of the modularity quality function (Rubinov & Sporns, 2011). *Q* was maximized using the Louvain algorithm (Blondel et al., 2008) implemented through the *community_louvain* function in the Brain Connectivity Toolbox (http://www.brain-connectivity-toolbox.net) with the default resolution parameter γ=1 and initial community affiliation based on ICs' assignment to canonical RSNs. Maximized *Q* values were used as a measure of modularity for each tvFC state. We assessed two additional basic nodal properties: (1) within module degree z-score that reflects the degree of connectivity of a node to another node in the same module, and (2) participation coefficients which is the fraction of a node's edge that connects to other nodes within the same module. These measures give an index of the separation and integration, respectively, of RSNs in each tvFC state.

4.4.8. Functional Mapping Gradients of Different tvFC States

A second core organizational principle is that the cortex follows a spatially continuous topographical arrangement along a global gradient which underpins its cognitive processes (Huntenburg et al., 2018; Mesulam, 1998). Of particular interest is the principle gradient which describes gradual transitions at the whole-cortex level, running from primary sensory and motor regions at one end to transmodal cortices (i.e., default mode network (DMN) in humans) at the other end. This spatial separation is thought to enable DMN to perform its commonly ascribed functions relating to information integration and abstraction (Margulies et al., 2016).

To generate functional mapping gradients, we first assigned our resting state data to 400 parcels based on an established parcellation scheme (Schaefer et al., 2018) and then replicated the steps to generate sliding windows and their covariance matrix as described previously (i.e., 45secs window width, L1 regularized inverse covariance matrices, and Fisher-z-transformation). A sliding window's assignment to a tvFC state was matched to our previous k-means clustering analysis. The average covariance matrix of all sliding windows corresponding to a given state was used to generate gradient maps using the BrainSpace toolbox (de Wael et al., 2019). 10 gradient maps per tvFC state were generated using a normalized angle kernel, dimensionally reduced via the diffusion embedding technique, and aligned to one another using Procrustes analysis. To calculate the distance of our derived principle gradient for each state, we took the median embedding value of DMN regions and calculated the Euclidean distance to both the median embedding value of the visual and somato-motor RSNs (Yeo et al., 2011) and then averaged these two distances to yield one value per state. These distance values were then compared to a distribution of distance values derived from randomly generated gradients which were sampled by generating covariance matrix from 1000 random sliding windows; we consider the distance value to be significant if it is higher than the 95^{th} percentile.

4.4.9. Task-based Activation and Functional Connectivity

Group analyses of task-related activity between trial > inter-trial periods were performed with one-sample t-tests using the general linear model in SPM12. Separate random effects ANCOVAs were then calculated on this contrast of interest for each of the FC state properties (e.g., dwell lifetime per state and transitions) as covariates. Clusters corrected for multiple comparisons using a familywise error (FWE) threshold of $P_{FWE} < .05$, with an extent threshold of 110 contiguous voxels, were considered significant. Region of interest analyses were performed by computing the mean parameter estimate of activation for functionally defined clusters for each condition and subject using the *spm_summarise* function.

RSNs are not conditional upon a task-free resting state, but have been shown to be heavily involved in task performance (Cole et al., 2014; Laird et al., 2011). To determine connectivity strength in task, we took the back reconstructed, individual-specific IC maps and applied them

to the task-based data. We calculated the correlation between all IC pairs but restricted the data to only trial time (i.e., when participants were viewing faces). These correlations were Fisher-z-transformed then averaged across trials per trial type (i.e., easy and ambiguous) to yield two connectivity matrix per participant. In comparing connectivity matrixes derived from rs-fMRI connectivity to task-fMRI, we ran a Mantel's test with 5,000 permutation (alpha=.05) (Diniz-Filho et al., 2013).

4.5. Results

4.5.1. Brain States Identified by Time-Varying Functional Connectivity

Based on anatomical, functional properties, and similarities to RSNs identified in previous studies (Laird et al., 2011), the selected 46 ICs derived from group-ICA were categorized into nine functional domains (Supplementary Fig. A4.1): Emotion/Interoception (EI), Basal Ganglia (BG), Motor/Visuospatial (MVS), Visual Perception (VIS), Default Mode Network (DMN), Cognitive (COG), Auditory (AUD), Language (LNG), Cerebellum (CB).

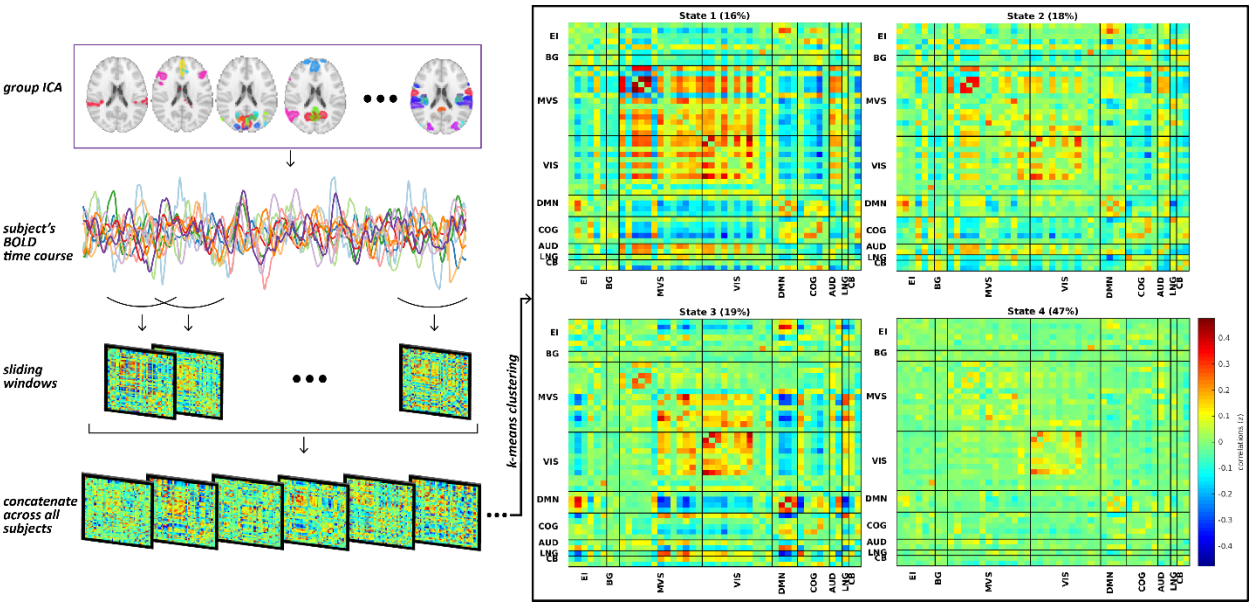

Fig. 4.1. *Overview of time-varying functional connectivity (tvFC) analysis. Left: Schematic depicting the computation of tvFC states. First, group independent component analysis was run to create spatially independent components (ICs). Second, covariance matrices or functional connectivity are computed on temporally windowed portions of the resting-state fMRI scan*

between the IC's. Finally, tvFC matrices from all participants are clustered using the k-means algorithm, yielding cluster centroids and cluster membership assignment for all windows. Right: Cluster centroids corresponding to the four tvFC states identified. Proportion of scan time spent in each state across participants are shown in parentheses next to the state number. Matrices show all pairwise correlations between ICs grouped into nine RSNs [EI: Emotion/Interoception; BG: Basal Ganglia; MVS: Motor/Visuospatial; VIS: Visual Perception; DMN: Default Mode Network; COG: Cognitive; AUD: Auditory; LNG: Language; CB: Cerebellum]. Warm and cold colours depict positive and negative correlations, respectively.

tvFC during the rs-fMRI acquisition is best represented by four FC states (Fig. 4.1), as assessed by the elbow criterion (Supplementary Fig. A4.2). Each tvFC state has a unique spatial connectivity profile and we sought to understand how their network properties and topology differed. To assist in this interpretation, we investigated the modularity and functional mapping gradients of each tvFC state (Fig. 4.2). State 1 (16% overall dwell lifetime) is characterized primarily by positive correlations within and between the motor and visual domains as well as negative correlations/anti-correlations between these networks and other networks (with exception of the auditory domain). State 2 (18% overall dwell lifetime) shows hypo-connectivity between networks with some intra-correlation within a select number of ICs in the motor and visual domains. State 3 (19% overall dwell lifetime) shows relatively prominent anticorrelations between ICs from the DMN domain and those from the motor and visual domains and demonstrates pronounced modularity (as indexed by the maximized *Q* value (Fig. 4.2A)). The DMN also demonstrates strong positive within-module degree z-score (Fig. 4.2B), suggesting that nodes within the DMN were highly connected to other nodes within the same module – an indication of high DMN modularity. State 4, occurring at the highest frequency (47% overall dwell lifetime), has weak overall correlations within and between networks with a large number of correlations centered around zero. Although its FC profile resembles State 2, it importantly differs in that it has high participation coefficients across RSNs (Fig. 4.2C) and the lowest modularity score of the four tvFC states, together suggesting high integration between the RSNs during this state.

We next consider functional gradient maps (Fig. 4.2D) which serves to provide a framework for the spatial ordering of large-scale networks. Across all four states, Gradient 1 accounts for the largest amount of variability in resting-state connectivity patterns across the cortex. It is

anchored at one end by the transmodal DMN regions and, at the other end, by unimodal regions corresponding to visual and somatomotor RSNs. When analyzing the distance or spread of Gradient 1, we found that State 1 and 3 significantly differed from chance (both 100th percentile) suggesting that these two tvFC states had greater separation between unimodal and transmodal regions (Supplementary Fig. A4.3). Distance values of State 2 and 4 did not significantly differ from chance.

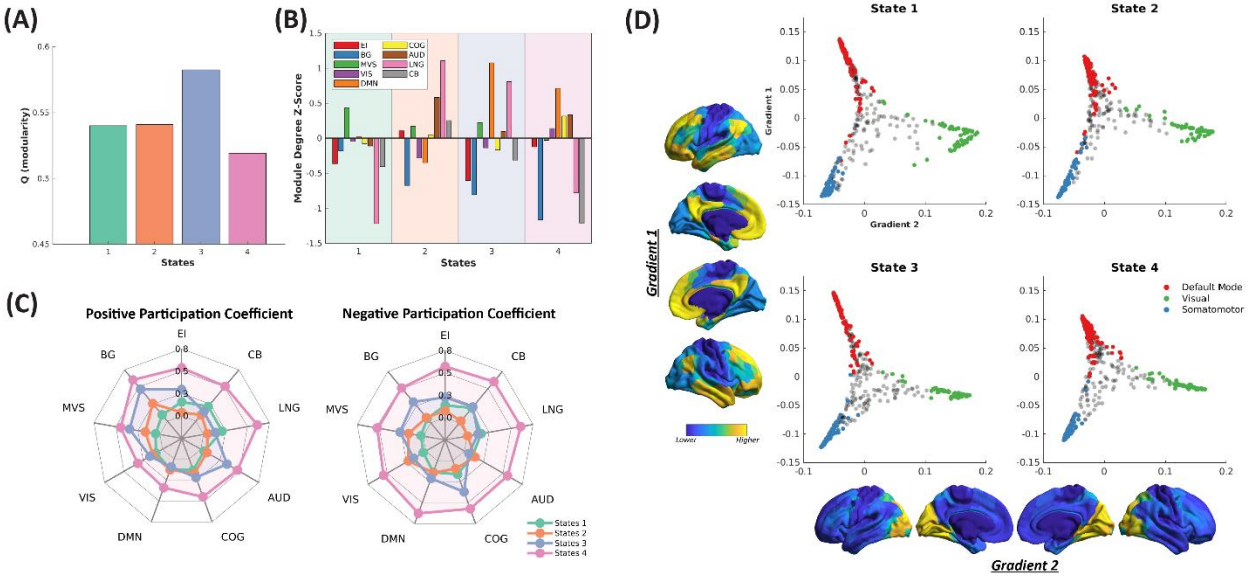

Fig. 4.2. *Description of time-varying functional connectivity (tvFC) states.* ***(A)*** *Bar plot of the modularity of each state. State 3 has the highest modularity indicating greatest dissociation between resting state networks (RSNs) whereas State 4 demonstrate the lowest.* ***(B)*** *Module degree z-score for each of the RSNs based on the network configuration of the tvFC states. Scores reflect the degree of connectivity of a node to another node in the same module/community.* ***(C)*** *Positive (left) and negative (right) participation coefficient for each RSNs given each tvFC state. Scores reflect the extent to which a node is connected to nodes in other modules.* ***(D)*** *Scatterplot of the low dimensional representation using the diffusion embedding algorithm between the first two gradients. Values depict the embedding value for Gradient 1 (y-axis) and 2 (x-axis). Regions corresponding to the default mode network (DMN), visual, and somatomotor regions are highlighted in red, green, and blue, respectively. Gradient 1 represents the dissociation between transmodal and unimodal areas on its two extremes. Gradient 2 depicts the dissociation between the visual and somatomotor networks. Brain images on the sides depict the embedding values for the first two gradients (vertically: Gradient 1; horizontally: Gradient 2) across the cortex with warmer (yellow) and colder (blue) colouring reflecting higher and lower values, respectively.*

4.5.2. FC State Properties at Rest Relates to Performance and Brain Activity in Task

Network cartographic profile at rest are thought to constrain network reconfiguration and brain activity in task. With this in mind, we hypothesized that variability in how one expresses different tvFC states at rest may translate to differences in performance in task. How long an individual dwelled in the modular State 3 at rest positively correlated with accuracy on easy trials (*rho*=.501, *p*=.003). Higher accuracy on easy trials was also marginally significantly correlated with a greater overall number of transitions between the four identified brain states (*rho*=.346, *p*=.052). No other behavioural measure (i.e., reaction time, accuracy, or urgency signal) significantly related to brain state characteristics after multiple comparison correction.

One might expect that variability in the prevalence tvFC states at rest may have a more indirect effect: the propensity to express a tvFC state may predispose brain activity during task which, in turn, drives behaviour. To this end, we tested whether dwell lifetime in each of the four tvFC states covaried with brain activity in task when comparing trial versus inter-trial periods across all trials. During trials, an array of regions involved in face processing including visual processing (i.e., lateral occipital), face processing (i.e., face processing, insula), executive function (i.e., dorsolateral prefrontal cortex), and motor regions (i.e., pre-central gyrus, supramarginal gyrus) demonstrated greater activation than intertrial periods (Fig. 4.3A). When considering the impact of FC states, we observed two significant clusters of brain regions who's activity scaled with longer dwell lifetime in State 3: one bilaterally in the thalamus (t=5.54; x=-6, y=-16, z=10) and one in the right caudate (t=4.66; x=18, y=4, z=18). Activity from these subcortical clusters were significantly related to participant's reaction time (overall: *rho*=.377, *p*=.006; easy: *rho*=.347, *p*=.013; ambiguous: *rho*=.404, *p*=.003) but not directly to performance accuracy (overall: *rho*=.102, *p*=.478; easy: *rho*=.228, *p*=.107; ambiguous: *rho*=-.110, *p*=.442). Rather, as Fig. 4.3C illustrates, the effect of the subcortical cluster's BOLD activity on accuracy appears to be partially mediated via reaction time. Moreover, BOLD activity from the subcortical clusters was significantly negatively correlated with participants' endogenous urgency signal (*rho*=-.452, *p*<.001); this relationship remained significant even after controlling for mean reaction time as a covariate (*rho*=-.358, *p*=.009). This provides converging evidence

that the dwell lifetime in State 3 relates to an increase likelihood of exhibiting a "braking" signal in task which helps to improve behavioural performance. Dwell lifetime in no other state, nor the overall number of transitions between states, demonstrated significant covariation with brain activity in task. Taken together, this suggests that the propensity to express certain brain states at rest can shape brain activity in task which, in turn, relates to behavioural performance.

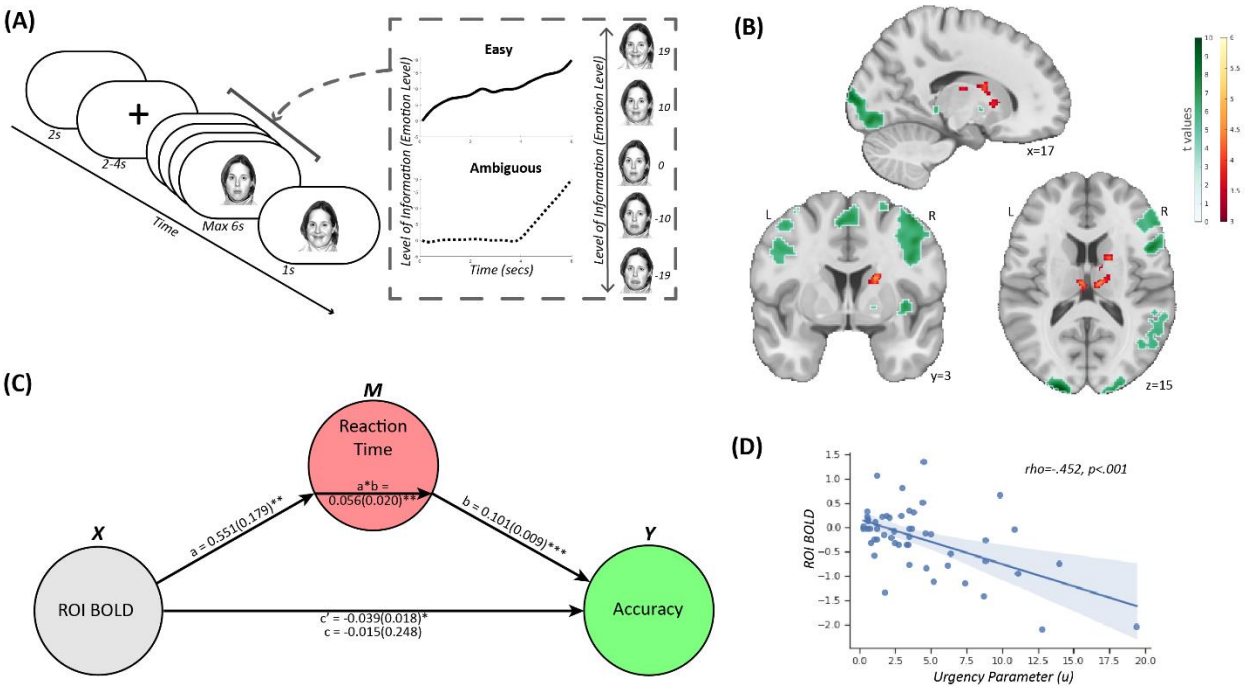

Fig. 4.3. *Relating time-varying functional connectivity (tvFC) state properties to behaviour.* ***(A)*** *Schematic of task design. Subjects viewed a short movie clip that slowly morphed from a neutral to either happy or sad facial expression. Easy and ambiguous trial types were interleaved throughout the blocks.* ***(B)*** *Signal contrasts between the trial and intertrial periods across all participants are depicted in green. When considering the effect of dwell lifetime in State 3 as a covariate on this contrast, we observe two significant clusters: one in the thalamus and another in the caudate (highlighted in yellow-red). In both instances, warmer colour indexes higher contrast values.* ***(C)*** *Mediation analysis for the association between the region of interest's (ROI; i.e., subcortical clusters) BOLD activity, mean reaction time, and overall accuracy. Path coefficients are shown next to arrows indicating each link in the analysis, with standard errors in parentheses. Path a refers to the path from BOLD activity to reaction time; path b refers to the direct link between reaction time and accuracy; path c is the relationship between BOLD activity and accuracy; and path c' refers to the total association between BOLD activity and accuracy, without the mediator (*=p <.05, **=p<.01, ***p<.0001).* ***(D)*** *Correlation between the cluster's BOLD activity and the urgency signal.*

4.5.3. Conservation of Network Configuration between Rest and Task is a Function of Task Difficulty

Although we established that a more pronounced global braking signal in task is observed among subjects with longer dwell lifetime in the modular brain State 3 at rest, our finding that dwell lifetime in State 3 only related to accuracy in easy trials leaves open the question how external task demands may influence network cartography. We addressed this by assessing whether FC configuration during rs-fMRI is preserved in task-fMRI and, if so, whether they may resemble a specific tvFC state. Moreover, we examined whether similarity between task and rest FC configuration may relate to behavioural performance. Within easy trials, the more similar the connectivity matrix in task-fMRI on easy trials was to that of the modular State 3, the better an individual performed on the easy trials in terms of accuracy (r=.408, Mantel's statistic: p=.003). Within ambiguous trials, closer resemblance between connectivity patterns and that of the low modularity State 4 was related to better accuracy on ambiguous trials (r=.395, Mantel's statistic: p=.004). We did not observe a significant relationship between dwell lifetime in any other FC states and behavioural performance metrics after multiple comparison correction.

4.6. Discussion

Cognitive processes are associated with altered brain activity and, by extension, functional connectivity. Understanding the intrinsic organization of brain networks at rest and in task can offer a context for the performance in task. Here, we provide evidence that individual differences in the prevalence of different network topology at rest relate to performance in a perceptual decision-making task. We utilized a dynamic approach to characterize fluctuations in FC configurations at rest and identified four distinct brain states. Results showed that individuals who had a propensity to more frequently express a tvFC state at rest with higher global modularity, especially of the DMN, were also more likely to demonstrate increased thalamic and caudate activity in task. This brain activity, in turn, served as a brake that slowed

decision time and improved accuracy in task. Next, we showed that network integration in task is dependent on task difficulty and that this relationship correlates with behavioural performance. These results underscore the importance of network topology in shaping behavioural performance when confronted with external tasks.

Why would the propensity to occupy a modular state at rest improve behavioural performance in task? A highly modular network architecture reduces the metabolic costs involved in maintaining the wiring of long-range, between-system connections (Bullmore & Sporns, 2012) which, though perhaps necessary for adaptive cognition, can only be sustained for brief periods of time. Critically, modularity is also behaviourally relevant – global brain network modularity measured during periods of rest is correlated with state-like (e.g., perception on a trail-by-trial basis (Boly et al., 2007; Sadaghiani et al., 2015)) as well as trait-like (e.g., working memory (Stevens et al., 2012)) aspects of cognition. Here, we add to this previous work by showing that the propensity to exhibit longer occupancy of a brain state of high modularity at rest improves behavioural performance in task. Our findings suggest a key role for subcortical structures, such as the thalamus and caudate, in mediating this relationship and the reason for this may be two-fold. First, the thalamus and basal ganglia may be uniquely poised to influence cognition as it forms part of a core circuit that support convergence of functionally diverse neural signals (Bell & Shine, 2016; Shafiei et al., 2018; Sherman, 2016). While a modular organization at rest may improve performance in task, a completely modular organization renders the brain limited in function. For example, without connectivity between networks, perceptual information from the visual cortex could never reach the motor cortex and dictate actions. Subcortical structures may play a key role in mediating the switch from a modular and segregated network configuration to one that is highly integrated when confronted with task demands. Second, the thalamus and basal ganglia serve as relays for the serial flow of information from structures involved in reward and motivation which can critically influence goal-directed cognition and subsequently drive motor output (Haber & Knutson, 2010). Our results suggest activity from these regions likely serve as a braking signal to pause, wait till enough information is accrued to make an informed decision, and consequently, improve performance accuracy. These findings dovetail with recent work implicating these subcortical regions in suppressing competing motor

actions (Dunovan et al., 2015; Meder et al., 2016) and to an endogenous urgency signal (Thura & Cisek, 2017; Yau et al., 2020), as in the present study.

During goal-orientated behaviour, more demanding cognitive functions may benefit from a less modular brain organization. As modules become more integrated, regions can change their module allegiance more quickly, potentially forming bridges of communication and foster flow of information in response to task demands (Bullmore & Sporns, 2012; Cole et al., 2014). Our results suggest that system-wide alterations in network topology facilitate more effective behavioural performance, but that this relationship is a function of task difficulty: in relatively straightforward easy trials, the more similar the network cartography was to a more modular brain state, the better individuals performed behaviourally; conversely, in ambiguous trials that require more complex working memory updating and cognitive control, resemblance of network cartography to a more integrated brain state resulted in better behavioural performance. This hypothesis has already garnered support from recent studies in network dynamics that suggest the extent to which the brain is globally integrated scales to task complexity and cognitive demand across blocks of similarly difficult trials (Cohen & D'Esposito, 2016; Hearne et al., 2017; Shine et al., 2016; Vatansever et al., 2017; Yue et al., 2017). Our findings extend these studies by demonstrating fluctuations in network topology can be identified even when task difficultly changes from one trial to the next, thus more closely mimicking natural settings. However, the specific cognitive demands that drive global integration remains unclear and warrants further investigation.

There are some important limitations to note in our study. First, we only tested one perceptual decision-making task and therefore do not know the generalizability of our results to other cognitive tasks. Second, FC fluctuations at rest may arise, in part, from stochastic noise (Handwerker et al., 2012). Though converging lines of evidence from computational models (Deco et al., 2011) and multimodal imaging (Tagliazucchi et al., 2012; Thompson et al., 2013) indicate a neural basis of tvFC, debate remains regarding whether these signals are spurious (Lurie et al., 2018). Finally, though we used a common sliding-window approach to estimate connectivity dynamics, there are many techniques used to estimate these metrics (e.g., Allen et

al., 2014; Lurie et al., 2018; Shappell et al., 2019; Yaesoubi et al., 2015) and further work should consider and compare robustness of different tvFC approaches in determining its relation to cognition.

Recognition that dynamic neuronal signalling is important in adaptive cognition and behaviour has been long established (Hebb, 1949) but the notion that signalling can be dynamic also in the absence of external task demands is relatively novel. Our results indicate that connectivity patterns between brain regions are continuously changing both at rest as well as in task. Performance on a cognitive task may not depend entirely on changes during the task itself, but also on the propensity of an individual to express certain patterns of intrinsic network organization. Thus, understanding examining individual differences in intrinsic network profile can help elucidate potential mechanisms underpinning disrupted cognition.

CHAPTER 5: General Discussion

A critical question in neuroscience is how a person, and by proxy the brain, arrives at a decision. We frequently navigate dynamic decision environments where sensory information changes from one moment to the next and can contain unreliable information. How does the brain support adaptive choices in these changing and ambiguous environments? Theories as to how decisions are formed stretch back centuries, but only in the recent decades have neuroscientists begun to chip away at the biological basis of perceptual decisions. This is driven largely by the convergence of computational models and non-human primate neurophysiology. In this doctoral thesis, I attempted to bridge this research to human perceptual decisions by employing various non-invasive neuroimaging modalities. The central aim of this thesis was to study the correlates of decision parameters in the human brain and examine whether decision formation may be influenced by an urgency signal. In brief, we tested potential neural correlates of hypothesized decision parameters in Chapter 2. We demonstrate that MVPA can be used to infer sensory evidence from fMRI BOLD activity by relating it to model parameters from a hierarchical Bayesian model of the DDM. Moreover, the paradigm we developed can probe the dynamics of perceptual decision-making and tease apart predictions made by a pure evidence accumulation versus urgency gating model. Our results point to the caudate as a potential source of an inverse-urgency signal. We extended this in Chapter 3 and examined how perceptual decisions unfold over time. We provide evidence that a decision variable captured by EEG reflects the combined influence of both sensory evidence and an evidence-independent, time-variant urgency signal. In Chapter 4, we highlight how individual variability in the functional organization of the brain may influence behavioural performance in task. We demonstrate how this may be mediated by activity of subcortical regions that are involved with generating an inverse-urgency signal. This final chapter presents a general discussion of the common themes from the questions we have considered, the limitations in our findings, and highlights some potential avenues for future research.

5.1. Probing Decision-Related Neural Activity from Individual Brain Regions/Signals Using Non-Invasive Recordings in Humans

A particularly rich vein of research in perceptual decision-making has been driven by applying evidence accumulation models to study neural mechanisms underlying simple choice paradigms based on visual sensory evidence, such as the random dot motion task. These tasks have allowed researchers to accurately characterize the sensory information in the decision environment, fit computational models to behaviour, and identify neural activity that reflects core ingredients of perceptual decisions (e.g., sensory evidence and decision variables) using single-cell recordings in non-human primates (Gold & Shadlen, 2007). We sought to adapt these tasks for use with neuroimaging modalities (i.e., fMRI and EEG) for data acquisition in humans. Neuroimaging techniques provide us with a way to non-invasively acquire whole-brain recording to assess the contribution of different brain regions, and their connectivity, to perceptual decisions. Building on previous work (O'Connell et al., 2012; Thura et al., 2012), we designed and employed a dynamic visual discrimination task across our three studies. This task involved the presentation of a neutral facial emotion that gradually morphed into a happy or sad expression. Subjects were asked to respond whenever they felt confident enough to predict what the final emotion will be, and to respond both as accurately and as quickly as possible. We used the subject's RT distribution, along with accuracy, to estimate decision parameters in our computational models and then searched for their neural correlates using neuroimaging modalities.

5.1.1. CPP Signalling in Humans as a Homologue to LIP Signalling in Monkeys

Researchers have long searched for brain region(s) that demonstrate activity which closely mirror the estimated decision variable from evidence accumulation models like the DDM. One of the pivotal findings in the field of perceptual decision-making is the discovery that dynamic activity of single neurons in the LIP of the monkey cortex can be well-described by an evidence accumulation process during the random dot motion task (Gold & Shadlen, 2007; Hanks et al., 2006; Roitman & Shadlen, 2002; Shadlen & Newsome, 2001). Significance advances in non-invasive assays have opened opportunities for translating this finding, as well as other detailed

characterisations of decision mechanisms, from animal neurophysiology to the human brain. In particular, the high temporal resolution of EEG naturally lends itself to serve as an appropriate non-invasive alternative to single cell recording. In our study (Chapter 3), we were able to identify a domain-general CPP signal from scalp EEG in human subjects. This neural signal displayed hallmarks of a decision variable: it gradually evolved in time, ramped steeply close to decision, and peaked just before the time of response. We formally test this notion with a hierarchical Bayesian implementation of the DDM to demonstrate that the buildup of the CPP signal reflected the evidence accrued as related to the drift rate parameter at a trial-by-trial level. Our analysis further suggested that the relationship between CPP buildup and drift rate was dependent on the trial type, and on individual differences in the tendency to wait for more information before deliberation. In brief, CPP buildup did not differ between correct or incorrect trials, was related to higher drift rate in trials of higher ambiguity in sensory information, and was still detected in subjects who tended to respond early despite high ambiguity. These findings are in line with recent work suggesting that the CPP is mediated by subjective evidence and perceived decision confidence, over and above the actual sensory evidence in the environment (Herding et al., 2019; Tagliabue et al., 2019), thus contradicting the original assumption that the CPP solely varies with the available sensory information (O'Connell et al., 2012). Our findings also point to the potential involvement of an additional urgency parameter (discussed in Chapter 5.3). In a similar vein, firing rates of LIP and other fronto-parietal neurons thought to reflect a decision variable in non-human primates have also been shown to encode a signal of subjective sensory experience and decision confidence (de Lafuente & Romo, 2005; Grimaldi et al., 2015; Kiani & Shadlen, 2009; Pouget et al., 2016). Taken together, our findings suggest that the CPP signal may relate to similar, or even homologue, mechanisms reflected in the neuronal processes identified in the LIP of non-human primates.

While EEG is a versatile, inexpensive, and portable neuroimaging modality, a key limitation is that it provides a very indirect reflection of the neural processes underlying brain functions. The recording captured by a single electrode can reflect the summed activity of hundreds of thousand of pyramidal neurons. Moreover, the shape and conductivity of the skull and scalp

strongly influence the EEG signal. Attempts to identify the spatial, cortical origin of signals detected on the scalp by using source localization are limited by issues in the forward problem (that is, estimating the brain, skull, and scalp surface boundaries which can distort EEG signals), and importantly, the lack of a unique solution for the inverse problem (that is, how to calculate the relationship between the potential at the scalp and the dipole amplitude in the brain) (Akalin Acar & Makeig, 2013; Asadzadeh et al., 2020). Thus, to infer where in the brain a scalp EEG signal originates require certain assumptions and constraints to attain a unique solution. This does not mean the source localization of EEG signals is uninformative. Source localization algorithms like minimum norm estimates and their generalization (e.g., low resolution electrical tomography) have yielded results that are largely anatomically concordant with fMRI BOLD localization (Grech et al., 2008; Phillips et al., 2002). Although our results suggest that the CPP acts as a decision variable, without knowing the specific neural origin of the signal, it is hard to contextualize this finding in the decision circuitry. A brain region that encodes a decision variable should be connected to regions that encode the sensory information and to regions that are involved with the appropriate (motor) response. As it stands, we do not know if CPP matches these criteria, and to our knowledge, the cortical origin of this signal has yet to be tested. Though the CPP is captured from a parietal site on the scalp suggesting it is likely under the greatest influence of activity from parietal pyramidal neurons, we cannot definitively draw this conclusion. Thus, an interesting next step may be to apply source localization to identify the neural origins of the CPP. Alternatively, and perhaps a more precise methodology, one could use simultaneous acquisition of EEG and fMRI data to characterize the temporal dynamics of a decision variable, such as the CPP, on a trial-by-trial level in spatially well-defined neural networks.

5.1.2. Neural Representation of Sensory Evidence in the Human Brain

Given that perceptual decisions are hypothesized to result from the gathering of sensory information from the environment, another interesting question to address is where and how in the brain is the relevant sensory information represented. For example, it is established in the non-human primate literature that, during the random dot motion task, neurons within the area MT encode the sensory decision variable (i.e., motion direction) based on their receptive

field, and project to the LIP to inform a decision variable (Katz et al., 2016; Mazurek et al., 2003; Perrone, 2004). Extending this to humans is difficult as non-invasive assays of the human brain cannot differentiate between motion directions in the random dot task. As such, there is a need to use alternative stimuli sets whose representations in the brain are discriminable by neuroimaging modalities. Previous EEG studies have shown that the early N170 component – a face-sensitive visually evoked ERP – and a late parietal component can discriminate face from car stimuli (Philiastides et al., 2006; Philiastides & Sajda, 2006). However, this stimulus is not ideal for a dynamic task as faces and cars do not naturally transition, and artificial manipulation is required to modulate the level of sensory information available between the two options (e.g., blurred masks or jumbling pixels of face and car images). Moreover, EEG is generally ill-suited for discriminating neural correlates of sensory information as its captured signals reflect the summed activity of an extensive pool of neurons that are likely sensitive to different sensory information. In this thesis, we first opted to use fMRI due to its higher spatial resolution and exploited the well-characterized face-processing system in the human brain. fMRI BOLD activations to different facial emotions can be decoded with MVPA and machine-learning techniques (Haxby et al., 2000; Wegrzyn et al., 2015). Facial emotions also naturally transition from one to the next and were therefore ideally suited for our dynamic paradigm.

Although a number of previous studies have attempted to characterize how sensory information is represented in the human brain using averaged fMRI BOLD activity, their findings have been highly discrepant (reviewed in Chapter 1.5.1). In Chapter 2, we attempted to reconcile this issue by taking a new approach of using MVPA to decode information from patterns of BOLD activity. MVPA is arguably a better methodology to detect more precisely *what* information is accumulated and *where* (Haxby et al., 2001; Norman et al., 2006). While univariate analysis focuses on the difference in mean BOLD signal, MVPA focuses on decoding the informational content of activation patterns encoded in different regions (Davis & Poldrack, 2013). We exploited this methodology to decode patterns of activity related to either happy or sad expressions in a training task, allowing us to infer the extent to which a voxel carried neural signals in favour of each choice alternative. We then applied the individual decoders to our dynamic task, and with hierarchical Bayesian modelling, we tested whether allowing the drift

rate of the DDM to vary with the multivariate "code" of sensory representation in regions previously implicated in face-processing (Haxby et al., 2000; Wegrzyn et al., 2015) could improve model fit. While facial emotion could be decoded from the BOLD activity from all of our regions of interest, only the MVPA code from the fusiform gyrus contributed to the DDM and related to the estimated drift rate at a trial-by-trial level. This suggests that the fusiform gyrus may be central to decoding and feeding the information forward in our task. As with the CPP in our EEG experiment, we found that the relationship between the fusiform MVPA code and drift rate was contingent on trial type and on individual differences in the tendency to respond early or late. However, in contrast to the CPP buildup which we found to be present regardless of the amount of sensory information in the decision environment, the fusiform MVPA code was only related to drift rate when there was sufficient evidence. The fusiform MVPA code was not found to contribute to evidence accumulation in responses made during the early portion of the ambiguous trials where there were low levels of sensory evidence. This likely suggests that the fusiform MVPA code is a more direct representation of the sensory evidence, mirroring closely the amount of information available. On the other hand, the CPP signal is more characteristic of a decision variable that integrates lower-level sensory information and appears to be under some other influence that drives its buildup, independent of sensory evidence. We demonstrate that the fusiform gyrus can be used to provide a window into decision processes and the computations they implement, specifically in the context of facial emotion stimuli. As with MT firing being informative for motion detection, activity from the fusiform should not be misconceived as a central function in accumulating evidence for *all* decisions. Presumably, different areas would be involved if the decision depended on different categories of stimulus features. We used facial emotion as an example of sensory information in perceptual decision-making but testing with other forms of sensory information is warranted. We believe that our approach of combining MVPA with DDM can serve as a template for future fMRI studies.

MVPA has been ambitiously advertised as a means of "reading" the brain (Norman et al., 2006). However, it should be noted that there are several caveats with employing an MVPA approach. Compared to traditional univariate analyses, MVPA may be better suited to revealing the

informational content coded in activation patterns in the brain, but it is by no means a perfect description of this representation (Ritchie et al., 2017). Classifiers, especially more complex non-linear ones, can be too informationally greedy. The information the classifier uses as a basis of the discrimination may not be constrained to the information the brain actually exploits to make the distinction. How a classifier exploits information in neural data can be deeply opaque. Moreover, the biological plausibility of decoding methods is often overlooked. While fMRI has superior spatial resolution compared to EEG, BOLD is nonetheless an indirect measure of the underlying neural processes, and a voxel reflects the average activity of hundreds of thousands of neurons. Regardless of performing univariate or multivariate analysis, all fMRI studies face this inherent limitation. In our study (Chapter 2), we show that our activation "code" of the fusiform gyrus – derived from support vector machine-learning weights – has psychological plausibility as it links to observed behaviour, and specifically, the drift rate parameter. Moreover, we show that the fusiform MVPA code is transferred between relevant up-stream and down-stream brain regions (discussed below in Chapter 5.2.1) suggesting biological plausibility. Nonetheless, we must remain cautious in how we interpret our findings. Further understanding of the assumptions that different machine-learning techniques make, in addition to identifying their strengths and weaknesses for specific representational questions, may be essential in revealing and interpreting how information may be represented in the brain to make decisions possible.

5.2. Decisions in the Context of Brain Networks

Thus far, we have discussed our findings from individual brain regions/signals. However, we know that the coordinated activity between a multitude of brain regions contributes to successful decision formation and execution. Visual information flows through dorsal and ventral visual streams responsible for action specification and action selection, respectively (reviewed in Chapter 1.3 and depicted in Fig. 1.3) (Cisek, 2007; Goodale & Milner, 1992).

5.2.1. Informational Connectivity of Sensory Evidence During Task

After providing evidence that the MVPA code from the fusiform gyrus represents sensory information in the brain, we sought to contextualize this finding in light of the decision circuitry. To this end, we took advantage of the spatial resolution of fMRI and its ability to probe the whole brain, including ventral and subcortical structures that may be more difficult to capture by scalp EEG. In Chapter 2, we used generalized psychophysiological-interaction analysis (McLaren et al., 2012) to identify which brain regions not only temporally coactivated with the fusiform gyrus – thus reflecting FC – but also whether these connections were modulated by the fusiform MVPA code. We interpreted this as reflecting informational connectivity, which charts the flow of information during the task (Anzellotti et al., 2017). We found that the neural representation of sensory evidence from the fusiform MVPA code is relayed between regions of lower-level sensory processing areas (e.g., lateral occipital area), as well as dorsal stream areas involved in action specification (e.g., inferior parietal sulcus, superior parietal lobule, supramarginal gyrus, and frontal eye fields). This resembles findings from non-human primate physiology studies that suggest sensory evidence from the area MT projects to the LIP where a decision variable is formed and then converted into action (Gold & Shadlen, 2007; Hanks et al., 2006). Here, we provide a more global view of the decision circuitry that may be involved in perceptual decisions during our task. However, due to the low temporal resolution of fMRI, we were unable to temporally tease apart the flow of information during the decision process. Simultaneous single-cell recording from area MT, LIP, and the prefrontal cortex in macaque monkeys have shown that perceptual decisions are not simple feed-forward processes, but result from complex temporal dynamics including feedforward and feedback interactions between frontal and posterior cortex (Siegel et al., 2015); whether this principle holds true in the human brain remains to be tested.

5.2.2. Individual Variations in the Organization of Human Brain Networks Affects Task Performance

While connectivity between brain regions may change in response to task demands, the organization of these connections are thought to be dominated by certain intrinsic configurations or RSNs (Laird et al., 2011; Yeo et al., 2011) with substantially more modest

contributions from task-state (Cole et al., 2014; Gratton et al., 2018). This view of brain function highlights the role of individual brain regions within the context of broader neural networks. For example, the informational connectivity of the fusiform MVPA code we observe in Chapter 2 involves visual perception, cognitive, and motor/visuospatial networks. RSNs do not work independently and the dynamics between RSNs are thought to reflect the array of cognitive architectures that the brain has available (Bertolero et al., 2018). Critically, functional network architecture identified using resting-state FC is also present during task performance and may reflect the route by which activity flows during cognitive task performance (Cole et al., 2014; Cole et al., 2016). In tandem, there is growing recognition of the importance of time-sensitive descriptions of brain activity, and that the traditional analysis technique of averaging across extended periods of fMRI scan-time may obfuscate the time-varying reconfiguration in global network structures (Allen et al., 2014; Lurie et al., 2018). In Chapter 4, we found that individuals who more frequently expressed a brain state (or FC configuration) with higher global modularity/segregation were also more likely to perform better behaviourally in task. Our findings suggest a key role for the thalamus and caudate in mediating this relationship by serving as an inverse urgency signal (discussed below in Chapter 5.3). In the context of evidence accumulation models, slower responses (e.g., by raising the decision threshold) likely allow for more information to be accrued before choice commitment, in turn, improving accuracy. These subcortical structures may also play a key role in mediating the switch between modular and integrated brain states (Bell & Shine, 2016; Bullmore & Sporns, 2012; Shafiei et al., 2018; Sherman, 2016). This is important as more demanding cognitive functions benefit from a more integrated brain organization that fosters the flow of information in response to task demands, but can be too metabolically demanding to sustain over long periods of time (Bullmore & Sporns, 2012; Shine et al., 2016). In our task, ambiguous trials with low sensory information are arguably more difficult, requiring greater cognitive control, and more complex working memory updating. In line with our hypothesis, we found that the more a subject's FC configuration during ambiguous trials resembled an integrated brain state, the better the subject performed. Conversely, subjects' FC configuration resembled a more modular brain state during easy trials, and the degree of this resemblance related to how well

the subject performed on these trials. We discussed at the beginning of this thesis (Chapter 1.3) how the neural architecture of perceptual decision-making can be split into four systems: sensory, decision, motor, and performance monitoring. While distinct, these systems are thought to be constantly interacting as information flows from occipital to motor areas (Cisek, 2007). In a situation where sensory information is abundant, the default baseline (i.e., rest) connectivity between different RSNs pertaining to these four systems may be sufficient in conveying information flow to inform a decision. However, in situations where sensory information is weak or ambiguous, there may be a greater need to form stronger bridges of communication between RSNs, for example, to exert action selection mechanisms. Taken together, our results help contextualize perceptual decisions in the framework of brain connectivity and networks.

5.2.3. Limitations of Functional Connectivity

A potential issue with how we address brain connectivity in both Chapter 2 and 4 is that we assume it is determined by FC. This method ignores a fundamental assumption in neuroscience: anatomical connections between brain regions provide the structural basis for functional interactions between them. Thus, the propensity for two regions to interact should vary in proportion to the density and efficacy of the projections connecting them, and FC is thought to reconfigure around the underlying large-scale anatomical structure of the human cerebral cortex (Honey et al., 2009). For example, it has been shown that functional activation to faces in the fusiform gyrus can be predicted by structural connectivity alone (as measured by diffusion-weighted imaging) (Saygin et al., 2011). While recent studies suggest there is strong evidence for the biological plausibility of FC (Deco et al., 2011; Handwerker et al., 2012; Tagliazucchi et al., 2012; Thompson et al., 2013), studies that use FC to infer brain connectivity, as we do in our studies, do not explicitly consider the relevant anatomical skeleton. A better understanding of the nature of the structure-function relationship may help further guide our understanding of how cognition is achieved. Future work can expand the findings from our study, and the combination of structural and functional connectivity techniques (e.g., voxel-to-voxel tractography) may help more finely characterize the relationship between brain connectivity and function.

5.3. Role of an Evidence-Independent Urgency Signal

While the DDM has been a reliable workhorse for describing extant neural data, recent work contends that this standard account provides an incomplete picture of how neural responses contribute to the timing of perceptual decisions, especially in the face of noisy or changing sensory information (Churchland et al., 2008; Thura & Cisek, 2017). In the highly complex and dynamic environment we inhabit, making accurate and timely decisions is a considerable challenge since the information the brain receives is almost always to some degree unreliable. Decisions may not be merely driven by accumulation of noisy sensory evidence, but also by a time-varying urgency signal that helps curtail deliberation in the face of ambiguous information (Cisek et al., 2009).

The urgency signal is thought to grow with time and ubiquitously elevate a decision variable towards decision thresholds, such that less sensory evidence is required for decisions commitment as elapsed decision time increases. This contradicts the traditional DDM which assumes an integrating decision variable is based solely on sensory evidence. In tasks that present constant evidence (e.g., where dot motion coherence remains unchanged throughout a trial), the DDM and the urgency gating model make very similar predictions about neural activity and behaviour (Thura et al., 2012). In both, the predicted decision variable grows at a rate proportional to the subject's estimate of the strength of evidence, and reaches some threshold level of activity at the time decision is made. In the DDM, this is attributed to the accumulation of sensory evidence, whereas in the urgency gating model, this is attributed to an endogenous urgency signal that grows with time. In order to distinguish the predictions made from these two computational models, one must track either the sensory evidence available or the urgency signal. However, since the urgency signal is posited to arise endogenously, it difficult to explicitly manipulate naturally without creating artificial scenarios where speed is encouraged over accuracy (Hanks et al., 2014; Heitz & Schall, 2012). In our paradigm, by changing the sensory information in the decision environment, we can accurately characterize the sensory information available at any given time and compare our captured neural signal to that predicted by our models. Moreover, by having trials of differing ambiguity of sensory

information (i.e., easy and ambiguous), we were able to more clearly see when suboptimal decision policies were in place and to offer the opportunity to understand their computational substrates (e.g., higher urgency).

Results from our studies suggest an urgency signal can be observed in naïve human participants. Our participants were not trained on the dynamic paradigm we employed, were allowed to freely respond, and were not incentivised to choose one decision strategy over another (e.g., rewarding subjects based on performance). We nevertheless observed two broad groups of individuals: those who tended to wait for more sensory information to be available when the decision environment is ambiguous, and those who tended to respond early with incomplete and ambiguous information. Participants appear to inherently vary in their motivations to complete the task, and by formally testing with an urgency gating model, we demonstrate that those of higher urgency (i.e., early responders) tended to choose speed over accuracy, despite not being explicit prompted to do so. This contradicts previous work that suggests models incorporating a time-varying parameter only fit behaviour of highly trained monkeys and not humans performing a limited number of trials (Hawkins et al., 2015). In addition to these behavioural findings, we provide evidence that a dynamically growing neural decision variable, namely the CPP captured by EEG (Chapter 3), nonetheless ramps up in time among early responders who make decisions despite very ambiguous sensory information in the decision environment. This resembles previous finding in macaque monkeys where firing rates in the LIP grew in time even on trials where sensory evidence was entirely ambiguous (i.e., 0% motion coherence during the random dot motion task) (Churchland et al., 2008). One potential interpretation of this finding is that the decision variable is subject to an urgency signal, in close conjunction with subjective evidence and perceived decision confidence (Braunlich & Seger, 2016). We formally tested this notion and found that our predicted neural signal from an urgency gating model accurately fitted with the observed CPP buildup at a trial-by-trial level – this was not the case for neural signals predicted by the DDM.

Our results also shed light into where in the brain an urgency signal may arise. While the neural correlates of an urgency signal have been formally tested in non-human primates (Thura &

Cisek, 2014, 2017), this model has yet to be extended to humans. We demonstrate using fMRI (Chapter 2), that late compared to early responders exhibited greater caudate activity on ambiguous compared to easy trials. Moreover, BOLD signal from the caudate was inversely related to subjects' estimated urgency signal. In Chapter 4, we found that individuals who exhibited a propensity to demonstrate a modular FC organization at rest – argued to be a less metabolically-demanding and more optimal configuration when not engaged in external task (Bullmore & Sporns, 2012) – were also more likely to exhibit greater thalamus and caudate activity during the task. Consistent with our observations in Chapter 2, we observed that a subject's average activity from these subcortical regions inversely related to their estimated urgency parameter. Taken together, our findings indicate that urgency may be rooted in subcortical activity. We posit that this is linked to braking signals generated by the indirect dopaminergic pathway originating from a striatal population of projection neurons (Frank & Claus, 2006). This ties in with basal ganglia's hypothesized role in action selection: multiple possible actions generated by the cortex are received by the basal ganglia, which acts as a gating mechanism, selecting the behavioural response that is considered most appropriate, and suppressing alternative signals (Bogacz & Gurney, 2007; Cisek, 2007; Frank et al., 2007). However, in none of our studies did we directly measure dopamine or the indirect pathway *per se*. Future research is needed to more directly test the link between dopamine (e.g., tyrosine depletion, Parkinson patients, or positron emission tomography studies) and the urgency signal in human decision-making.

The research presented in this thesis lends support to the notion that the formation of perceptual decisions is influenced by an evidence-independent, time-variant variable, and these studies are among the first to formally test the neural correlates of an urgency signal in naïve human subjects. However, it is important to acknowledge that this concept is relatively nascent and remains a debated topic (Thura et al., 2012; Winkel et al., 2014). Though our trial types are modelled after previous work testing the urgency gating model in macaques (Thura et al., 2012), there are several drawbacks to this task paradigm. First, our trial types may encourage individuals to choose between speed and accuracy, perhaps exaggerating the effects of urgency. Second, subjects were asked to make an inference about the future, and not

necessarily to make a judgement based on the current available sensory information. Third, urgency may be only one of the explanations for our findings. There is a plethora of computational models that have attempted to describe observed behaviour and this thesis only considers two possible variants. Though we found that the urgency gating model was a better fit to our data than to the DDM, it shares similar assumptions with other models such as the collapsing bound model or leaky-competing-accumulator (Evans et al., 2020; Thura, 2016). Direct comparison of a more comprehensive range of models may help better elucidate which hypothesized mechanisms are actually closest to the ground-truth of how perceptual decisions are formed. We believe that better characterization of the urgency signal (or lack thereof) at the neural level is an important future goal for cognitive neuroscientists and can provide us with a more mechanistically principled and refined understanding of the cognitive underpinnings of perceptual decisions.

5.4. Use and Limitations of Computational Models

David Marr, a pioneer in Computational Neuroscience, postulated in his famous three-step recipe of brain modelling that to understand the brain one must: (i) formulate the problem and identify its normative solution (i.e., the way it behaves optimally), (ii) search for computational models that accomplish the optimal solution, and (iii) elucidate implementations of such algorithm(s) in the brain (Marr, 1982; Marr & Poggio, 1979). In this thesis, I have demonstrated how computational models (e.g., DDM and urgency gating model) can be harnessed to provide insight into the latent psychological processes that underlie decisions. The ability to model behaviour provides a powerful analysis tool for mechanistic understanding of the processes by which decisions are forged in the brain at group, subject, or even trial level. This is achieved by formalizing conceptual models into mathematical terms, thus eliminating the vagueness in terminology, and enforcing a rigorous and precise way of testing relevant components or parameters. Such quantitative descriptors or model parameters can provide a bridge between mental and neuronal processes and allow us to test how they map onto each other (e.g., urgency signal mapping inversely to subcortical activity). Moreover, model

parameters may serve as additional biomarkers that can disentangle symptom clusters as they probe a more basic level of understanding, independent of diagnostic category (Huys et al., 2016).

The foregoing discussion illustrates the benefits of anchoring neuroimaging data to principled quantitative models of behavioural data. However, it is important to note an obvious caveat to this approach: the insight computational models provide about an individual's disposition is limited to the abstractions assumed by the model. A model must trade-off between parsimony (i.e., economy of parameters) and comprehensiveness (i.e., goodness of fit) in its assumptions: too simple a model and you risk not being able explain your observed data; too complex a model and you risk overfitting and becoming unable to generalize outside your dataset. Ultimately, it is the estimate of the model parameters that serves as a proxy for underlying decision dynamics. Computational models are typically optimized for behavioural data, with their validity assessed by its fit to accuracy and RT data. However, they remain agnostic about the precise implementation of the algorithms at the neural level. While behavioural data can be comprehensively explained by parsimonious models with a minimal set of parameters, the underlying neural implementations are probably far more complex – it is unlikely that neural signals have a simple one-to-one relation with model parameters. Moreover, many other hypotheses can be generated that are consistent with the observed link but differ in the mechanics that explain the link (e.g., the identified region may simply relay or mirror the signal of interest). Results from our studies, as well as other studies, that use model parameters based on behavioural data to identify neural signals should be considered in light of this key limitation. Over the coming years, new neural data will undoubtedly help further constrain and update our modelling framework. Development of new devices, new methods of measurement, and new experimental paradigms are required to support computational models that respect the complexity of brain structure and function. Such advances can help us determine whether model parameters reflect underlying neural processes, or remain abstractions disconnected from this ground-truth.

5.5. Beyond Perceptual Decisions

Though this thesis centers on perceptual decision-making, not all decisions revolve around perception. Understanding how the brain overcomes the challenges associated with perceptual decision-making may illuminate broader principles of computation that extend to a range of cognitive operations. A common engine for decision-making could be one that drives the observer from a state of ambiguity towards a decision based on the information gathered from the environment, while simultaneously faced with a growing pressure to commit to a choice as time elapses. Whether such principles are idiosyncratic to perceptual decision-making or have further implications is an intriguing and important question.

For example, decisions are often driven by their "value" (or in economic terms, "utility") with the selected option being the one with the highest subjective value. One may choose between eating an apple or a cake not based on its perceptual properties, but by its perceived value or taste. However, our understanding of perceptual decisions suggests evidence needs to be accrued from the external decision environment. This is difficult to reconcile with in value-based decision-making, as deliberations are made based on internal evidence – that is, the subjective value assigned to each option. One approach has been to include an attention parameter to the DDM, which is hypothesized to modulate the drift rate during choice accumulation. Eye tracking data suggest that greater time is spent fixated on objects/stimuli of higher value, and that this fixation time or attention moderates the drift rate across time (Krajbich et al., 2010; Krajbich & Rangel, 2011; Mormann et al., 2010). More recently, it has been proposed that the hippocampus may carry internal evidence to support deliberations about value, and damage to this region impacts the ability to draw on such internal evidence, resulting in stochastic choices and longer reaction times (Bakkour et al., 2019). Others have emphasized the role of the striatum and ventromedial prefrontal cortex in encoding the expected value of a decision (Summerfield & Tsetsos, 2012). For example, the neural correlates of a decision variable estimated using the DDM for a value-based, compared to a perceptual, decision-making task was found to not only involve parietal regions implicated in integrating sensory evidence, but also frontal regions that encode valuation (Polanía et al., 2014). There is

less knowledge about how a time-variant parameter like urgency may come into play in value-based decisions. Recent evidence suggest both choice and saccadic vigour vary with subjective economic value (Yoon et al., 2018; Yoon et al., 2019), potentially reflecting a global influence of the urgency signal during both decision and action. This resembles a study performed with macaques, which showed that both the decision time and the vigour of movement used to report decisions related to an urgency signal in a perceptual task (Thura & Cisek, 2014). However, to our knowledge, the influence of an urgency parameter on value-based decision-making has yet to be formally tested and could be an interesting avenue to pursue in future research.

Understanding perceptual decisions can also give us insight into what may have gone awry in neurological and psychiatric disorders where cognitive dysfunction is apparent. For example, the phenomenon of misperceiving one object as another, or the belief that there is a percept despite no sensory signals (i.e., hallucinations), are present in conditions such as schizophrenia (Limongi et al., 2018; Powers et al., 2017; Tek et al., 2002). Such illusory or phantom percepts may be a result of dysfunctions in the perceptual system when the brain regions responsible for generating a decision variable (e.g., fronto-parietal) incorrectly interpret weak sensory evidence coming from lower-level sensory regions (e.g., visual) (Summerfield et al., 2006). More broadly, clinical disorders may also be amenable to pathophysiological abnormalities in the decision formation process. For example, elevated urgency may be etiologically tied to disorders of impulsivity (discussed in Chapter 1.4), while excessively diminished urgency may cause lack of motivation and blunting of reward sensitivity, potentially posing vulnerability to conditions such as depression and anhedonia (Carland et al., 2019). If indeed our understanding of perceptual decisions can be translated to the broader neuroscience discipline, it can potentially assist in generating a unifying framework in understanding the cognitive underpinnings of decision-making. Ultimately, better understanding will lead to better treatment options to correct or ameliorate cognitive dysfunctions present in a variety of clinical disorders. Future work that provides a more refined understanding of the underlying neural mechanisms can lead to new therapies that target brain systems in ways we cannot currently imagine.

5.6. Conclusion

The original research presented in this thesis helps bridge some of the gaps in our understanding of human perceptual decisions. I have shown how neural correlates of decision-making can be addressed at different timescales using different neuroimaging modalities, specifically fMRI and EEG. Moreover, our research highlights some new approaches that can be used to connect theoretical insights concerning the computations that support decision formation to neuronal activity. The field of cognitive neuroscience is at an important juncture: the current age of big data and open science, with the ability to acquire and manipulate extremely high-dimensional, multimodal datasets (e.g., cognitive, neuroimaging, clinical, and genetic), holds great promise in uncovering the complex cognitive underpinnings of human decision-making. However, it poses a data analysis challenge, and can be like finding needles of understanding in haystacks of data. Having a clearly articulated analytic goal in mind is paramount to research endeavours. I hope the work from this thesis can serve as a guide to orient future research.

Though we have covered much ground in this doctoral thesis, the study of decision-making extends far beyond what I have presented here. Decision-making is a fundamental human behaviour and a palimpsest of intellectual disciplines, including neuroscience, psychology, mathematics, sociology, economics, political science, and philosophy, to name a few. This speaks to the far-reaching implications of decision-making. A nuanced understanding of human decisions, and the neural mechanisms that support it, can improve decision-making in many situations and potentially ameliorate dysfunctions when it has gone awry.

APPENDIX

Supplementary Materials from Chapter 2

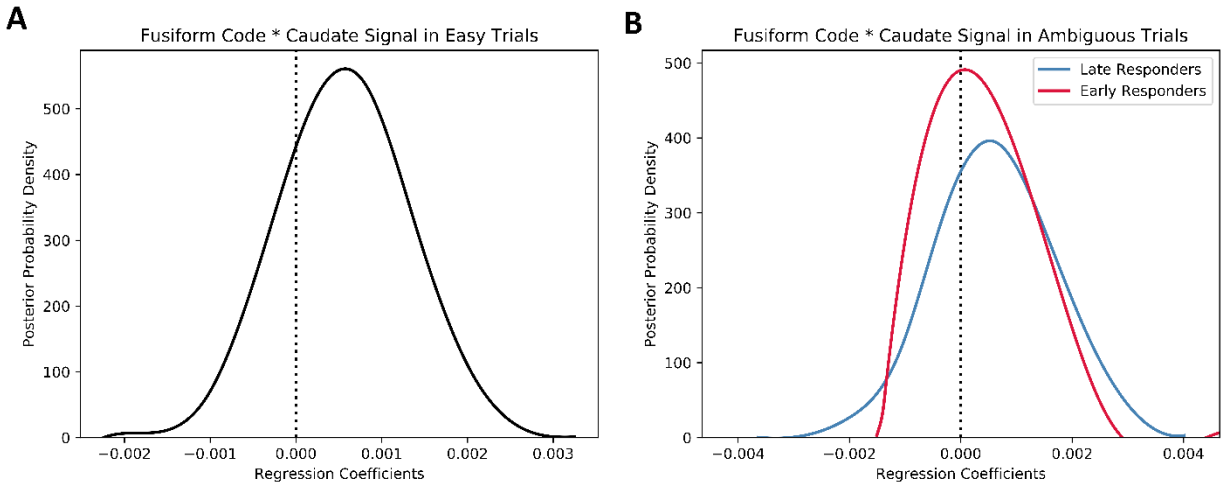

Supplementary Fig. A2.1*. A striatal "urgency" signal may interact with fusiform code depending on task demands. To test this hypothesis, we adapted our HDDM model to assess whether caudate activity, within the significant clusters, could alter decision parameters. As with our HDDM models with fusiform code, we split our data three-ways based on: (1) easy trials across all subjects, (2) ambiguous trials among late responders, and (3) ambiguous trials among early responders. Adding caudate BOLD activity did not improve model fit, as assessed by DIC, beyond a model with only fusiform code. There was weak evidence that the degree to which fusiform code impacted drift rate was modulated by variance in caudate activity in easy trials (79.02% of posterior probability >0) and in ambiguous trials among late responders (71.98% of posterior probability >0). It had little to no effect on ambiguous trials among early responders (54.35% of posterior probability > 0). To test whether caudate may convey information regarding facial emotions, we ran a SVM classifier per participant restricted to the caudate to decode happy and sad faces in the training task. We found that, as opposed to the fusiform and other face processing areas, caudate activity did not accurately decode facial emotions better than chance. Thus, although caudate activity reflected parts of the evidence accumulation process, it did not appear to reflect information processing of facial emotion stimuli nor affect decision parameters as estimated by HDDM.*

Supplementary Table A2.1. *Raw deviance information criterion (DIC) values comparing HDDM model fit of the seven neural models relative to base.*

Region Name	**Difference in DIC value (relative to base)**
Amygdala	653.49
Anterior Temporal	650.22
Fusiform Gyrus	-26.29
Inferior Occipital	662.75
Insula	672.19
Intraparietal Sulcus	683.00
Superior Temporal	668.38

Supplementary Table A2.2. *Psychophysiological interaction (PPI) from a left and right fusiform seed as parametrically modulated by the multivariate fusiform code for emotion. Related to Fig. 2.5.*

Region	x	y	z	t stat	Number of Voxels
L Fusiform Gyrus Seed					
L lateral occipital	-18	-92	22	7.03	24
R lateral occipital	38	-80	32	10.79	1202
L cerebellum	-14	-74	-44	10.44	267
R cerebellum	22	-70	-44	8.26	170
R lateral occipital	48	-70	4	7.86	30
R lateral occipital	40	-70	-24	7.26	39
R fusiform gyrus	30	-68	-4	7.53	93
R inferior temporal	54	-54	-14	10.04	551
L fusiform gyrus	-42	-48	-20	23.96	3359
L lateral occipital	-12	-48	54	8.03	252
R superior temporal sulcus	56	-44	4	9.45	489
R superior parietal lobule	30	-44	50	8.49	56
L intraparietal sulcus	-48	-42	48	9.40	360
R supramarginal gyrus	60	-38	24	7.28	75
R intraparietal sulcus	50	-36	54	9.66	182
L supramarginal gyrus	-60	-36	26	7.55	42
L superior temporal sulcus	-50	-34	4	7.78	111
R premotor cortex	32	-2	52	8.99	122
L premotor cortex	-26	0	50	7.68	35
L inferior frontal gyrus	-42	14	20	9.13	651
R inferior frontal gyrus	48	16	22	11.00	143
R orbitofrontal cortex	32	26	-18	7.59	27
R middle frontal gyrus	54	34	8	9.07	80

R Fusiform Gyrus Seed					
R fusiform gyrus	26	-82	-8	9.14	94
R lateral occipital	26	-82	-22	7.80	53
L cerebellum	-24	-80	-30	7.12	33
L lateral occipital	-48	-78	18	7.44	35
L cerebellum	10	-76	-44	7.77	89
L lateral occipital	-42	-70	-2	8.86	266
R cerebellum	36	-70	-28	7.32	36
L cerebellum	-26	-66	-50	8.30	161
L lateral occipital	-26	-64	48	7.22	31
R superior temporal sulcus	46	-58	4	7.02	31
R precuneus	12	-54	48	7.1	63
R fusiform gyrus	44	-48	-16	18.27	898
R cerebellum	44	-48	-38	8.83	25
L supramarginal gyrus	-42	-40	50	7.65	164
R superior temporal sulcus	46	-20	-8	8.87	44
L postcentral gyrus	-54	-18	34	7.21	41

Supplementary Table A2.3. *Spearman correlations between urgency signal and factors from BIS-11 (Patton et al., 1995) and BIS/BAS (Carver & White, 1994; Heym et al., 2008). No correlations survive significance test (alpha=.05) after a Bonferroni correction for multiple comparison.*

	Questionnaire	***r***	***p***
BIS-11	Attentional	-0.0751	0.6237
	Motor	-0.2139	0.1584
	Non-planning	0.0733	0.6324
BIS/BAS	BAS Drive	-0.1791	0.2390
	BAS Fun Seeking	-0.0456	0.7664
	BAS Reward Responsiveness	-0.3721	0.0118
	BIS Anxiety	-0.0324	0.8328
	BIS FFFS-Fear	0.0389	0.7998

Supplementary Table A2.4. *Spearman's correlations between participants' optimized parameters as determined by varying levels of Gaussian noise (N) compared to an N of 6, as used in the main text. Values reflect Spearman's r.*

Optimized Parameter	***N*=4**	***N*=5**	***N*=7**	***N*=8**
UGM (μ)	0.9941	0.9940	0.9904	0.9897
DDM (T)	0.9771	0.9750	0.9683	0.9717

Supplementary Materials from Chapter 3

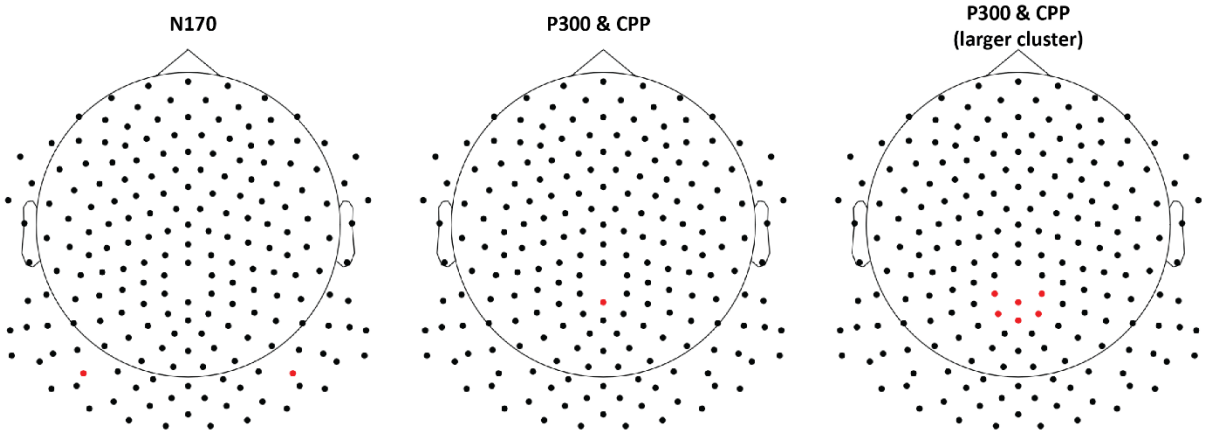

Supplementary Fig. A3.1. *Topomap of 256-channel HydroCel GSN v1.0 (Adult). Channels/electrodes used for the ERP of interest is highlighted in red.*

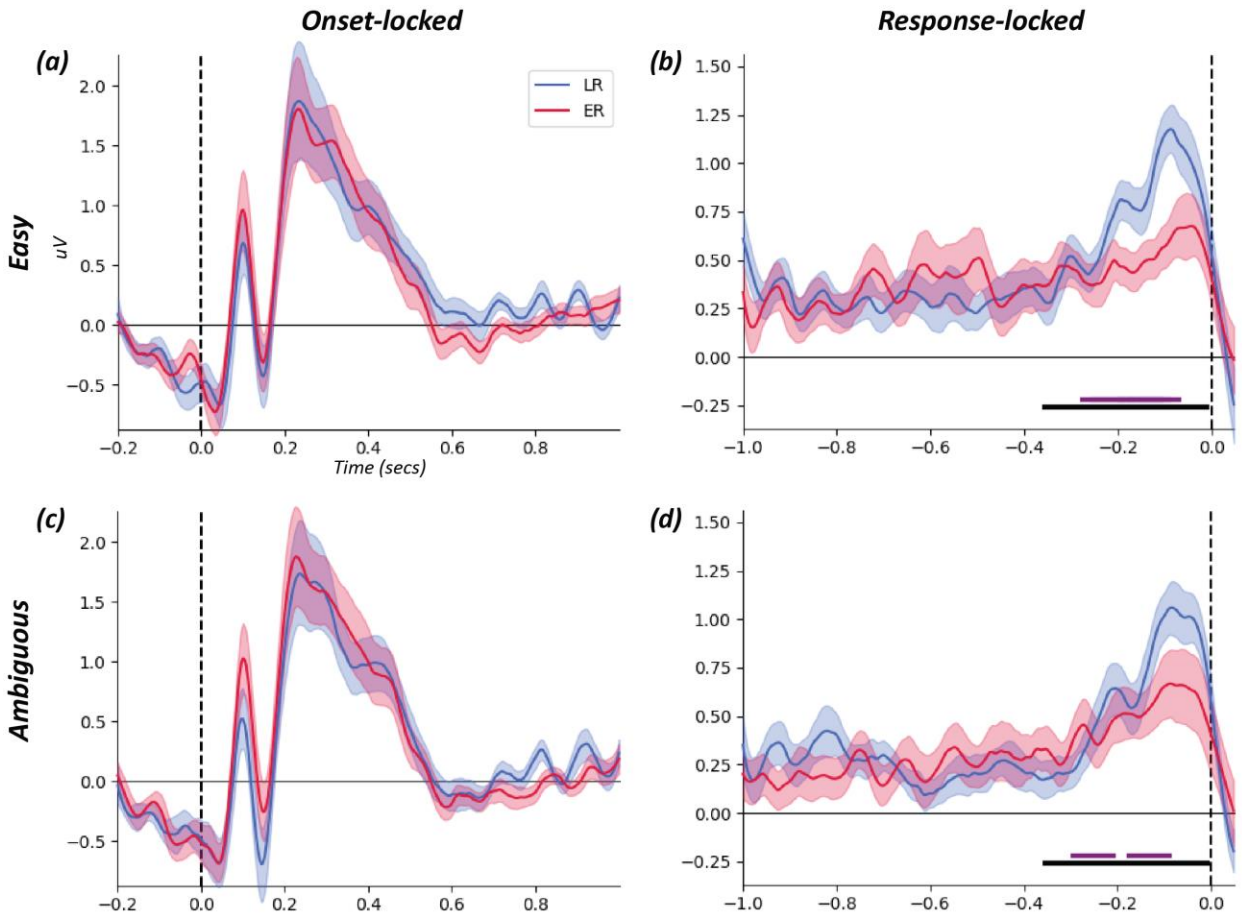

Supplementary Fig. A3.2. *Grand average waveforms from 5 posterior electrode sites surrounding Pz (*E101, E100, E129, E119, E110, E128*) closely resembles waveforms from the single electrode site Pz (Fig. 3.5 in main text). The onset-locked P300 signal is depicted in the left-hand column for* ***(a)*** *easy and* ***(c)*** *ambiguous trials. The response-locked CPP signal is depicted in the right hand column for* ***(b)*** *easy and* ***(d)*** *ambiguous trials.*

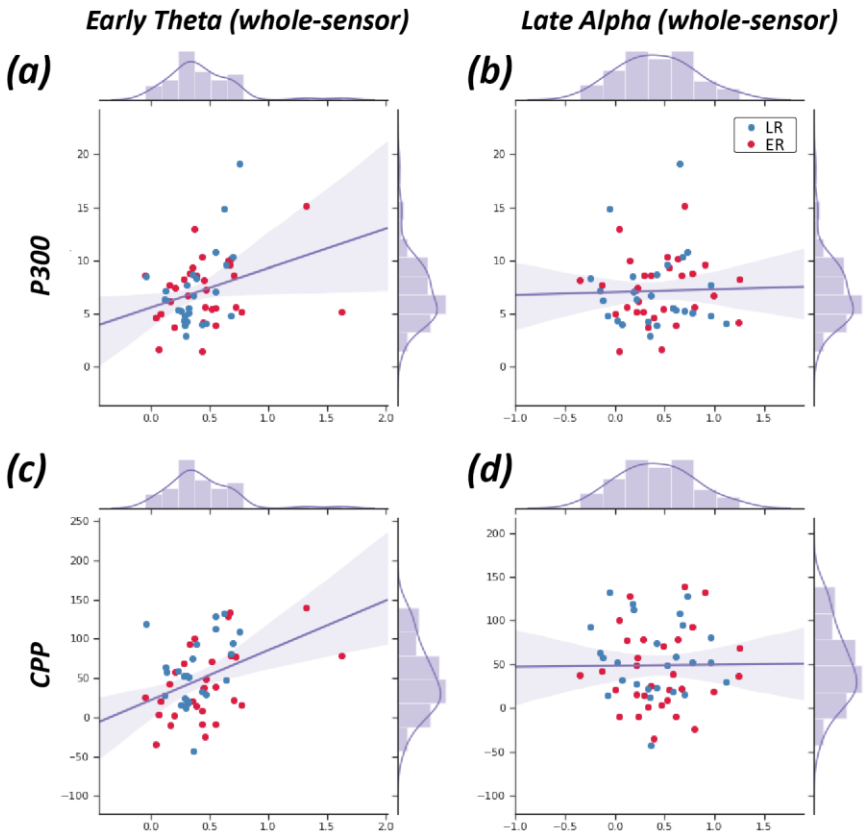

Supplementary Fig. A3.3. *Relationship between the early theta and late alpha power with our ERPS of interest. Power was derived by averaging across all electrodes. Early theta was significantly positively related to both P300 amplitude (rho=.312, p=.018) and CPP amplitude (rho=.382, p=.003). Late alpha did not relate to either P300 amplitude (rho=.07, p=.606) or CPP amplitude (rho=.011, p=.937). Each dot represents a subject, with blue and red representing LRs and ERs, respectively.*

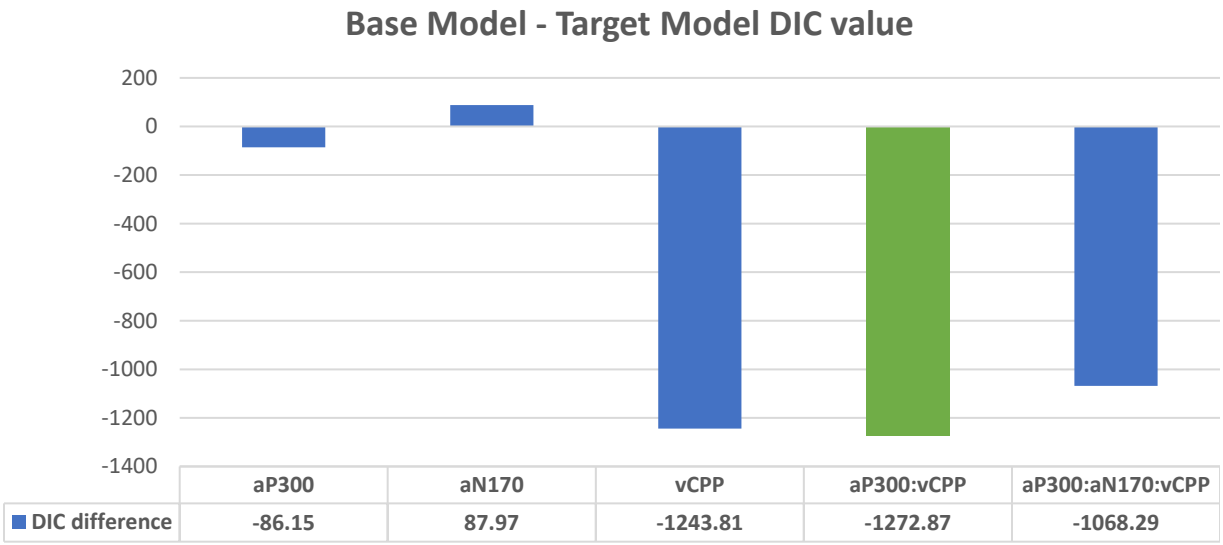

Supplementary Fig. A3.4. *DIC values when comparing HDDM model fit that allows for decision parameters (decision threshold (a) and drift rate (v)) to vary by neural signals (N170, P300, and CPP). The best fitting model is one where decision threshold is allowed to vary with P300 maximum amplitude and drift rate to vary with CPP build up (highlighted in green).*

Supplementary Table A3.1. *Breakdown of posterior probabilities from HDDM when considering trail-by-trial modulation of P300 on decision threshold (a) and CPP on drift rate (v). These findings are depicted in Fig 3.6a and 3.6b in the main text.*

	Condition	Group	Posterior Probability > 0	Posterior Probability < 0
P300	Easy	LR	58.31	41.69
		ER	11.96	88.04
	Ambiguous	LR	99.20	0.80
		ER	21.27	78.73
CPP	Easy	LR	22.49	77.51
		ER	0.01	99.99
	Ambiguous	LR	88.10	11.90
		ER	97.98	2.02

Supplementary Table A3.2. *Breakdown of posterior probabilities from HDDM when considering trail-by-trial modulation of P300 on decision threshold (a) and CPP on drift rate (v), as well as their interaction with condition (easy or ambiguous trial types). These findings are depicted in Fig 3.6c and 3.6d in the main text.*

Interaction	Group	Posterior Probability > 0	Posterior Probability < 0
P300 x condition	LR	95.33	4.67
	ER	57.49	42.51
CPP x condition	LR	91.41	8.59
	ER	99.9	0.1

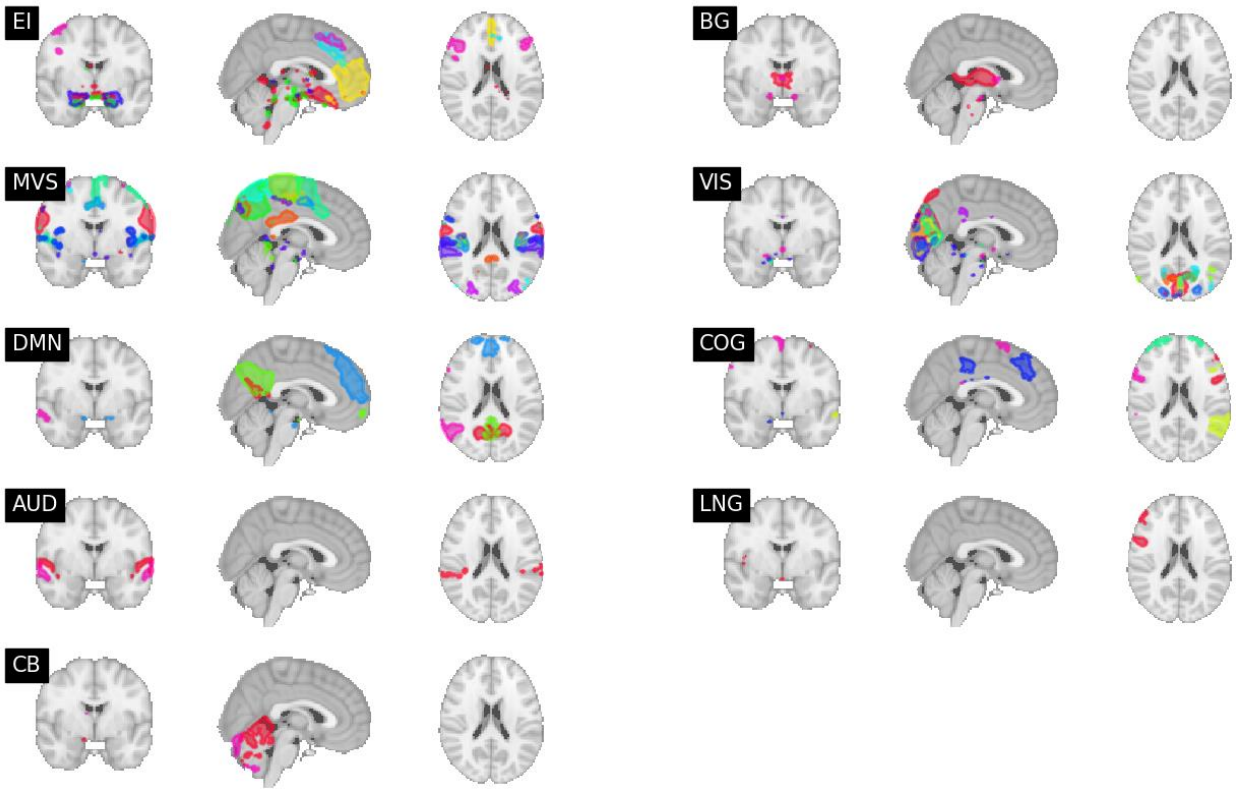

Supplementary Fig. A4.1. *Independent components grouped according to RSNs. Each colour depicts one independent component within each of the nine RSNs [EI: Emotion/Interoception; BG: Basal Ganglia; MVS: Motor/Visuospatial; VIS: Visual Perception; DMN: Default Mode Network; COG: Cognitive; AUD: Auditory; LNG: Language; CB: Cerebellum]*

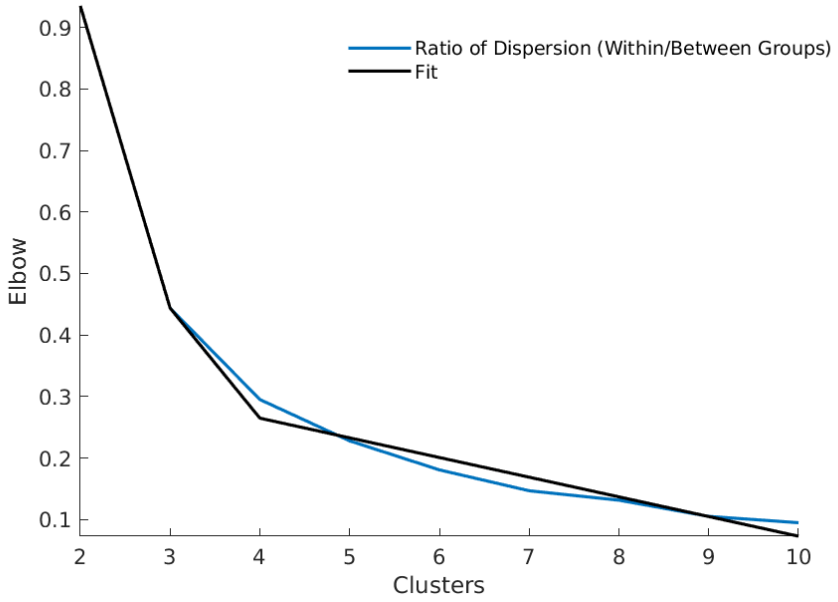

Supplementary Fig. A4.2. *Elbow criterion of cluster validity index, computed as the ratio of within- to between-cluster distance and indexes the optimal number of clusters (k) for k-means clustering.*

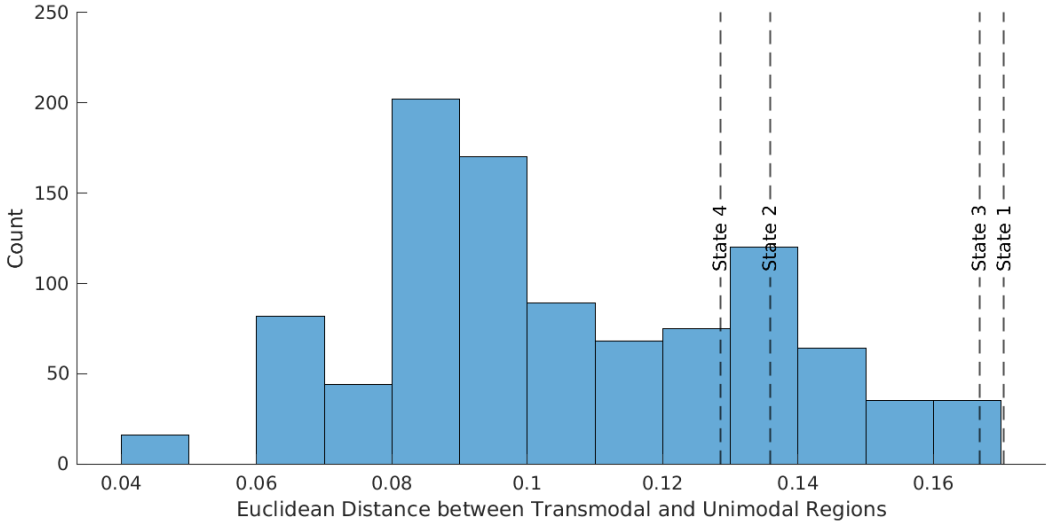

Supplementary Fig. A4.3. *Euclidean distance between transmodal and unimodal regions. This was determined as the average Euclidean distance between the median embedding value of DMN regions against the median embedding value of the visual and somato-motor RSNs for the principle gradient map of each tvFC state (highlighted with dotted lines). This was compared again a distribution of distance values derived from randomly generated gradients which were sampled by generating covariance matrix from 1,000 randomly selected sliding windows.*

REFERENCES

Akalin Acar, Z., & Makeig, S. (2013). Effects of Forward Model Errors on EEG Source Localization. *Brain Topography, 26*(3), 378-396. doi:10.1007/s10548-012-0274-6

Allen, E. A., Damaraju, E., Plis, S. M., Erhardt, E. B., Eichele, T., & Calhoun, V. D. (2014). Tracking whole-brain connectivity dynamics in the resting state. *Cereb Cortex, 24*(3), 663-676. doi:10.1093/cercor/bhs352

Andersen, R. A., Asanuma, C., Essick, G., & Siegel, R. (1990). Corticocortical connections of anatomically and physiologically defined subdivisions within the inferior parietal lobule. *Journal of Comparative Neurology, 296*(1), 65-113.

Anzellotti, S., Caramazza, A., & Saxe, R. (2017). Multivariate pattern dependence. *PLOS Computational Biology, 13*(11), e1005799. doi:10.1371/journal.pcbi.1005799

Asadzadeh, S., Yousefi Rezaii, T., Beheshti, S., Delpak, A., & Meshgini, S. (2020). A systematic review of EEG source localization techniques and their applications on diagnosis of brain abnormalities. *J Neurosci Methods, 339*, 108740. doi:10.1016/j.jneumeth.2020.108740

Aupperle, R. L., Melrose, A. J., Stein, M. B., & Paulus, M. P. (2012). Executive function and PTSD: Disengaging from trauma. *Neuropharmacology, 62*(2), 686-694.

Averbeck, B. B., Latham, P. E., & Pouget, A. (2006). Neural correlations, population coding and computation. *Nature Reviews Neuroscience, 7*(5), 358-366.

Bakkour, A., Palombo, D. J., Zylberberg, A., Kang, Y. H. R., Reid, A., Verfaellie, M., . . . Shohamy, D. (2019). The hippocampus supports deliberation during value-based decisions. *eLife, 8*, e46080. doi:10.7554/eLife.46080

Banca, P., Vestergaard, M. D., Rankov, V., Baek, K., Mitchell, S., Lapa, T., . . . Voon, V. (2015). Evidence Accumulation in Obsessive-Compulsive Disorder: the Role of Uncertainty and Monetary Reward on Perceptual Decision-Making Thresholds. *Neuropsychopharmacology, 40*(5), 1192-1202. doi:10.1038/npp.2014.303

Banz, B. C., Yip, S. W., Yau, Y. H., & Potenza, M. N. (2016). Behavioral addictions in addiction medicine: from mechanisms to practical considerations. In *Progress in brain research* (Vol. 223, pp. 311-328): Elsevier.

Başar, E., Başar-Eroglu, C., Karakaş, S., & Schürmann, M. (2001). Gamma, alpha, delta, and theta oscillations govern cognitive processes. *International Journal of Psychophysiology, 39*(2-3), 241-248.

Bassett, D. S., Yang, M., Wymbs, N. F., & Grafton, S. T. (2015). Learning-induced autonomy of sensorimotor systems. *Nat Neurosci, 18*(5), 744-751. doi:10.1038/nn.3993

Bechara, A., Damasio, H., Tranel, D., & Anderson, S. W. (1998). Dissociation Of working memory from decision making within the human prefrontal cortex. *J Neurosci, 18*(1), 428-437. doi:10.1523/jneurosci.18-01-00428.1998

Beck, A., Ward, C., Mendelson, M., Mock, J., & Erbaugh, J. (1961). An Inventory for Measuring Depression. *Arch Gen Psychiatry, 4*(6), 561 - 571.

Bell, A. J., & Sejnowski, T. J. (1995). An information-maximization approach to blind separation and blind deconvolution. *Neural computation, 7*(6), 1129-1159.

Bell, P. T., & Shine, J. M. (2016). Subcortical contributions to large-scale network communication. *Neurosci Biobehav Rev, 71*, 313-322. doi:10.1016/j.neubiorev.2016.08.036

Benady-Chorney, J., Aumont, E., Yau, Y., Zeighami, Y., Bohbot, V. D., & West, G. L. (2020). Action video game experience is associated with increased resting state functional connectivity in the caudate nucleus and decreased functional connectivity in the hippocampus. *Computers in Human Behavior, 106*, 106200.

Benady-Chorney, J., Yau, Y., Zeighami, Y., Bohbot, V. D., & West, G. L. (2018). Habitual action video game players display increased cortical thickness in the dorsal anterior cingulate cortex. *Neuroreport, 29*(5), 393-396.

Berret, B., Castanier, C., Bastide, S., & Deroche, T. (2018). Vigour of self-paced reaching movement: cost of time and individual traits. *Scientific Reports, 8*(1), 10655. doi:10.1038/s41598-018-28979-6

Bertolero, M. A., Yeo, B. T. T., Bassett, D. S., & D'Esposito, M. (2018). A mechanistic model of connector hubs, modularity and cognition. *Nature Human Behaviour, 2*(10), 765-777. doi:10.1038/s41562-018-0420-6

Bigdely-Shamlo, N., Mullen, T., Kothe, C., Su, K.-M., & Robbins, K. A. (2015). The PREP pipeline: standardized preprocessing for large-scale EEG analysis. *Frontiers in neuroinformatics, 9*, 16.

Blondel, V. D., Guillaume, J.-L., Lambiotte, R., & Lefebvre, E. (2008). Fast unfolding of communities in large networks. *Journal of statistical mechanics: theory and experiment, 2008*(10), P10008.

Bogacz, R., & Gurney, K. (2007). The basal ganglia and cortex implement optimal decision making between alternative actions. *Neural computation, 19*(2), 442-477.

Boly, M., Balteau, E., Schnakers, C., Degueldre, C., Moonen, G., Luxen, A., . . . Laureys, S. (2007). Baseline brain activity fluctuations predict somatosensory perception in humans. *Proceedings of the National Academy of Sciences, 104*(29), 12187-12192.

Bowman, N. E., Kording, K. P., & Gottfried, J. A. (2012). Temporal integration of olfactory perceptual evidence in human orbitofrontal cortex. *Neuron, 75*(5), 916-927. doi:10.1016/j.neuron.2012.06.035

Brants, M., Baeck, A., Wagemans, J., & de Beeck, H. P. (2011). Multiple scales of organization for object selectivity in ventral visual cortex. *NeuroImage, 56*(3), 1372-1381. doi:10.1016/j.neuroimage.2011.02.079

Braun, U., Schafer, A., Walter, H., Erk, S., Romanczuk-Seiferth, N., Haddad, L., . . . Bassett, D. S. (2015). Dynamic reconfiguration of frontal brain networks during executive cognition in humans. *Proc Natl Acad Sci U S A, 112*(37), 11678-11683. doi:10.1073/pnas.1422487112

Braunlich, K., & Seger, C. A. (2016). Categorical evidence, confidence, and urgency during probabilistic categorization. *NeuroImage, 125*, 941-952. doi:10.1016/j.neuroimage.2015.11.011

Britten, K. H., Shadlen, M. N., Newsome, W. T., & Movshon, J. A. (1993). Responses of neurons in macaque MT to stochastic motion signals. *Visual neuroscience, 10*(6), 1157-1169.

Bullmore, E., & Sporns, O. (2012). The economy of brain network organization. *Nat Rev Neurosci, 13*(5), 336-349.

Calhoun, V. D., Adali, T., Pearlson, G. D., & Pekar, J. J. (2001). A method for making group inferences from functional MRI data using independent component analysis. *Hum Brain Mapp, 14*(3), 140-151.

Calhoun, Vince D., Miller, R., Pearlson, G., & Adalı, T. (2014). The Chronnectome: Time-Varying Connectivity Networks as the Next Frontier in fMRI Data Discovery. *Neuron, 84*(2), 262-274. doi:https://doi.org/10.1016/j.neuron.2014.10.015

Cao, H., Plichta, M. M., Schäfer, A., Haddad, L., Grimm, O., Schneider, M., . . . Tost, H. (2014). Test–retest reliability of fMRI-based graph theoretical properties during working memory, emotion processing, and resting state. *NeuroImage, 84*, 888-900.

Carland, M. A., Thura, D., & Cisek, P. (2019). The Urge to Decide and Act: Implications for Brain Function and Dysfunction. *Neuroscientist, 25*(5), 491-511. doi:10.1177/1073858419841553

Carver, C. S., & White, T. L. (1994). Behavioral inhibition, behavioral activation, and affective responses to impending reward and punishment: The BIS/BAS Scales. *Journal of Personality and Social Psychology, 67*, 319-333.

Cavanagh, J. F., Figueroa, C. M., Cohen, M. X., & Frank, M. J. (2011a). Frontal theta reflects uncertainty and unexpectedness during exploration and exploitation. *Cerebral Cortex, 22*(11), 2575-2586.

Cavanagh, J. F., Frank, M. J., Klein, T. J., & Allen, J. J. (2010). Frontal theta links prediction errors to behavioral adaptation in reinforcement learning. *NeuroImage, 49*(4), 3198-3209.

Cavanagh, J. F., Wiecki, T. V., Cohen, M. X., Figueroa, C. M., Samanta, J., Sherman, S. J., & Frank, M. J. (2011b). Subthalamic nucleus stimulation reverses mediofrontal influence over decision threshold. *Nature neuroscience, 14*(11), 1462-1467. doi:10.1038/nn.2925

Chamberlain, S. R., & Sahakian, B. J. (2007). The neuropsychiatry of impulsivity. *Curr Opin Psychiatry, 20*(3), 255-261. doi:10.1097/YCO.0b013e3280ba4989

Chang, C., & Glover, G. H. (2010). Time-frequency dynamics of resting-state brain connectivity measured with fMRI. *NeuroImage, 50*(1), 81-98. doi:10.1016/j.neuroimage.2009.12.011

Choi, J. E., Vaswani, P. A., & Shadmehr, R. (2014). Vigor of movements and the cost of time in decision making. *Journal of Neuroscience, 34*(4), 1212-1223.

Churchland, A. K., Kiani, R., & Shadlen, M. N. (2008). Decision-making with multiple alternatives. *Nature neuroscience, 11*(6), 693.

Ciric, R., Rosen, A. F. G., Erus, G., Cieslak, M., Adebimpe, A., Cook, P. A., . . . Satterthwaite, T. D. (2018). Mitigating head motion artifact in functional connectivity MRI. *Nature Protocols, 13*(12), 2801-2826. doi:10.1038/s41596-018-0065-y

Ciric, R., Wolf, D. H., Power, J. D., Roalf, D. R., Baum, G. L., Ruparel, K., . . . Satterthwaite, T. D. (2017). Benchmarking of participant-level confound regression strategies for the control of motion artifact in studies of functional connectivity. *NeuroImage, 154*, 174-187. doi:https://doi.org/10.1016/j.neuroimage.2017.03.020

Cisek, P. (2007). Cortical mechanisms of action selection: the affordance competition hypothesis. *Philos Trans R Soc Lond B Biol Sci, 362*(1485), 1585-1599. doi:10.1098/rstb.2007.2054

Cisek, P., & Kalaska, J. F. (2005). Neural correlates of reaching decisions in dorsal premotor cortex: specification of multiple direction choices and final selection of action. *Neuron, 45*(5), 801-814.

Cisek, P., Puskas, G. A., & El-Murr, S. (2009). Decisions in changing conditions: the urgency-gating model. *The Journal of neuroscience, 29*(37), 11560-11571.

Cohen, J. R. (2018). The behavioral and cognitive relevance of time-varying, dynamic changes in functional connectivity. *NeuroImage, 180*, 515-525. doi:https://doi.org/10.1016/j.neuroimage.2017.09.036

Cohen, J. R., & D'Esposito, M. (2016). The segregation and integration of distinct brain networks and their relationship to cognition. *Journal of Neuroscience, 36*(48), 12083-12094.

Cole, M. W., Bassett, D. S., Power, J. D., Braver, T. S., & Petersen, S. E. (2014). Intrinsic and task-evoked network architectures of the human brain. *Neuron, 83*(1), 238-251.

Cole, M. W., Ito, T., Bassett, D. S., & Schultz, D. H. (2016). Activity flow over resting-state networks shapes cognitive task activations. *Nature neuroscience, 19*(12), 1718-1726. doi:10.1038/nn.4406

Cole, M. W., Reynolds, J. R., Power, J. D., Repovs, G., Anticevic, A., & Braver, T. S. (2013). Multi-task connectivity reveals flexible hubs for adaptive task control. *Nature neuroscience, 16*(9), 1348.

Coutanche, M., & Thompson-Schill, S. (2013). Informational connectivity: identifying synchronized discriminability of multi-voxel patterns across the brain. *Front Hum Neurosci, 7*(15). doi:10.3389/fnhum.2013.00015

Cox, S. M., Yau, Y., Larcher, K., Durand, F., Kolivakis, T., Delaney, J. S., . . . Leyton, M. (2017). Cocaine cue-induced dopamine release in recreational cocaine users. *Scientific Reports, 7*, 46665.

Dadar, M., Zeighami, Y., Yau, Y., Fereshtehnejad, S.-M., Maranzano, J., Postuma, R. B., . . . Collins, D. L. (2018). White matter hyperintensities are linked to future cognitive decline in de novo Parkinson's disease patients. *NeuroImage: Clinical, 20*, 892-900.

Damaraju, E., Allen, E. A., Belger, A., Ford, J. M., McEwen, S., Mathalon, D. H., . . . Calhoun, V. D. (2014). Dynamic functional connectivity analysis reveals transient states of dysconnectivity in schizophrenia. *Neuroimage Clin, 5*, 298-308. doi:10.1016/j.nicl.2014.07.003

Davis, T., LaRocque, K. F., Mumford, J. A., Norman, K. A., Wagner, A. D., & Poldrack, R. A. (2014). What do differences between multi-voxel and univariate analysis mean? How subject-, voxel-, and trial-level variance impact fMRI analysis. *NeuroImage, 97*, 271-283. doi:10.1016/j.neuroimage.2014.04.037

Davis, T., & Poldrack, R. A. (2013). Measuring neural representations with fMRI: practices and pitfalls. *Ann N Y Acad Sci, 1296*, 108-134. doi:10.1111/nyas.12156

de Lafuente, V., Jazayeri, M., & Shadlen, M. N. (2015). Representation of Accumulating Evidence for a Decision in Two Parietal Areas. *The Journal of neuroscience, 35*(10), 4306-4318. doi:10.1523/jneurosci.2451-14.2015

de Lafuente, V., & Romo, R. (2005). Neuronal correlates of subjective sensory experience. *Nat Neurosci, 8*(12), 1698-1703. doi:10.1038/nn1587

de Wael, R. V., Benkarim, O., Paquola, C., Lariviere, S., Royer, J., Tavakol, S., . . . Bernhardt, B. C. (2019). BrainSpace: a toolbox for the analysis of macroscale gradients in neuroimaging and connectomics datasets. *bioRxiv*, 761460. doi:10.1101/761460

Deco, G., Jirsa, V., & McIntosh, A. (2011). Emerging concepts for the dynamical organization of resting-state activity in the brain. *Nat Rev Neurosci, 12*(1), 43 - 56.

Ding, L., & Gold, J. I. (2010). Caudate encodes multiple computations for perceptual decisions. *J Neurosci, 30*(47), 15747-15759. doi:10.1523/jneurosci.2894-10.2010

Ding, L., & Gold, J. I. (2012). Separate, causal roles of the caudate in saccadic choice and execution in a perceptual decision task. *Neuron, 75*(5), 865-874. doi:10.1016/j.neuron.2012.07.021

Diniz-Filho, J. A. F., Soares, T. N., Lima, J. S., Dobrovolski, R., Landeiro, V. L., de Campos Telles, M. P., . . . Bini, L. M. (2013). Mantel test in population genetics. *Genetics and molecular biology, 36*(4), 475-485. doi:10.1590/S1415-47572013000400002

Ditterich, J. (2006). Evidence for time-variant decision making. *European Journal of Neuroscience, 24*(12), 3628-3641. doi:10.1111/j.1460-9568.2006.05221.x

Donchin, E., & Coles, M. G. H. (1988). Is the P300 component a manifestation of context updating? *Behavioral and Brain Sciences, 11*(3), 357-374. doi:10.1017/S0140525X00058027

Douw, L., Wakeman, D. G., Tanaka, N., Liu, H., & Stufflebeam, S. M. (2016). State-dependent variability of dynamic functional connectivity between frontoparietal and default networks relates to cognitive flexibility. *Neuroscience, 339*, 12-21. doi:https://doi.org/10.1016/j.neuroscience.2016.09.034

Drugowitsch, J., Moreno-Bote, R., Churchland, A. K., Shadlen, M. N., & Pouget, A. (2012). The cost of accumulating evidence in perceptual decision making. *J Neurosci, 32*(11), 3612-3628. doi:10.1523/jneurosci.4010-11.2012

Duchaine, B., & Yovel, G. (2015). A Revised Neural Framework for Face Processing. *Annual Review of Vision Science, 1*(1), 393-416. doi:10.1146/annurev-vision-082114-035518

Dunovan, K., Lynch, B., Molesworth, T., & Verstynen, T. (2015). Competing basal ganglia pathways determine the difference between stopping and deciding not to go. *eLife, 4*, e08723. doi:10.7554/eLife.08723

Eimer, M. (2011). The face-sensitivity of the n170 component. *Front Hum Neurosci, 5*, 119-119. doi:10.3389/fnhum.2011.00119

Erhardt, E. B., Rachakonda, S., Bedrick, E. J., Allen, E. A., Adali, T., & Calhoun, V. D. (2011). Comparison of multi-subject ICA methods for analysis of fMRI data. *Human brain mapping, 32*(12), 2075-2095.

Esteban, O., Markiewicz, C. J., Blair, R. W., Moodie, C. A., Isik, A. I., Erramuzpe, A., . . . Gorgolewski, K. J. (2019). fMRIPrep: a robust preprocessing pipeline for functional MRI. *Nature methods, 16*(1), 111-116. doi:10.1038/s41592-018-0235-4

Evans, N. J., Trueblood, J. S., & Holmes, W. R. (2020). A parameter recovery assessment of time-variant models of decision-making. *Behavior Research Methods, 52*(1), 193-206. doi:10.3758/s13428-019-01218-0

Evans, N. J., & Wagenmakers, E.-J. (2019). Evidence accumulation models: Current limitations and future directions.

Fineberg, N. A., Chamberlain, S. R., Goudriaan, A. E., Stein, D. J., Vanderschuren, L. J., Gillan, C. M., . . . Potenza, M. N. (2014). New developments in human neurocognition: clinical, genetic, and brain imaging correlates of impulsivity and compulsivity. *CNS Spectr, 19*(1), 69-89. doi:10.1017/s1092852913000801

Finn, E. S., Shen, X., Scheinost, D., Rosenberg, M. D., Huang, J., Chun, M. M., . . . Constable, R. T. (2015). Functional connectome fingerprinting: identifying individuals using patterns of brain connectivity. *Nature neuroscience, 18*(11), 1664-1671. doi:10.1038/nn.4135

Fiorenzato, E., Strafella, A. P., Kim, J., Schifano, R., Weis, L., Antonini, A., & Biundo, R. (2019). Dynamic functional connectivity changes associated with dementia in Parkinson's disease. *Brain, 142*(9), 2860-2872. doi:10.1093/brain/awz192

Fonov, V. S., Evans, A. C., McKinstry, R. C., Almli, C., & Collins, D. (2009). Unbiased nonlinear average age-appropriate brain templates from birth to adulthood. *NeuroImage, 47*, S102.

Forstmann, B. U., Anwander, A., Schafer, A., Neumann, J., Brown, S., & Wagenmakers, E. J. (2010). Cortico-striatal connections predict control over speed and accuracy in perceptual decision making. *Proc Natl Acad Sci USA, 107*, 15916-15920.

Foster, D. W., Hoff, R. A., Pilver, C. E., Yau, Y. H., Steinberg, M. A., Wampler, J., . . . Potenza, M. N. (2015). Correlates of gambling on high-school grounds. *Addictive Behaviors, 51*, 57-64.

Frank, M. J., & Claus, E. D. (2006). Anatomy of a decision: Striato-orbitofrontal interactions in reinforcement learning, decision making, and reversal. *Psychol Rev, 113*(2), 300-326. doi:10.1037/0033-295x.113.2.300

Frank, M. J., Gagne, C., Nyhus, E., Masters, S., Wiecki, T. V., Cavanagh, J. F., & Badre, D. (2015). fMRI and EEG Predictors of Dynamic Decision Parameters during Human Reinforcement Learning. *The Journal of neuroscience, 35*(2), 485-494. doi:10.1523/jneurosci.2036-14.2015

Frank, M. J., Samanta, J., Moustafa, A. A., & Sherman, S. J. (2007). Hold your horses: impulsivity, deep brain stimulation, and medication in parkinsonism. *Science, 318*(5854), 1309-1312.

Friedman, J., Hastie, T., & Tibshirani, R. (2008). Sparse inverse covariance estimation with the graphical lasso. *Biostatistics, 9*(3), 432-441.

Friston, K. J., Holmes, A. P., Worsley, K. J., Poline, J.-P., Frith, C. D., & Frackowiak, R. S. J. (1994). Statistical parametric maps in functional imaging: A general linear approach. *Human brain mapping, 2*(4), 189-210. doi:10.1002/hbm.460020402

Geerligs, L., Renken, R. J., Saliasi, E., Maurits, N. M., & Lorist, M. M. (2015a). A Brain-Wide Study of Age-Related Changes in Functional Connectivity. *Cereb Cortex, 25*(7), 1987-1999. doi:10.1093/cercor/bhu012

Geerligs, L., Rubinov, M., Cam, C., & Henson, R. N. (2015b). State and Trait Components of Functional Connectivity: Individual Differences Vary with Mental State. *J Neurosci, 35*(41), 13949-13961. doi:10.1523/JNEUROSCI.1324-15.2015

Gelman, A., & Rubin, D. B. (1992). Inference from iterative simulation using multiple sequences. *Statistical science, 7*(4), 457-472.

Gelman, A., Stern, H. S., Carlin, J. B., Dunson, D. B., Vehtari, A., & Rubin, D. B. (2013). *Bayesian data analysis*: Chapman and Hall/CRC.

Gießing, C., Thiel, C. M., Alexander-Bloch, A. F., Patel, A. X., & Bullmore, E. T. (2013). Human brain functional network changes associated with enhanced and impaired attentional task performance. *Journal of Neuroscience, 33*(14), 5903-5914.

Glaze, C. M., Kable, J. W., & Gold, J. I. (2015). Normative evidence accumulation in unpredictable environments. *eLife, 4*. doi:10.7554/eLife.08825

Gluth, S., Rieskamp, J., & Buchel, C. (2012). Deciding when to decide: time-variant sequential sampling models explain the emergence of value-based decisions in the human brain. *J Neurosci, 32*(31), 10686-10698. doi:10.1523/jneurosci.0727-12.2012

Gold, J. I., & Shadlen, M. N. (2007). The neural basis of decision making. *Annu. Rev. Neurosci., 30*, 535-574.

Gonzalez-Castillo, J., Hoy, C. W., Handwerker, D. A., Robinson, M. E., Buchanan, L. C., Saad, Z. S., & Bandettini, P. A. (2015). Tracking ongoing cognition in individuals using brief, whole-brain functional connectivity patterns. *Proceedings of the National Academy of Sciences, 112*(28), 8762-8767.

Goodale, M. A., & Milner, A. D. (1992). Separate visual pathways for perception and action. *Trends Neurosci, 15*(1), 20-25. doi:10.1016/0166-2236(92)90344-8

Gould, I. C., Nobre, A. C., Wyart, V., & Rushworth, M. F. (2012). Effects of decision variables and intraparietal stimulation on sensorimotor oscillatory activity in the human brain. *J Neurosci, 32*(40), 13805-13818. doi:10.1523/jneurosci.2200-12.2012

Gramfort, A., Luessi, M., Larson, E., Engemann, D., Strohmeier, D., Brodbeck, C., . . . Hämäläinen, M. (2013). MEG and EEG data analysis with MNE-Python. *Frontiers in Neuroscience, 7*(267). doi:10.3389/fnins.2013.00267

Gramfort, A., Luessi, M., Larson, E., Engemann, D. A., Strohmeier, D., Brodbeck, C., . . . Hämäläinen, M. S. (2014). MNE software for processing MEG and EEG data. *NeuroImage, 86*, 446-460. doi:https://doi.org/10.1016/j.neuroimage.2013.10.027

Gratton, C., Laumann, T. O., Nielsen, A. N., Greene, D. J., Gordon, E. M., Gilmore, A. W., . . . Petersen, S. E. (2018). Functional Brain Networks Are Dominated by Stable Group and Individual Factors, Not Cognitive or Daily Variation. *Neuron, 98*(2), 439-452.e435. doi:10.1016/j.neuron.2018.03.035

Grech, R., Cassar, T., Muscat, J., Camilleri, K. P., Fabri, S. G., Zervakis, M., . . . Vanrumste, B. (2008). Review on solving the inverse problem in EEG source analysis. *Journal of NeuroEngineering and Rehabilitation, 5*(1), 25. doi:10.1186/1743-0003-5-25

Grimaldi, P., Lau, H., & Basso, M. A. (2015). There are things that we know that we know, and there are things that we do not know we do not know: Confidence in decision-making. *Neurosci Biobehav Rev, 55*, 88-97. doi:10.1016/j.neubiorev.2015.04.006

Haber, S. N., & Knutson, B. (2010). The reward circuit: linking primate anatomy and human imaging. *Neuropsychopharmacology, 35*(1), 4-26. doi:10.1038/npp.2009.129

Handwerker, D. A., Roopchansingh, V., Gonzalez-Castillo, J., & Bandettini, P. A. (2012). Periodic changes in fMRI connectivity. *NeuroImage, 63*(3), 1712-1719. doi:10.1016/j.neuroimage.2012.06.078

Hanks, T., Kiani, R., & Shadlen, M. N. (2014). A neural mechanism of speed-accuracy tradeoff in macaque area LIP. *eLife, 3*, e02260. doi:10.7554/eLife.02260

Hanks, T. D., Ditterich, J., & Shadlen, M. N. (2006). Microstimulation of macaque area LIP affects decision-making in a motion discrimination task. *Nature neuroscience, 9*(5), 682.

Hanks, T. D., Kopec, C. D., Brunton, B. W., Duan, C. A., Erlich, J. C., & Brody, C. D. (2015). Distinct relationships of parietal and prefrontal cortices to evidence accumulation. *Nature, 520*(7546), 220-223. doi:10.1038/nature14066

Harry, B., Williams, M., Davis, C., & Kim, J. (2013). Emotional expressions evoke a differential response in the fusiform face area. *Front Hum Neurosci, 7*(692). doi:10.3389/fnhum.2013.00692

Hawkins, G. E., Forstmann, B. U., Wagenmakers, E. J., Ratcliff, R., & Brown, S. D. (2015). Revisiting the evidence for collapsing boundaries and urgency signals in perceptual decision-making. *J Neurosci, 35*(6), 2476-2484. doi:10.1523/jneurosci.2410-14.2015

Haxby, J. V., Gobbini, M. I., Furey, M. L., Ishai, A., Schouten, J. L., & Pietrini, P. (2001). Distributed and overlapping representations of faces and objects in ventral temporal cortex. *Science, 293*(5539), 2425-2430. doi:10.1126/science.1063736

Haxby, J. V., Hoffman, E. A., & Gobbini, M. I. (2000). The distributed human neural system for face perception. *Trends in cognitive sciences, 4*(6), 223-233. doi:https://doi.org/10.1016/S1364-6613(00)01482-0

Haynes, J. D., & Rees, G. (2005). Predicting the stream of consciousness from activity in human visual cortex. *Curr Biol, 15*(14), 1301-1307. doi:10.1016/j.cub.2005.06.026

Hearne, L. J., Cocchi, L., Zalesky, A., & Mattingley, J. B. (2017). Reconfiguration of Brain Network Architectures between Resting-State and Complexity-Dependent Cognitive Reasoning. *J Neurosci, 37*(35), 8399-8411. doi:10.1523/JNEUROSCI.0485-17.2017

Hebb, D. O. (1949). *The organization of behavior; a neuropsychological theory*. Oxford, England: Wiley.

Heekeren, H. R., Marrett, S., Bandettini, P. A., & Ungerleider, L. G. (2004). A general mechanism for perceptual decision-making in the human brain. *Nature, 431*(7010), 859-862. doi:http://www.nature.com/nature/journal/v431/n7010/suppinfo/nature02966_S1.html

Heekeren, H. R., Marrett, S., & Ungerleider, L. G. (2008). The neural systems that mediate human perceptual decision making. *Nature Reviews Neuroscience, 9*(6), 467-479.

Heitz, Richard P., & Schall, Jeffrey D. (2012). Neural Mechanisms of Speed-Accuracy Tradeoff. *Neuron, 76*(3), 616-628. doi:https://doi.org/10.1016/j.neuron.2012.08.030

Heitz, R. P., & Schall, J. D. (2013). Neural chronometry and coherency across speed–accuracy demands reveal lack of homomorphism between computational and neural mechanisms of evidence accumulation. *Philosophical Transactions of the Royal Society B: Biological Sciences, 368*(1628), 20130071.

Hendriks, M. H. A., Daniels, N., Pegado, F., & Op de Beeck, H. P. (2017). The Effect of Spatial Smoothing on Representational Similarity in a Simple Motor Paradigm. *Frontiers in Neurology, 8*, 222. doi:10.3389/fneur.2017.00222

Henson, R., & Friston, K. (2007). Convolution models for fMRI. *Statistical parametric mapping: The analysis of functional brain images*, 178-192.

Herding, J., Ludwig, S., von Lautz, A., Spitzer, B., & Blankenburg, F. (2019). Centro-parietal EEG potentials index subjective evidence and confidence during perceptual decision making. *NeuroImage, 201*, 116011. doi:10.1016/j.neuroimage.2019.116011

Heym, N., Ferguson, E., & Lawrence, C. (2008). An evaluation of the relationship between Gray's revised RST and Eysenck's PEN: Distinguishing BIS and FFFS in Carver and White's BIS/BAS scales. *Personality and Individual Differences, 45*(8), 709-715. doi:https://doi.org/10.1016/j.paid.2008.07.013

Hillyard, S. A., & Kutas, M. (1983). Electrophysiology of cognitive processing. *Annu Rev Psychol, 34*(1), 33-61.

Hillyard, S. A., Squires, K. C., Bauer, J. W., & Lindsay, P. H. (1971). Evoked potential correlates of auditory signal detection. *Science, 172*(3990), 1357-1360.

Himberg, J., & Hyvarinen, A. (2003). *Icasso: software for investigating the reliability of ICA estimates by clustering and visualization.* Paper presented at the 2003 IEEE XIII Workshop on Neural Networks for Signal Processing (IEEE Cat. No. 03TH8718).

Ho, T. C., Brown, S., & Serences, J. T. (2009). Domain General Mechanisms of Perceptual Decision Making in Human Cortex. *The Journal of neuroscience, 29*(27), 8675-8687. doi:10.1523/jneurosci.5984-08.2009

Honey, C. J., Sporns, O., Cammoun, L., Gigandet, X., Thiran, J. P., Meuli, R., & Hagmann, P. (2009). Predicting human resting-state functional connectivity from structural connectivity. *Proceedings of the National Academy of Sciences, 106*(6), 2035. doi:10.1073/pnas.0811168106

Huntenburg, J. M., Bazin, P.-L., & Margulies, D. S. (2018). Large-scale gradients in human cortical organization. *Trends in cognitive sciences, 22*(1), 21-31.

Hutchison, R. M., Womelsdorf, T., Allen, E. A., Bandettini, P. A., Calhoun, V. D., Corbetta, M., . . . Gonzalez-Castillo, J. (2013). Dynamic functional connectivity: promise, issues, and interpretations. *NeuroImage, 80*, 360-378.

Huys, Q. J. M., Maia, T. V., & Frank, M. J. (2016). Computational psychiatry as a bridge from neuroscience to clinical applications. *Nature neuroscience, 19*(3), 404-413. doi:10.1038/nn.4238

Jackson, A. F., & Bolger, D. J. (2014). The neurophysiological bases of EEG and EEG measurement: A review for the rest of us. *Psychophysiology, 51*(11), 1061-1071.

Jacobs, J., Hwang, G., Curran, T., & Kahana, M. J. (2006). EEG oscillations and recognition memory: Theta correlates of memory retrieval and decision making. *NeuroImage, 32*(2), 978-987. doi:https://doi.org/10.1016/j.neuroimage.2006.02.018

James, G., Witten, D., Hastie, T., & Tibshirani, R. (2013). *An introduction to statistical learning* (Vol. 112): Springer.

Jueptner, M., & Weiller, C. (1998). A review of differences between basal ganglia and cerebellar control of movements as revealed by functional imaging studies. *Brain: a journal of neurology, 121*(8), 1437-1449.

Kassam, K. S., Markey, A. R., Cherkassky, V. L., Loewenstein, G., & Just, M. A. (2013). Identifying Emotions on the Basis of Neural Activation. *PLOS ONE, 8*(6), e66032. doi:10.1371/journal.pone.0066032

Katz, L. N., Yates, J. L., Pillow, J. W., & Huk, A. C. (2016). Dissociated functional significance of decision-related activity in the primate dorsal stream. *Nature, 535*(7611), 285-288. doi:10.1038/nature18617

Kelly, C., Biswal, B. B., Craddock, R. C., Castellanos, F. X., & Milham, M. P. (2012). Characterizing variation in the functional connectome: promise and pitfalls. *Trends in cognitive sciences, 16*(3), 181-188. doi:https://doi.org/10.1016/j.tics.2012.02.001

Kelly, S. P., & O'Connell, R. G. (2013). Internal and external influences on the rate of sensory evidence accumulation in the human brain. *Journal of Neuroscience, 33*(50), 19434-19441.

Keuken, M. C., Müller-Axt, C., Langner, R., Eickhoff, S. B., Forstmann, B. U., & Neumann, J. (2014). Brain networks of perceptual decision-making: an fMRI ALE meta-analysis. *Front Hum Neurosci, 8*(445). doi:10.3389/fnhum.2014.00445

Kiani, R., & Shadlen, M. N. (2009). Representation of confidence associated with a decision by neurons in the parietal cortex. *Science, 324*(5928), 759-764.

Kim, J. N., & Shadlen, M. N. (1999). Neural correlates of a decision in the dorsolateral prefrontal cortex of the macaque. *Nat Neurosci, 2*(2), 176-185. doi:10.1038/5739

Kirschner, M., Schmidt, A., Hodzic-Santor, B., Burrer, A., Manoliu, A., Zeighami, Y., . . . Habermeyer, B. (2020). Orbitofrontal-striatal structural alterations linked to negative symptoms at different stages of the schizophrenia spectrum. *medRxiv*.

Klimesch, W. (1999). EEG alpha and theta oscillations reflect cognitive and memory performance: a review and analysis. *Brain research reviews, 29*(2-3), 169-195.

Klimesch, W. (2012). α-band oscillations, attention, and controlled access to stored information. *Trends in cognitive sciences, 16*(12), 606-617. doi:10.1016/j.tics.2012.10.007

Kloosterman, N. A., de Gee, J. W., Werkle-Bergner, M., Lindenberger, U., Garrett, D. D., & Fahrenfort, J. J. (2019). Humans strategically shift decision bias by flexibly adjusting sensory evidence accumulation. *eLife, 8*, e37321. doi:10.7554/eLife.37321

Krajbich, I., Armel, C., & Rangel, A. (2010). Visual fixations and the computation and comparison of value in simple choice. *Nat Neurosci, 13*(10), 1292-1298. doi:10.1038/nn.2635

Krajbich, I., & Rangel, A. (2011). Multialternative drift-diffusion model predicts the relationship between visual fixations and choice in value-based decisions. *Proc Natl Acad Sci U S A, 108*(33), 13852-13857. doi:10.1073/pnas.1101328108

Kriegeskorte, N., Goebel, R., & Bandettini, P. (2006). Information-based functional brain mapping. *Proc Natl Acad Sci U S A, 103*(10), 3863-3868. doi:10.1073/pnas.0600244103

Kriegeskorte, N., & Kievit, R. A. (2013). Representational geometry: integrating cognition, computation, and the brain. *Trends Cogn Sci, 17*(8), 401-412. doi:10.1016/j.tics.2013.06.007

Krienen, F. M., Yeo, B. T., & Buckner, R. L. (2014). Reconfigurable task-dependent functional coupling modes cluster around a core functional architecture. *Philosophical Transactions of the Royal Society B: Biological Sciences, 369*(1653), 20130526.

Kruschke, J. K. (2010). Bayesian data analysis. *WIREs Cognitive Science, 1*(5), 658-676. doi:10.1002/wcs.72

Kubanek, J., Snyder, L. H., Brunton, B. W., Brody, C. D., & Schalk, G. (2013). A low-frequency oscillatory neural signal in humans encodes a developing decision variable. *NeuroImage, 83*, 795-808. doi:10.1016/j.neuroimage.2013.06.085

Kwong, K. K., Belliveau, J. W., Chesler, D. A., Goldberg, I. E., Weisskoff, R. M., Poncelet, B. P., . . . Turner, R. (1992). Dynamic magnetic resonance imaging of human brain activity during primary sensory stimulation. *Proceedings of the National Academy of Sciences, 89*(12), 5675-5679. doi:10.1073/pnas.89.12.5675

LaConte, S., Strother, S., Cherkassky, V., Anderson, J., & Hu, X. (2005). Support vector machines for temporal classification of block design fMRI data. *NeuroImage, 26*(2), 317-329. doi:10.1016/j.neuroimage.2005.01.048

Laird, A. R., Fox, P. M., Eickhoff, S. B., Turner, J. A., Ray, K. L., McKay, D. R., . . . Fox, P. T. (2011). Behavioral interpretations of intrinsic connectivity networks. *J Cogn Neurosci, 23*(12), 4022-4037. doi:10.1162/jocn_a_00077

Lee, M. D., & Wagenmakers, E.-J. (2013). *Bayesian cognitive modeling: A practical course*. New York, NY, US: Cambridge University Press.

Lewis, J. W., & Van Essen, D. C. (2000). Corticocortical connections of visual, sensorimotor, and multimodal processing areas in the parietal lobe of the macaque monkey. *Journal of Comparative Neurology, 428*(1), 112-137.

Li, N., Ma, N., Liu, Y., He, X.-S., Sun, D.-L., Fu, X.-M., . . . Zhang, D.-R. (2013). Resting-state functional connectivity predicts impulsivity in economic decision-making. *Journal of Neuroscience, 33*(11), 4886-4895.

Limongi, R., Bohaterewicz, B., Nowicka, M., Plewka, A., & Friston, K. J. (2018). Knowing when to stop: Aberrant precision and evidence accumulation in schizophrenia. *Schizophr Res, 197*, 386-391. doi:https://doi.org/10.1016/j.schres.2017.12.018

Liu, T., & Pleskac, T. J. (2011). Neural correlates of evidence accumulation in a perceptual decision task. *J Neurophysiol, 106*(5), 2383-2398. doi:10.1152/jn.00413.2011

Lo, C.-C., & Wang, X.-J. (2006). Cortico–basal ganglia circuit mechanism for a decision threshold in reaction time tasks. *Nature neuroscience, 9*(7), 956-963.

Logothetis, N. K., Guggenberger, H., Peled, S., & Pauls, J. (1999). Functional imaging of the monkey brain. *Nature neuroscience, 2*(6), 555-562.

Lucci, G., Berchicci, M., Perri, R. L., Spinelli, D., & Di Russo, F. (2016). Effect of target probability on pre-stimulus brain activity. *Neuroscience, 322*, 121-128. doi:https://doi.org/10.1016/j.neuroscience.2016.02.029

Lurie, D., Kessler, D., Bassett, D., Betzel, R. F., Breakspear, M., Keilholz, S., . . . McIntosh, A. R. (2018). On the nature of time-varying functional connectivity in resting fMRI. *PsyArXiv*. doi:https://doi.org/10.31234/osf.io/xtzre

Mahmoudi, A., Takerkart, S., Regragui, F., Boussaoud, D., & Brovelli, A. (2012). Multivoxel pattern analysis for FMRI data: a review. *Computational and mathematical methods in medicine, 2012*, 961257-961257. doi:10.1155/2012/961257

Maia, T. V., & Frank, M. J. (2011). From reinforcement learning models to psychiatric and neurological disorders. *Nature neuroscience, 14*(2), 154-162. doi:10.1038/nn.2723

Mansfield, E. L., Karayanidis, F., Jamadar, S., Heathcote, A., & Forstmann, B. U. (2011). Adjustments of Response Threshold during Task Switching: A Model-Based Functional Magnetic Resonance Imaging Study. *The Journal of neuroscience, 31*(41), 14688-14692. doi:10.1523/jneurosci.2390-11.2011

Margulies, D. S., Ghosh, S. S., Goulas, A., Falkiewicz, M., Huntenburg, J. M., Langs, G., . . . Petrides, M. (2016). Situating the default-mode network along a principal gradient of macroscale cortical organization. *Proceedings of the National Academy of Sciences, 113*(44), 12574-12579.

Marr, D. (1982). Vision: A computational investigation into the human representation and processing of visual information.

Marr, D., & Poggio, T. (1979). A computational theory of human stereo vision. *Proceedings of the Royal Society of London. Series B. Biological Sciences, 204*(1156), 301-328.

Mars, R. B., Debener, S., Gladwin, T. E., Harrison, L. M., Haggard, P., Rothwell, J. C., & Bestmann, S. (2008). Trial-by-Trial Fluctuations in the Event-Related Electroencephalogram Reflect Dynamic Changes in the Degree of Surprise. *The Journal of neuroscience, 28*(47), 12539-12545. doi:10.1523/jneurosci.2925-08.2008

MATLAB. (2018). MATLAB and Statistics Toolbox Release 2018b. Natick, Massachusetts, United States: The MathWorks, Inc.

Matsui, T., Murakami, T., & Ohki, K. (2018). Neuronal Origin of the Temporal Dynamics of Spontaneous BOLD Activity Correlation. *Cerebral Cortex, 29*(4), 1496-1508. doi:10.1093/cercor/bhy045

Matzke, D., & Wagenmakers, E. J. (2009). Psychological interpretation of the ex-Gaussian and shifted Wald parameters: a diffusion model analysis. *Psychon Bull Rev, 16*(5), 798-817. doi:10.3758/pbr.16.5.798

Mazaika, P., Whitfield-Gabrieli, S., Reiss, A., & Glover, G. (2007). Artifact repair for fMRI data from high motion clinical subjects. *Human brain mapping*, 2007.

Mazurek, M. E., Roitman, J. D., Ditterich, J., & Shadlen, M. N. (2003). A Role for Neural Integrators in Perceptual Decision Making. *Cerebral Cortex, 13*(11), 1257-1269. doi:10.1093/cercor/bhg097

McLaren, D. G., Ries, M. L., Xu, G., & Johnson, S. C. (2012). A generalized form of context-dependent psychophysiological interactions (gPPI): a comparison to standard approaches. *NeuroImage, 61*(4), 1277-1286.

Meder, D., Haagensen, B. N., Hulme, O., Morville, T., Gelskov, S., Herz, D. M., . . . Siebner, H. R. (2016). Tuning the Brake While Raising the Stake: Network Dynamics during Sequential Decision-Making. *The Journal of neuroscience, 36*(19), 5417-5426. doi:10.1523/jneurosci.3191-15.2016

Mei, S., Yau, Y. H., Chai, J., Guo, J., & Potenza, M. N. (2016). Problematic Internet use, well-being, self-esteem and self-control: Data from a high-school survey in China. *Addictive Behaviors, 61*, 74-79.

Mesulam, M.-M. (1998). From sensation to cognition. *Brain: a journal of neurology, 121*(6), 1013-1052.

Michaud, A., Dadar, M., Pelletier, M., Zeighami, Y., Garcia-Garcia, I., Iceta, S., . . . Biertho, L. (2020). Neuroanatomical changes in white and grey matter after sleeve gastrectomy. *NeuroImage*, 116696.

Mishkin, M., Ungerleider, L. G., & Macko, K. A. (1983). Object vision and spatial vision: two cortical pathways. *Trends in Neurosciences, 6*, 414-417. doi:https://doi.org/10.1016/0166-2236(83)90190-X

Mormann, M. M., Malmaud, J., Huth, A., Koch, C., & Rangel, A. (2010). The drift diffusion model can account for the accuracy and reaction time of value-based choices under high and low time pressure. *Judgment and Decision Making, 5*(6), 437-449.

Mulder, M. J., van Maanen, L., & Forstmann, B. U. (2014). Perceptual decision neurosciences - a model-based review. *Neuroscience, 277*, 872-884. doi:10.1016/j.neuroscience.2014.07.031

Mumford, J. A., Turner, B. O., Ashby, F. G., & Poldrack, R. A. (2012). Deconvolving BOLD activation in event-related designs for multivoxel pattern classification analyses. *NeuroImage, 59*(3), 2636-2643.

Murphy, P. R., Boonstra, E., & Nieuwenhuis, S. (2016). Global gain modulation generates time-dependent urgency during perceptual choice in humans. *Nature Communications, 7*, 13526.

Nagano-Saito, A., Cisek, P., Perna, A. S., Shirdel, F. Z., Benkelfat, C., Leyton, M., & Dagher, A. (2012). From anticipation to action, the role of dopamine in perceptual decision making: an fMRI-tyrosine depletion study. *J Neurophysiol, 108*(2), 501-512. doi:10.1152/jn.00592.2011

Neseliler, S., Vainik, U., Dadar, M., Yau, Y. H., Garcia-Garcia, I., Scala, S. G., . . . Dagher, A. (2018). Neural and behavioral endophenotypes of obesity. *bioRxiv*, 348821.

Newman, M. E., & Girvan, M. (2004). Finding and evaluating community structure in networks. *Physical review E, 69*(2), 026113.

Newsome, W. T., Britten, K. H., & Movshon, J. A. (1989). Neuronal correlates of a perceptual decision. *Nature, 341*(6237), 52-54.

Nieuwenhuis, S., De Geus, E. J., & Aston-Jones, G. (2011). The anatomical and functional relationship between the P3 and autonomic components of the orienting response. *Psychophysiology, 48*(2), 162-175. doi:10.1111/j.1469-8986.2010.01057.x

Nieuwenhuis, S., Slagter, H. A., von Geusau, N. J., Heslenfeld, D. J., & Holroyd, C. B. (2005). Knowing good from bad: differential activation of human cortical areas by positive and negative outcomes. *European Journal of Neuroscience, 21*, 3161-3168.

Nomi, J. S., Vij, S. G., Dajani, D. R., Steimke, R., Damaraju, E., Rachakonda, S., . . . Uddin, L. Q. (2017). Chronnectomic patterns and neural flexibility underlie executive function. *NeuroImage, 147*, 861-871. doi:10.1016/j.neuroimage.2016.10.026

Noppeney, U., Ostwald, D., & Werner, S. (2010). Perceptual decisions formed by accumulation of audiovisual evidence in prefrontal cortex. *Journal of Neuroscience, 30*(21), 7434-7446.

Norman, K. A., Polyn, S. M., Detre, G. J., & Haxby, J. V. (2006). Beyond mind-reading: multi-voxel pattern analysis of fMRI data. *Trends in cognitive sciences, 10*(9), 424-430. doi:https://doi.org/10.1016/j.tics.2006.07.005

O'Connell, R. G., Dockree, P. M., & Kelly, S. P. (2012). A supramodal accumulation-to-bound signal that determines perceptual decisions in humans. *Nature neuroscience, 15*(12), 1729.

O'Toole, A. J., Jiang, F., Abdi, H., & Haxby, J. V. (2005). Partially distributed representations of objects and faces in ventral temporal cortex. *J Cogn Neurosci, 17*(4), 580-590. doi:10.1162/0898929053467550

Ogawa, S., Lee, T.-M., Kay, A. R., & Tank, D. W. (1990a). Brain magnetic resonance imaging with contrast dependent on blood oxygenation. *Proceedings of the National Academy of Sciences, 87*(24), 9868-9872.

Ogawa, S., Lee, T. M., Nayak, A. S., & Glynn, P. (1990b). Oxygenation-sensitive contrast in magnetic resonance image of rodent brain at high magnetic fields. *Magnetic resonance in medicine, 14*(1), 68-78.

Op de Beeck, H. P. (2010). Against hyperacuity in brain reading: spatial smoothing does not hurt multivariate fMRI analyses? *NeuroImage, 49*(3), 1943-1948. doi:10.1016/j.neuroimage.2009.02.047

Palestro, J. J., Weichart, E., Sederberg, P. B., & Turner, B. M. (2018). Some task demands induce collapsing bounds: Evidence from a behavioral analysis. *Psychon Bull Rev, 25*(4), 1225-1248. doi:10.3758/s13423-018-1479-9

Parasuraman, R., & Beatty, J. (1980). Brain events underlying detection and recognition of weak sensory signals. *Science, 210*(4465), 80-83.

Patton, J. H., Stanford, M. S., & Barratt, E. S. (1995). Factor structure of the Barratt impulsiveness scale. *Journal of Clinical Psychology, 51*(6), 768-774.

Pedersen, M. L., Frank, M. J., & Biele, G. (2017). The drift diffusion model as the choice rule in reinforcement learning. *Psychon Bull Rev, 24*(4), 1234-1251. doi:10.3758/s13423-016-1199-y

Pedregosa, F., Varoquaux, G., Gramfort, A., Michel, V., Thirion, B., Grisel, O., . . . Dubourg, V. (2011). Scikit-learn: Machine learning in Python. *Journal of machine learning research, 12*(Oct), 2825-2830.

Pedroni, A., Bahreini, A., & Langer, N. (2019). Automagic: Standardized preprocessing of big EEG data. *NeuroImage, 200*, 460-473. doi:10.1016/j.neuroimage.2019.06.046

Pereira, F., & Botvinick, M. (2011). Information mapping with pattern classifiers: a comparative study. *NeuroImage, 56*(2), 476-496. doi:10.1016/j.neuroimage.2010.05.026

Perrone, J. A. (2004). A visual motion sensor based on the properties of V1 and MT neurons. *Vision Research, 44*(15), 1733-1755. doi:https://doi.org/10.1016/j.visres.2004.03.003

Philiastides, M. G., & Heekeren, H. R. (2009). Chapter 8 - Spatiotemporal characteristics of perceptual decision making in the human brain. In J.-C. Dreher & L. Tremblay (Eds.), *Handbook of Reward and Decision Making* (pp. 185-212). New York: Academic Press.

Philiastides, M. G., Ratcliff, R., & Sajda, P. (2006). Neural Representation of Task Difficulty and Decision Making during Perceptual Categorization: A Timing Diagram. *The Journal of neuroscience, 26*(35), 8965-8975. doi:10.1523/jneurosci.1655-06.2006

Philiastides, M. G., & Sajda, P. (2006). Temporal characterization of the neural correlates of perceptual decision making in the human brain. *Cereb Cortex, 16*(4), 509-518. doi:10.1093/cercor/bhi130

Phillips, C., Rugg, M. D., & Friston, K. J. (2002). Anatomically Informed Basis Functions for EEG Source Localization: Combining Functional and Anatomical Constraints. *NeuroImage, 16*(3, Part A), 678-695. doi:https://doi.org/10.1006/nimg.2002.1143

Picton, T. W. (1992). The P300 wave of the human event-related potential. *J Clin Neurophysiol, 9*(4), 456-479. doi:10.1097/00004691-199210000-00002

Ploran, E. J., Nelson, S. M., Velanova, K., Donaldson, D. I., Petersen, S. E., & Wheeler, M. E. (2007). Evidence Accumulation and the Moment of Recognition: Dissociating Perceptual Recognition Processes Using fMRI. *The Journal of neuroscience, 27*(44), 11912-11924. doi:10.1523/jneurosci.3522-07.2007

Polanía, R., Krajbich, I., Grueschow, M., & Ruff, Christian C. (2014). Neural Oscillations and Synchronization Differentially Support Evidence Accumulation in Perceptual and Value-Based Decision Making. *Neuron, 82*(3), 709-720. doi:http://dx.doi.org/10.1016/j.neuron.2014.03.014

Polich, J. (2007). Updating P300: an integrative theory of P3a and P3b. *Clin Neurophysiol, 118*(10), 2128-2148. doi:10.1016/j.clinph.2007.04.019

Polyn, S. M., Natu, V. S., Cohen, J. D., & Norman, K. A. (2005). Category-specific cortical activity precedes retrieval during memory search. *Science, 310*(5756), 1963-1966. doi:10.1126/science.1117645

Pouget, A., Drugowitsch, J., & Kepecs, A. (2016). Confidence and certainty: distinct probabilistic quantities for different goals. *Nat Neurosci, 19*(3), 366-374. doi:10.1038/nn.4240

Power, J. D., & Petersen, S. E. (2013). Control-related systems in the human brain. *Current Opinion in Neurobiology, 23*(2), 223-228.

Powers, A. R., Mathys, C., & Corlett, P. (2017). Pavlovian conditioning–induced hallucinations result from overweighting of perceptual priors. *Science, 357*(6351), 596-600.

R Core Team. (2015). R: A language and environment for statistical computing. *R Foundation for Statistical Computing.* Retrieved from https://www.R-project.org/

Rabinovich, M. I., Friston, K. J., & Varona, P. (2012). *Principles of brain dynamics: global state interactions*: MIT Press.
Raschka, S. (2018). MLxtend: Providing machine learning and data science utilities and extensions to Python's scientific computing stack. *Journal of Open Source Software, 3*(24), 638.
Ratcliff, R., & McKoon, G. (2008). The diffusion decision model: theory and data for two-choice decision tasks. *Neural computation, 20*(4), 873-922. doi:10.1162/neco.2008.12-06-420
Ratcliff, R., Philiastides, M. G., & Sajda, P. (2009). Quality of evidence for perceptual decision making is indexed by trial-to-trial variability of the EEG. *Proceedings of the National Academy of Sciences, 106*(16), 6539-6544.
Ratcliff, R., Smith, P. L., Brown, S. D., & McKoon, G. (2016). Diffusion Decision Model: Current Issues and History. *Trends Cogn Sci, 20*(4), 260-281. doi:10.1016/j.tics.2016.01.007
Redgrave, P., Rodriguez, M., Smith, Y., Rodriguez-Oroz, M. C., Lehericy, S., Bergman, H., . . . Obeso, J. A. (2010). Goal-directed and habitual control in the basal ganglia: implications for Parkinson's disease. *Nature Reviews Neuroscience, 11*(11), 760-772. doi:10.1038/nrn2915
Reppert, T. R., Rigas, I., Herzfeld, D. J., Sedaghat-Nejad, E., Komogortsev, O., & Shadmehr, R. (2018). Movement vigor as a traitlike attribute of individuality. *J Neurophysiol, 120*(2), 741-757.
Ritchie, J. B., Kaplan, D. M., & Klein, C. (2017). Decoding the Brain: Neural Representation and the Limits of Multivariate Pattern Analysis in Cognitive Neuroscience. *The British Journal for the Philosophy of Science, 70*(2), 581-607. doi:10.1093/bjps/axx023
Robinson, J. E., Breakspear, M., Young, A. W., & Johnston, P. J. (2018). Dose-dependent modulation of the visually evoked N1/N170 by perceptual surprise: a clear demonstration of prediction-error signalling. *Eur J Neurosci*. doi:10.1111/ejn.13920
Rock, P., Roiser, J., Riedel, W., & Blackwell, A. (2014). Cognitive impairment in depression: a systematic review and meta-analysis. *Psychol Med, 44*(10), 2029-2040.
Rohrbaugh, J. W., Donchin, E., & Eriksen, C. W. (1974). Decision making and the P300 component of the cortical evoked response. *Perception & Psychophysics, 15*(2), 368-374.
Roitman, J. D., & Shadlen, M. N. (2002). Response of neurons in the lateral intraparietal area during a combined visual discrimination reaction time task. *J Neurosci, 22*(21), 9475-9489.
Rubinov, M., & Sporns, O. (2011). Weight-conserving characterization of complex functional brain networks. *NeuroImage, 56*(4), 2068-2079.
Sadaghiani, S., Poline, J.-B., Kleinschmidt, A., & D'Esposito, M. (2015). Ongoing dynamics in large-scale functional connectivity predict perception. *Proceedings of the National Academy of Sciences, 112*(27), 8463-8468. doi:10.1073/pnas.1420687112
Salvatier, J., Wiecki, T. V., & Fonnesbeck, C. (2016). Probabilistic programming in Python using PyMC3. *PeerJ Computer Science, 2*, e55.
San Martín, R., Appelbaum, L. G., Pearson, J. M., Huettel, S. A., & Woldorff, M. G. (2013). Rapid brain responses independently predict gain maximization and loss minimization during economic decision making. *Journal of Neuroscience, 33*(16), 7011-7019.
Sanz-Arigita, E. J., Schoonheim, M. M., Damoiseaux, J. S., Rombouts, S. A., Maris, E., Barkhof, F., . . . Stam, C. J. (2010). Loss of 'small-world' networks in Alzheimer's disease: graph analysis

of FMRI resting-state functional connectivity. *PLOS ONE, 5*(11), e13788. doi:10.1371/journal.pone.0013788

Satterthwaite, T. D., Elliott, M. A., Gerraty, R. T., Ruparel, K., Loughead, J., Calkins, M. E., . . . Wolf, D. H. (2013). An improved framework for confound regression and filtering for control of motion artifact in the preprocessing of resting-state functional connectivity data. *NeuroImage, 64*, 240-256. doi:https://doi.org/10.1016/j.neuroimage.2012.08.052

Sauseng, P., Griesmayr, B., Freunberger, R., & Klimesch, W. (2010). Control mechanisms in working memory: A possible function of EEG theta oscillations. *Neuroscience & Biobehavioral Reviews, 34*(7), 1015-1022. doi:https://doi.org/10.1016/j.neubiorev.2009.12.006

Saygin, Z. M., Osher, D. E., Koldewyn, K., Reynolds, G., Gabrieli, J. D., & Saxe, R. R. (2011). Anatomical connectivity patterns predict face selectivity in the fusiform gyrus. *Nat Neurosci, 15*(2), 321-327. doi:10.1038/nn.3001

Schaefer, A., Kong, R., Gordon, E. M., Laumann, T. O., Zuo, X. N., Holmes, A. J., . . . Yeo, B. T. T. (2018). Local-Global Parcellation of the Human Cerebral Cortex from Intrinsic Functional Connectivity MRI. *Cereb Cortex, 28*(9), 3095-3114. doi:10.1093/cercor/bhx179

Schag, K., Teufel, M., Junne, F., Preissl, H., Hautzinger, M., Zipfel, S., & Giel, K. E. (2013). Impulsivity in binge eating disorder: food cues elicit increased reward responses and disinhibition. *PLOS ONE, 8*(10).

Scott, B. B., Constantinople, C. M., Akrami, A., Hanks, T. D., Brody, C. D., & Tank, D. W. (2017). Fronto-parietal Cortical Circuits Encode Accumulated Evidence with a Diversity of Timescales. *Neuron, 95*(2), 385-398.e385. doi:10.1016/j.neuron.2017.06.013

Seabold, S., & Perktold, J. (2010). *Statsmodels: Econometric and statistical modeling with python.* Paper presented at the Proceedings of the 9th Python in Science Conference.

Shadlen, Michael N., & Kiani, R. (2013). Decision Making as a Window on Cognition. *Neuron, 80*(3), 791-806. doi:https://doi.org/10.1016/j.neuron.2013.10.047

Shadlen, M. N., & Newsome, W. T. (1996). Motion perception: seeing and deciding. *Proc Natl Acad Sci U S A, 93*(2), 628-633.

Shadlen, M. N., & Newsome, W. T. (2001). Neural basis of a perceptual decision in the parietal cortex (area LIP) of the rhesus monkey. *J Neurophysiol, 86*(4), 1916-1936.

Shafiei, G., Zeighami, Y., Clark, C. A., Coull, J. T., Nagano-Saito, A., Leyton, M., . . . Mišić, B. (2018). Dopamine Signaling Modulates the Stability and Integration of Intrinsic Brain Networks. *Cerebral Cortex, 29*(1), 397-409. doi:10.1093/cercor/bhy264

Shappell, H., Caffo, B. S., Pekar, J. J., & Lindquist, M. A. (2019). Improved state change estimation in dynamic functional connectivity using hidden semi-Markov models. *NeuroImage, 191*, 243-257. doi:https://doi.org/10.1016/j.neuroimage.2019.02.013

Shen, K., Hutchison, R. M., Bezgin, G., Everling, S., & McIntosh, A. R. (2015). Network structure shapes spontaneous functional connectivity dynamics. *J Neurosci, 35*(14), 5579-5588. doi:10.1523/jneurosci.4903-14.2015

Sherman, S. M. (2016). Thalamus plays a central role in ongoing cortical functioning. *Nat Neurosci, 19*(4), 533-541. doi:10.1038/nn.4269

Shine, James M., Bissett, Patrick G., Bell, Peter T., Koyejo, O., Balsters, Joshua H., Gorgolewski, Krzysztof J., . . . Poldrack, Russell A. (2016). The Dynamics of Functional Brain Networks:

Integrated Network States during Cognitive Task Performance. *Neuron, 92*(2), 544-554. doi:https://doi.org/10.1016/j.neuron.2016.09.018
Shirer, W. R., Ryali, S., Rykhlevskaia, E., Menon, V., & Greicius, M. D. (2012). Decoding subject-driven cognitive states with whole-brain connectivity patterns. *Cerebral Cortex, 22*(1), 158-165.
Siegel, M., Buschman, T. J., & Miller, E. K. (2015). Cortical information flow during flexible sensorimotor decisions. *Science, 348*(6241), 1352-1355. doi:10.1126/science.aab0551
Smith, J. L., Johnstone, S. J., & Barry, R. J. (2008). Movement-related potentials in the Go/NoGo task: The P3 reflects both cognitive and motor inhibition. *Clinical Neurophysiology, 119*(3), 704-714. doi:https://doi.org/10.1016/j.clinph.2007.11.042
Smith, P. L., & Ratcliff, R. (2004). Psychology and neurobiology of simple decisions. *Trends in Neurosciences, 27*(3), 161-168. doi:https://doi.org/10.1016/j.tins.2004.01.006
Smith, S. M., Miller, K. L., Salimi-Khorshidi, G., Webster, M., Beckmann, C. F., Nichols, T. E., . . . Woolrich, M. W. (2011). Network modelling methods for FMRI. *NeuroImage, 54*(2), 875-891.
Spiegelhalter, D. J., Best, N. G., Carlin, B. P., & Van Der Linde, A. (2002). Bayesian measures of model complexity and fit. *Journal of the royal statistical society: Series b (statistical methodology), 64*(4), 583-639.
Standage, D., You, H., Wang, D., & Dorris, M. (2011). Gain Modulation by an Urgency Signal Controls the Speed–Accuracy Trade-Off in a Network Model of a Cortical Decision Circuit. *Frontiers in Computational Neuroscience, 5*(7). doi:10.3389/fncom.2011.00007
Steinemann, N. A., O'Connell, R. G., & Kelly, S. P. (2018). Decisions are expedited through multiple neural adjustments spanning the sensorimotor hierarchy. *Nature Communications, 9*(1), 3627. doi:10.1038/s41467-018-06117-0
Stevens, A. A., Tappon, S. C., Garg, A., & Fair, D. A. (2012). Functional brain network modularity captures inter-and intra-individual variation in working memory capacity. *PLOS ONE, 7*(1).
Stevens, L., Verdejo-García, A., Goudriaan, A. E., Roeyers, H., Dom, G., & Vanderplasschen, W. (2014). Impulsivity as a vulnerability factor for poor addiction treatment outcomes: a review of neurocognitive findings among individuals with substance use disorders. *Journal of substance abuse treatment, 47*(1), 58-72.
Stevens, W. D., & Spreng, R. N. (2014). Resting-state functional connectivity MRI reveals active processes central to cognition. *Wiley Interdisciplinary Reviews: Cognitive Science, 5*(2), 233-245. doi:10.1002/wcs.1275
Summerfield, C., Egner, T., Mangels, J., & Hirsch, J. (2006). Mistaking a house for a face: neural correlates of misperception in healthy humans. *Cerebral Cortex, 16*(4), 500-508.
Summerfield, C., & Tsetsos, K. (2012). Building Bridges between Perceptual and Economic Decision-Making: Neural and Computational Mechanisms. *Frontiers in Neuroscience, 6*, 70-70. doi:10.3389/fnins.2012.00070
Sutton, S., Braren, M., Zubin, J., & John, E. (1965). Evoked-potential correlates of stimulus uncertainty. *Science, 150*(3700), 1187-1188.
Swaminathan, S. K., Masse, N. Y., & Freedman, D. J. (2013). A comparison of lateral and medial intraparietal areas during a visual categorization task. *J Neurosci, 33*(32), 13157-13170. doi:10.1523/JNEUROSCI.5723-12.2013

Swick, D., Pineda, J., & Foote, S. (1994). Effects of systemic clonidine on auditory event-related potentials in squirrel monkeys. *Brain Res Bull, 33*(1), 79-86.

Tagliabue, C. F., Veniero, D., Benwell, C. S. Y., Cecere, R., Savazzi, S., & Thut, G. (2019). The EEG signature of sensory evidence accumulation during decision formation closely tracks subjective perceptual experience. *Scientific Reports, 9*(1), 4949-4949. doi:10.1038/s41598-019-41024-4

Tagliazucchi, E., Von Wegner, F., Morzelewski, A., Brodbeck, V., & Laufs, H. (2012). Dynamic BOLD functional connectivity in humans and its electrophysiological correlates. *Front Hum Neurosci, 6*(339). doi:10.3389/fnhum.2012.00339

Tajima, S., Drugowitsch, J., & Pouget, A. (2016). Optimal policy for value-based decision-making. *Nature Communications, 7*(1), 12400. doi:10.1038/ncomms12400

Tek, C., Gold, J., Blaxton, T., Wilk, C., McMahon, R. P., & Buchanan, R. W. (2002). Visual Perceptual and Working Memory Impairments in Schizophrenia. *Arch Gen Psychiatry, 59*(2), 146-153. doi:10.1001/archpsyc.59.2.146

Thompson, G. J., Merritt, M. D., Pan, W.-J., Magnuson, M. E., Grooms, J. K., Jaeger, D., & Keilholz, S. D. (2013). Neural correlates of time-varying functional connectivity in the rat. *NeuroImage, 83*, 826-836.

Thura, D. (2016). How to discriminate conclusively among different models of decision making? *J Neurophysiol, 115*(5), 2251-2254. doi:10.1152/jn.00911.2015

Thura, D., Beauregard-Racine, J., Fradet, C.-W., & Cisek, P. (2012). Decision making by urgency gating: theory and experimental support. *J Neurophysiol, 108*(11), 2912-2930. doi:10.1152/jn.01071.2011

Thura, D., & Cisek, P. (2014). Deliberation and Commitment in the Premotor and Primary Motor Cortex during Dynamic Decision Making. *Neuron, 81*(6), 1401-1416. doi:http://dx.doi.org/10.1016/j.neuron.2014.01.031

Thura, D., & Cisek, P. (2016). Modulation of premotor and primary motor cortical activity during volitional adjustments of speed-accuracy trade-offs. *Journal of Neuroscience, 36*(3), 938-956.

Thura, D., & Cisek, P. (2017). The Basal Ganglia Do Not Select Reach Targets but Control the Urgency of Commitment. *Neuron, 95*(5), 1160-1170.e1165. doi:https://doi.org/10.1016/j.neuron.2017.07.039

Tosoni, A., Galati, G., Romani, G. L., & Corbetta, M. (2008). Sensory-motor mechanisms in human parietal cortex underlie arbitrary visual decisions. *Nature neuroscience, 11*(12), 1446-1453. doi:10.1038/nn.2221

Tottenham, N., Tanaka, J. W., Leon, A. C., McCarry, T., Nurse, M., Hare, T. A., . . . Nelson, C. (2009). The NimStim set of facial expressions: judgments from untrained research participants. *Psychiatry Res, 168*(3), 242-249. doi:10.1016/j.psychres.2008.05.006

Tremblay, C., Abbasi, N., Zeighami, Y., Yau, Y., Dadar, M., Rahayel, S., & Dagher, A. (accepted). Sex effects on brain structure in de novo Parkinson's disease: a multi-modal neuroimaging study. *Brain*.

Tremel, J. J., & Wheeler, M. E. (2015). Content-specific evidence accumulation in inferior temporal cortex during perceptual decision-making. *NeuroImage, 109*, 35-49. doi:10.1016/j.neuroimage.2014.12.072

Tversky, A., & Kahneman, D. (1981). The framing of decisions and the psychology of choice. *Science, 211*(4481), 453-458. doi:10.1126/science.7455683

Twomey, D. M., Murphy, P. R., Kelly, S. P., & O'Connell, R. G. (2015). The classic P300 encodes a build-to-threshold decision variable. *European Journal of Neuroscience, 42*(1), 1636-1643.

Ungerleider, L., Mishkin, M., Ingle, D., Goodale, M., & Mansfield, R. (1982). Analysis of visual behavior.

Vallat, R. (2018). Pingouin: statistics in Python. *Journal of Open Source Software, 3*(31), 1026.

van den Heuvel, M. P., Stam, C. J., Kahn, R. S., & Hulshoff Pol, H. E. (2009). Efficiency of functional brain networks and intellectual performance. *J Neurosci, 29*(23), 7619-7624. doi:10.1523/jneurosci.1443-09.2009

Van Horn, J. D., Grafton, S. T., & Miller, M. B. (2008). Individual variability in brain activity: a nuisance or an opportunity? *Brain Imaging Behav, 2*(4), 327.

van Vugt, M., Simen, P., Nystrom, L., Holmes, P., & Cohen, J. (2012). EEG Oscillations Reveal Neural Correlates of Evidence Accumulation. *Frontiers in Neuroscience, 6*(106). doi:10.3389/fnins.2012.00106

van Vugt, M. K., Beulen, M. A., & Taatgen, N. A. (2019). Relation between centro-parietal positivity and diffusion model parameters in both perceptual and memory-based decision making. *Brain Res, 1715*, 1-12.

Vanrullen, R., & Thorpe, S. J. (2001). The time course of visual processing: from early perception to decision-making. *Journal of cognitive neuroscience, 13*(4), 454-461.

Vatansever, D., Menon, D. K., & Stamatakis, E. A. (2017). Default mode contributions to automated information processing. *Proceedings of the National Academy of Sciences, 114*(48), 12821-12826. doi:10.1073/pnas.1710521114

Verleger, R., Jaśkowski, P., & Wascher, E. (2005). Evidence for an Integrative Role of P3b in Linking Reaction to Perception. *Journal of Psychophysiology, 19*(3), 165-181. doi:10.1027/0269-8803.19.3.165

Voon, V. (2014). Models of impulsivity with a focus on waiting impulsivity: translational potential for neuropsychiatric disorders. *Current Addiction Reports, 1*(4), 281-288.

Voskuilen, C., Ratcliff, R., & Smith, P. L. (2016). Comparing fixed and collapsing boundary versions of the diffusion model. *Journal of Mathematical Psychology, 73*, 59-79. doi:10.1016/j.jmp.2016.04.008

Wager, T. D., Kang, J., Johnson, T. D., Nichols, T. E., Satpute, A. B., & Barrett, L. F. (2015). A Bayesian Model of Category-Specific Emotional Brain Responses. *PLOS Computational Biology, 11*(4), e1004066. doi:10.1371/journal.pcbi.1004066

Wegrzyn, M., Riehle, M., Labudda, K., Woermann, F., Baumgartner, F., Pollmann, S., . . . Kissler, J. (2015). Investigating the brain basis of facial expression perception using multi-voxel pattern analysis. *Cortex, 69*, 131-140. doi:https://doi.org/10.1016/j.cortex.2015.05.003

Wheeler, M. E., Woo, S. G., Ansel, T., Tremel, J. J., Collier, A. L., Velanova, K., . . . Yang, T. (2015a). The Strength of Gradually Accruing Probabilistic Evidence Modulates Brain Activity during a Categorical Decision. *Journal of Cognitive Neuroscience, 27*(4), 705-719. doi:10.1162/jocn_a_00739

Wheeler, M. E., Woo, S. G., Ansel, T., Tremel, J. J., Collier, A. L., Velanova, K., . . . Yang, T. (2015b). The strength of gradually accruing probabilistic evidence modulates brain activity during a categorical decision. *J Cogn Neurosci, 27*(4), 705-719. doi:10.1162/jocn_a_00739

White, C. N., Mumford, J. A., & Poldrack, R. A. (2012). Perceptual Criteria in the Human Brain. *The Journal of neuroscience, 32*(47), 16716-16724. doi:10.1523/jneurosci.1744-12.2012
White, C. N., Ratcliff, R., Vasey, M. W., & McKoon, G. (2010). Using diffusion models to understand clinical disorders. *Journal of Mathematical Psychology, 54*(1), 39-52. doi:10.1016/j.jmp.2010.01.004
Wiecki, T. V., Sofer, I., & Frank, M. J. (2013). HDDM: Hierarchical Bayesian estimation of the Drift-Diffusion Model in Python. *Frontiers in neuroinformatics, 7*, 14-14. doi:10.3389/fninf.2013.00014
Williams, M. A., Dang, S., & Kanwisher, N. G. (2007). Only some spatial patterns of fMRI response are read out in task performance. *Nature neuroscience, 10*(6), 685-686.
Winkel, J., Keuken, M. C., van Maanen, L., Wagenmakers, E.-J., & Forstmann, B. U. (2014). Early evidence affects later decisions: Why evidence accumulation is required to explain response time data. *Psychon Bull Rev, 21*(3), 777-784.
Winkler, I., Haufe, S., & Tangermann, M. (2011). Automatic classification of artifactual ICA-components for artifact removal in EEG signals. *Behavioral and Brain Functions, 7*(1), 30.
Woodworth, R. S., Barber, B., & Schlosberg, H. (1954). *Experimental psychology*: Oxford and IBH Publishing.
Wyart, V., de Gardelle, V., Scholl, J., & Summerfield, C. (2012). Rhythmic fluctuations in evidence accumulation during decision making in the human brain. *Neuron, 76*(4), 847-858. doi:10.1016/j.neuron.2012.09.015
Yaesoubi, M., Allen, E. A., Miller, R. L., & Calhoun, V. D. (2015). Dynamic coherence analysis of resting fMRI data to jointly capture state-based phase, frequency, and time-domain information. *NeuroImage, 120*, 133-142.
Yang, T., & Shadlen, M. N. (2007). Probabilistic reasoning by neurons. *Nature, 447*(7148), 1075-1080.
Yarkoni, T., Poldrack, R. A., Nichols, T. E., Van Essen, D. C., & Wager, T. D. (2011). Large-scale automated synthesis of human functional neuroimaging data. *Nature methods, 8*(8), 665-670.
Yau, M. Y. H., & Potenza, M. N. (2015). Gambling disorder and other behavioral addictions: recognition and treatment. *Harvard review of psychiatry, 23*(2), 134.
Yau, Y., Dadar, M., Taylor, M., Zeighami, Y., Fellows, L. K., Cisek, P., & Dagher, A. (2020). Neural Correlates of Evidence and Urgency During Human Perceptual Decision-Making in Dynamically Changing Conditions. *Cerebral Cortex*. doi:10.1093/cercor/bhaa129
Yau, Y., Zeighami, Y., Baker, T., Larcher, K., Vainik, U., Dadar, M., . . . Mišić, B. (2018). Network connectivity determines cortical thinning in early Parkinson's disease progression. *Nature Communications, 9*(1), 1-10.
Yau, Y. H., Potenza, M. N., Mayes, L. C., & Crowley, M. J. (2015). Blunted feedback processing during risk-taking in adolescents with features of problematic Internet use. *Addictive Behaviors, 45*, 156-163.
Yeo, B. T., Krienen, F. M., Sepulcre, J., Sabuncu, M. R., Lashkari, D., Hollinshead, M., . . . Polimeni, J. R. (2011). The organization of the human cerebral cortex estimated by intrinsic functional connectivity. *J Neurophysiol, 106*(3), 1125-1165.

Yoon, T., Geary, R. B., Ahmed, A. A., & Shadmehr, R. (2018). Control of movement vigor and decision making during foraging. *Proceedings of the National Academy of Sciences, 115*(44), E10476-E10485. doi:10.1073/pnas.1812979115

Yoon, T., Jaleel, A., Ahmed, A. A., & Shadmehr, R. (2019). Saccade vigor partly reflects the subjective economic value of the visual stimulus. *bioRxiv*, 770560. doi:10.1101/770560

Yue, Q., Martin, R. C., Fischer-Baum, S., Ramos-Nunez, A. I., Ye, F., & Deem, M. W. (2017). Brain Modularity Mediates the Relation between Task Complexity and Performance. *J Cogn Neurosci, 29*(9), 1532-1546. doi:10.1162/jocn_a_01142

Zalesky, A., Fornito, A., Cocchi, L., Gollo, L. L., & Breakspear, M. (2014). Time-resolved resting-state brain networks. *Proc Natl Acad Sci U S A, 111*(28), 10341-10346. doi:10.1073/pnas.1400181111

Zhang, J., & Rowe, J. B. (2014). Dissociable mechanisms of speed-accuracy tradeoff during visual perceptual learning are revealed by a hierarchical drift-diffusion model. *Front Neurosci, 8*, 69. doi:10.3389/fnins.2014.00069

Zheng, Y.-Q., Zhang, Y., Yau, Y., Zeighami, Y., Larcher, K., Misic, B., & Dagher, A. (2019). Local vulnerability and global connectivity jointly shape neurodegenerative disease propagation. *PLoS biology, 17*(11).

Zou, Q., Miao, X., Liu, D., Wang, D. J., Zhuo, Y., & Gao, J. H. (2015). Reliability comparison of spontaneous brain activities between BOLD and CBF contrasts in eyes-open and eyes-closed resting states. *NeuroImage, 121*, 91-105. doi:10.1016/j.neuroimage.2015.07.044